University of Zurich[UZH]

Tree Rings as Indicators of Different Reactions to Drought in Urban Trees

GEO 511 Master's Thesis

Author
Nicola Paltenghi
15-058-506

Supervised by
Prof. Dr. Paolo Cherubini (paolo.cherubini@wsl.ch)

Faculty representative
Prof. Dr. Markus Egli

30.09.2021
Department of Geography, University of Zurich

GEO 511, Master Thesis
Geography Department
University of Zurich

Tree Rings as Indicators of Different Reactions to Drought in Urban Trees

NICOLA PALTENGHI
SUPERVISED BY PROF. DR. PAOLO CHERUBINI
FACULTY MEMBER PROF. DR. MARKUS EGLI

30-September-2021

Abstract

The consequences of global warming are decrease in the precipitation and increase variations in precipitation regimes. The evapotranspiration will increase, as responses of the increment in temperature. Such conditions are likely to sharp the magnitude and duration of the drought events in the next decades within the cities. The tree growth responses to the drought events are considered in order to gain knowledge about trees specific reaction to climate (through the SPEI). The trees reactions are analysed as follows: a) the trees growth responses along with the drought events occurrence, b) the velocity and the ability of the trees to regain the earlier growth patterns or as close as possible to previous standards, and, in the end, c) the ability of the trees to maintain the growth responses in a period following the drought events, also by considering a succession of drought events.

The tree ring width is measured to indicate the trees growth responses to urban environment. Tree ring width values are cross-dated, de-trended and statistically treated. The tree ring width indexes are compared with the climatic indexes. It is explored the long-term relationship through the Mann - Kendall statistics. 8 driest years are selected and 3 time periods are created: periods during the drought events (PDDE), periods before the drought events (PBDE) and periods after the drought events (PADE). ANOVA and Tukey's honest significance test are use to assess the similarities within the tree species. In the end, 3 tolerance indexes are built in order to have a comparison among the different tree species. The tree species are then evaluated through PCA cluster analysis in order to classify the tree species depending on their resistance, resilience and recovery.

Generally, 15 out of 19 tree species show a weak to moderate long-term relationship to SPEI data. 12 out of the 19 tree species showed a significant reduction in growth during the drought events. 3 out of 19 species show a significant lower tree growth during the PDDE concerning the PADE. No tree species show a significant difference between tree growth in the PBDE compared to PADE. PCA and cluster analysis allow to classify the tree species in 4 groups: *Sophora japonica* is strongly discriminated against, because it has the highest recovery value and the lowest resistance value. *Betula pendula*, *Pyrus communis* and *Paulownia tormentosa* represents another cluster. Similar to *Sophora japonica*, these tree species show strong recovery values and weak resistances values. *Amelanchier lamarckii*, *Fraxinus excelsior*, *Pinus rufinerve* and *Prunus umineko* tend to show relatively strong recovery and resilience values and moderate resistance values. The remaining tree species, *Crataegus levigata and lavellei*, *Magnolia kobus*, *Ailanthus altissima*, *Tilia altissima*, *Cercidiphyllum japonicum*, *Robinia pseudoacacia*, *Acer platanoides and rufinerve*, *Picea omorika* and *Catalpa bignoinioides* are the tree species in the last class. This latter class seems to have similar values of resistance, resilience and recovery: They show moderate resistance, resilience and recovery values.

Contents

1 Introduction

1.1 Context

Climate change is a phenomenon that is considered in the scientific literature to be one of the consequences of increased anthropogenic greenhouse gases emissions and the understanding of its effects is a current challenge (IPCC, 2018: Myhre et al., 2013: Barzagli and Mani, 2019: Haines et al., 2019). Climate change has led to drastic environmental and meteorological changes and an increase in exceptional conditions all over the world (Haines et al., 2019). It is broadly congruous in the scientific community that the effects of climate change are characterized by the alteration in temperature and precipitation regimes (IPCC, 2018: Myhre et al., 2013: Barzagli and Mani, 2019: Haines et al., 2019). The rise in the mean annual temperature, the change in precipitation pattern and the increase in the intra-annual variation are responsible for the extreme climate occurrences (Zang et al., 2014). Drought is an extreme climate event that occurs during exceptional high temperature and anomalous precipitation regime, in general, characterized by absence or extremely low rainfall for a prolonged period (Barzagli and Mani, 2019). Drought increase had been widely studied in the last decades and forecasting agree that drought occurrence is likely to increase in both frequency and magnitude in the next decades (IPCC, 2018: Schär et al., 2004). The impacts of the drought on the environment are fundamental to be studied and understood because they are damaging for the ecosystems and the society. As a matter of fact, the drought events are a constraint to trees growth and productivity, because they reduce trees fitness and in severe situations, they are likely to be a cause of the trees die-offs (Churkina and Running, 1998: Flexas and Medrano, 2002: Luyssaert et al., 2010: Reddy et al., 2004). Therefore, the knowledge about trees specific responses during previous and current severe drought events occurrence are fundamental to be studied, in order to understand the trees abilities to maintain living activities in the future climate (Bolte et al., 2009).

The same argument can be used to describe climate change within a city. However, the impacts of the climate change are likely to be severer within a city in comparison to forests. As a matter of fact, it is expected that cities will experience sharper warming, because of factors shaping the microclimate. For instance, the cities are likely to experience a chain of events, which are likely to contribute to the temperature increase, such as the warm island effect, the sunlight reflection by the buildings' walls, the thermal conductivity of asphalt, the absence of evapotranspiration, cooling of water reserves and plants, etc. A possible countermeasure to mitigate the worsening of climatic conditions within a city is the use of the cooling effect of plants' evapotranspiration, which would lead to a decrease in temperature (Munalula et al., 2017). Besides, urban areas populated by trees are likely to mitigate extreme climate effects through the creation of shadows and the ability to participate in the creation of a cold wind system. However, the increased frequency and magnitude of drought events is also a pressing issue for trees within cities, as worsening climatic conditions also affect the livability of urban trees. The observation and study of tree growth responses during earlier drought events within a city is a key task in understanding how climatic events affect the living conditions of trees during future urban scenarios (Parlow et al., 2011: Stadt Zürich, 2020).

The dendrochronology allows the detection of the trees signs of growth by analyzing the annual growth patterns found in the wood. Analyzing a longer time series, a sequences (chronology) of growth patterns allows to evaluate tree health and the environmental conditions the tree grew in, at species or population level (Fritts, 1976: Schweingrüber, 1988). Consequently, dendrochronology is a proven tool to recognize growth patterns and the tree's reaction and adaptation to extreme climatic conditions (Cook, 1990). Such knowledge is fundamental to observe the tree growth response during the drought events and, furthermore, it allows to estimate tree growth patterns in the period after the drought events, what is known as legacy effect. (Navarro-Cerrillo et al., 2018: Anderegg et al., 2020). For instance, the consequences of the trees growing patterns during the earlier drought events can last for years and impact the present tree growth responses (Bose et al., 2020). Therefore, dendrochronology allows the study of trees growth responses during and after the succession of past drought events. As suggested by the study of Bose and colleagues (2020), Anderegg and colleagues (2020) and Lloret and colleagues (2011), the tree growth responses are evaluated quantitatively following these three characteristics: a) the trees growth responses along with the drought events occurrence, b) the velocity and the ability of the trees to regain the earlier growth patterns or as close as possible to previous standards, and, in the end, c) the ability of the trees to maintain the growth responses in a period following the drought events, also by considering a succession of drought events (Zang et al., 2014: Bose et al., 2020).

The scientific community agrees on rising greenhouse gases atmospheric concentration as cause of the global warming and the subsequent drought occurrence increase in the next decades (Kew et al., 2019: IPCC, 2018: Dai et al., 2018). It is congruous in the scientific community that consequences of global warming will decrease the precipitation occurrence and it will increase variations in precipitation regimes. Furthermore, the evapotranspiration will increase, as responses of the increment in temperature. Such conditions are likely to increase the occurrence and duration of the drought events in the next decades (Dai et al., 2018). As a matter of fact, expectations (IPCC, 2018) are congruous that this regimes will continue and sharp in the future. Trees are endangered by future climatic variations, conservative measure are required accordingly (Lin et al., 2020). As suggested by Dai and colleagues (2018), the knowledge about the development of trees water use efficiency in responses to increasing atmospheric greenhouse gases concentration are fundamental. Trees water use efficiency is strongly bound to the ability of the trees to respond to the environmental drivers by fulfilling the 3 characteristics listed in the previous paragraph. As a matter of fact, augmenting tree water use efficiency will decrease the evaporation demand within a city. Therefore, the 3 appropriate trees' responses to climate change, allows a mitigation and reduction of the impacts of drought events in a city (Dai et al., 2018).

Such evaluations are likely to help the urban foresters in the forest management strategies. For instance, the selection of tree species to be planted at a specific location is constrained by the environmental conditions and therefore require a careful analysis of the tolerance and capabilities of adaptation a tree or plant has, in order to estimate the best growth responses under future climate. As a matter of fact, it is likely that the increase in drought frequency and magnitude increments the trees vulnerability and/or mortality (Churkina and Running, 1998: Flexas and Medrano, 2002: Luyssaert et al., 2010: Reddy et al., 2004). Therefore, the species of trees, which develop the best growth responses to drought events or the best ability to regain past growth pattern, is preferred by foresters (Zang et al., 2014: Bose et al., 2020). The discovery of which tree species is likely to be

less vulnerable to extreme climate events is one of the Grün Stadt Zürich (GSZ) topics of interest. GSZ is a service department of the Civil Engineering and Waste Management Department (TED) of the City of Zurich and it is responsible for the construction, care and maintenance of urban green spaces, such as parks, sports facilities, urban forests, cemeteries, bathing facilities and playgrounds.

GSZ (GSZ) considers the vulnerability and mortality of the trees in urban spaces one of the sensitive topics to be studied and understood (Batllori et al., 2020). Especially, GSZ is interested in the trees growth responses to the increase in drought frequency and magnitude within the urban spaces (Stadt Zürich, 2020). For instance, GSZ planned and developed delicate projects ("die Richtplanung", "das Grünbuch" and "die Fachplanung Hitzeminderung") to challenge the climate change effects within the city and the consideration about urban trees is relevant: the objectives are displayed as follow:
"*Drought, heat and heavy rain will increase in the coming years. Heatwaves will become more frequent, longer and more intense. We are already feeling this in the cities. Cities like Zurich act as heat islands, where it can be up to 10° C hotter than in the surrounding area. This has problematic effects on our lives. Therefore, we must not only combat the causes of climate change but also its symptoms. Heat mitigation planning is one instrument for this. We have the big task of how to adapt our city to the heat according to the latest knowledge. The city must also plan how it can grow in its limited spatial conditions and still create enough open spaces. We want to hand over to the next generations a city that is at least as livable as we find it today and as well adapted to climate change as possible. There are various planning elements: guideline planning, the green book and also the specialised planning for heat reduction. The sectoral planning shows that densification and adaptation to climate change are not contradictory. The city can not be transformed overnight. But we are setting the course for a climate−friendly city here and now.*" (translated from: Stadt Zürich, 2020).

City trees and park trees play an important role in the plan of GSZ. As a matter of fact, they are likely to be helpful in the mitigation of extreme climate conditions within urban spaces. Therefore, the employment of urban trees are likely to make the city more livable for its citizens. For instance, an increment in the number of urban trees, which develop the best growth responses to the past drought events, is likely to help extreme climate mitigation and reduce trees vulnerability/mortality within the city. Therefore, the plantation of trees, which develop the best growth responses to past drought events in urban spaces, is likely to have a mutual benefit within the city in the future. That means the trees contribute to the increase in the quality of life for the citizens and they contribute to the preservation of the fragile urban ecosystem (Stadt Zürich, 2020).

This master thesis considers urban and park trees from the city of Zurich provided by the GSZ. These trees are cut by the foresters because they are deemed too damaged to survive and they are considered dangerous for people. The trees can be of any species present in the city of Zurich, of any age and grown in every place, where GSZ has planted them.

This master thesis considers before the tree ring width measurements as indicators of trees growth responses to city environment. Tree ring width values are de-trended and statistically treated to have a comparable measuring unit among the different samples. The second step considers the construction of climatic indexes with the R software (SPEI, SPI, the duration of the drought events, the severity of the drought events, the

intensity of the drought events and the frequency of the drought events).

Once samples are ready and measured, the tree ring width indexes are compared with the climatic indexes. The first step considers the exploration of the long-term connection between tree ring width measurements and climatic index values. Statistics are used to assess the number of connections between the measures.

After the long term trend identification of the tree growth, the actual relationship between the driest years and the tree ring width measurements. This latter is achieved by researching and selecting the years with strongest drought and 2 time periods related to the occurrence of the drought events (the period before the drought events and periods after the drought events). These measures are compared with the ring width measurements and they are statistically assessed in order to discover the amount of relationship between the tree growth during the 3 periods. Such a way allows this thesis to have a perspective about the tree species growth pattern depending on climate drivers.

In the end, 3 tolerance indexes are built in order to have a comparison among the different tree species. Such indexes consider the tree growth during the 3 drought events period above mentioned and they allow the discovery of different tree species patterns. The tree species are then evaluated through cluster analysis in order to classify the tree species depending on their resistance, resilience and recovery pattern.

1.2 Aims of the study, hypothesis and research questions

The scientific community agrees that the increasing greenhouse gas emissions are responsible for global warming and the subsequent drought occurrence increase (Kew et al., 2019). Decrease in precipitation and the sharpening of the fluctuations in precipitation pattern combined to increase in evaporation caused by the rising temperature are responsible for the increasing drought occurrence in the last decades (Dai et al., 2018). The forecasting (IPCC, 2018) is confident that this trend will continue in the next decades and therefore, predictive measures are needed (Lin et al., 2020). Some recent discoveries showed the importance of specific trees in the increased water use efficiency under rising atmospheric greenhouse gases concentration, which would decrease the evaporation demand (Dai et al., 2018). Increase in trees' water use efficiency under high atmospheric greenouse gases concentration would mitigate and reduce the impact of drought events (Dai et al., 2018).

This master thesis aims to figure out which tree species will be more is more adapted to the conditions found in an urban environment like in the city of Zurich. With the aid of the dendrochronology, I study tree growth in the last 40 years in the city of Zurich. Dendrochronology would help in the understanding of the last 40 years of trees' responses to climatic factors within the city of Zurich. In particular, the drought period and trees reactions to drought are analyzed with dendrochronology in combination with meteorological data. On one hand, this master thesis, it should be possible to identify trees species, which are characterized by the capacity to withstand or to be less vulnerable to events of extreme drought or to post-drought periods. On the other hand, it should be possible to identify which tree species have less ability to cope with the drought period. This master thesis considers tree samples (stem discs or cores), historical meteorological data (from 1981 to 2020) and computer software to calculate meteorological indices and tree-related indices.

The research questions and hypothesis are thereafter listed:
Q1: How does the drought events occurrence and magnitude evolved during the last decades of climate change?
Q2: What is the impact of the drought pattern change on the trees' growth within the city of Zurich?
Q3: Are the signs of drought events visible from the tree ring width measurements?
Q4: Do consecutive drought events impact tree growth differently from a single event?
Q5: Do tree species react differently and/or with different timing to drought events?
Q6: Which tree species maintain the best growth pattern during the past drought events in the city of Zurich?
Q7: Which tree species keep the best growth pattern after the drought events in the city of Zurich?
Q8: Which tree species regain the best growth pattern, or the closest as before the drought events in the city of Zurich?
Q9: Which tree species will be most suitable to be planted in Zurich in the future?
The hypothesis is the following:
The drought occurrence increased in the last decades due to climate change. Temperature and precipitation pattern change have influences on the trees' growth within the city of Zurich. Trees suffer the drought increase in both magnitude and occurrence and the signs are visible in tree ring growth. As a matter of fact, it is expected that trees growth decrease during the drought events and effects last years later the occurrence of the drought events. Therefore, the succession of several drought events in a relatively short period, prevents the trees to compensate for the growth and it brings to a gradual loss in growth. The last 4 questions should be discovered through the work of this thesis and there are few basic knowledge to list expectations.

2 Methods

2.1 General descriptions

The detection and the methodology to study the effects of climate warming were challenging tasks for GSZ. The objective of GSZ was to understand how and how much the increasing of drought events occurrence within Zurich affected the livability of its citizens.

To answer the questions, 3 different methods were applied. The methodology allowed to consider and combine climatic drivers, dendrochronology issues and comparison between the two disciplines. The first intention of this thesis was to analyse and discover which climatic drivers caused the increase in drought events occurrence during the last decades (Richman and Leslie, 2015) in the city of Zurich. Moreover, the magnitude and variation of the drought events was assessed (Kim et al., 2020), within the city of Zurich in the last 40 years. As a matter of fact, the 40 years period allowed to have a comparison between the recent drought events and the older ones, where drought was less effective (Brunner et al., 2019). The research step about drought detection and calculation is described in the section "Meteorological data".

Furthermore, the trees growth response under climate change were analysed, in order to discover, how trees reacted to the increasing drought events occurrence (Huang et al., 2018). Tree samples were collected and analysed at the WSL laboratory of Birsmendorf in order to retrieve information about tree growth patterns.

The trees' growth was taken under consideration from 1981 to 2020 because it was coherent with the climatic indices above explained and it considered the age of trees, which sometimes did not reach the 40 years. The trees growth pattern was addressed through the measurements of the ring width and thereafter, the raw ring width was treated to have a standard measure comparable between different tree species. The steps concerning the dendrochronology issues are addressed in section "Tree growth parameters".

In the end, a relationship between tree species growth and drought occurrence and magnitude was discovered (Clark et al., 2016). In order to discover the relationship between trees growth and drought occurrence and magnitude, the construction of the tolerance indexes was considered. This step combined the ring width measurements with the climatic factors. The calculations and the methodology for the comparison are described in section "Comparison between drought and tree growth indices".

2.2 Study site

Zurich is the largest city in Switzerland and the capital of the canton of the same name and it is one of the cities with the highest quality of life (MERCER LLC, 2019). Zurich city is located in the northeast of Switzerland in the eastern Swiss midlands and lies at the northern edge of the lake of the same name, where the river Limmat leaves the lake. A little further north, at Zurich's largest park, the Platzspitz, the Sihl River flows from the southwest into the Limmat. To the west, the city extends along the Limmat valley. Zurich borders are represented by the morphology: to the north, Zurich extends beyond the Zürichberg and Käferberg mountains into the Glatt valley. The eastern boundary is formed by the Adlisberg and Öschbrig (696 m.a.s.l.), while the south-western boundary is formed by the Uetliberg (FDHA, FSO, 2020).

The municipal area of the city of Zurich covers an area of around a bit less than 100 km^2. It encompasses the upper part of the Limmattal nature and settlement area, a section of the northern Swiss Mittelland. The canalised and partly straightened Limmat does not flow roughly in the middle of the valley, but always along the right (north-eastern) edge of the valley. At 392 meters above sea level, the lowest point of the municipality is reached on the Limmat near Oberengstringen. On its western side, the Limmat valley is flanked by the wooded heights of the Albis chain, the Uetliberg and the Buechhoger, on which the western municipal boundary runs. The Uetliberg, the town's local mountain, is the highest point in the vicinity at 870 metres above sea level. To the south, the municipal ground extends into the lower Sihl valley. To the northeast of the Limmat valley is a chain of hills that marks the watershed between the Limmat and Glatt rivers. The height of the most forest-covered hilltops increases from northwest to southeast: Hönggerberg (541 m above sea level), Käferberg (with Waidberg, 571 m above sea level), Zürichberg (676 m above sea level) and Adlisberg (701 m above sea level). Between Käferberg and Zürichberg is the completely built-up Milchbucks saddle (around 470 m above sea level), an important transition from the Limmat to the Glatt valley. The northernmost part of the municipality extends into the plain of the Glattal and into the depression that connects the Glattal and the Furttal. Part of the Katzensee (nature reserve) and the Büsisee, both of which are drained by the Katzenbach to the Glatt, also belong to the municipal area (DETEC: FOEN, 2020).

Zurich lies in the temperate climate zone. Zurich's climate is characterised on the one hand by the winds

from westerly directions, which often bring precipitation, and on the other hand by the Bise (easterly or north-easterly wind), which is usually associated with high-pressure conditions and brings cooler weather phases than would be expected on average in all seasons. The Föhn, which is important in the Alpine valleys and at the edge of the Alps, does not normally have any special climatic effects on Zurich. The annual mean temperature at the measuring station of the Federal Office of Meteorology and Climatology (MeteoSwiss) in Zurich-Affoltern at 444 meters above sea level is $9.4°C$, with the coldest monthly mean temperatures in January ($0.3°C$) and the warmest in July ($18.8°C$). On average, around 92 frost days and 21 ice days can be expected here. There are around 46 summer days on average per year, while there are normally 8.5 heat days. The Zurich-Affoltern measuring station has an average of 1531 hours of sunshine per year. The 1054 mm of precipitation falls throughout the year, with higher amounts being measured in the summer half-year and especially during the three summer months due to convective precipitation than in winter (FDHA: MeteoSwiss, 2020).

A general overview of the place and the location of the sample sites can be seen in figure 1, where it is displayed Zurich city from a satellite and the respective location of the tree samples.

Figure 1: Satellite image of Zurich city. The map shows the location of the trees (red signs) within the city. Map downloaded from Open Street Map package in QGIS v.3.14.16 under the MapTile plugin.

2.3 Tree species

GSZ provided several samples of different tree species for the analysis: *Pyrus communis*, *Robinia pseudoacacia*, *Acer platanoides and rufinerve*, *Aesculus hippocastanum*, *Betula pendula*, *Catalpa bignonioides*, *Crataegus levigata and lavellei*, *Platanus x hispanica*, *Sophora japonica*, *Tilia europea*, *Cercidiphyllum japonicum*, *Magnolia kobus*, *Paulownia tormentosa*, *Picea omorika*, *Prunus umineko*, *Ailanthus altissima*, *Amelanchier lamarckii*, *Pinus sylvestris* and *Fraxinus excelsior*. All these tree species were analysed in the WSL laboratory of Birsmendorf. However, some species were challenging to be measured and some did not have a high number of specimens to compare the results within the species. Therefore, in this thesis only a few species were selected

for more detailed analysis and statistical comparison. The selected species for this master thesis were 19. Some species had a low number of samples, therefore, some analyses might be inaccurate because there was not a direct comparison within the same species. However, GSZ provided the tree samples and there was no possibility to collect them individually. The tree species and the number of samples that were at disposal for the analysis, are displayed in tables 1 and 31 in the appendix.

Table 1: Number of samples for every tree species

Tree species	No. of samples
Robinia pseudoacacia	16
Prunus umineko	11
Acer platanoides and rufinerve	6
Tilia europea	6
Platanus x hispanica	6
Betula pendula	5
Ailanthus altissima	4
Crataegus levigata and lavellei	2
Magnolia kobus	2
Picea omorika	2
Aesculus hippocastanum	1
Catalpa bignonioides	1
Sophora japonica	1
Cercidiphyllum japonicum	1
Paulownia tormentosa	1
Amelanchier lamarckii	1
Pinus sylvestris	1
Fraxinus excelsior	1
Pyrus communis	1

2.4 Meteorological data

Some of the studies above mentioned (Brunner et al., 2019: Dai et al., 2018: Kew et al., 2019: Kim et al., 2020: Lin et al., 2020: Richman and Leslie, 2015) addressed change in precipitation pattern and decrease in magnitude. They discovered temperature increase connected with the change in evapotranspiration pattern, as the main drivers to cause drought events. In this analysis, drought was therefore defined with threshold values applied on monthly precipitation and mean monthly temperature. As showed in literature (Chen et al., 2013: Li et al., 2012: McKee et al., 1993: Morid et al., 2006: Nedealcov et al., 2015: Pei et al., 2020: Vicente-Serrano et al., 2010: Tan et al., 2015: Wang et al., 2012), drought stress was defined and estimated with indices, which combined climatic factors, such as mean monthly temperature and mean monthly precipitation. The indices were standard precipitation evapotranspiration index (SPEI), developed by Vicente-Serrano (2010) and standard precipitation index (SPI), developed by McKee and colleagues (1993). However, drought frequency and magnitude were challenging to be assessed by SPEI and SPI alone. Therefore, further meteorological indices were created, because they were more specific, fitted for the purpose and simplified the complexity of

the SPEI and SPI. For instance, the last step of the climate parameters dealt with the creation of drought indices from SPEI and SPI: vegetative SPEI, duration of drought, frequency of drought, the severity of drought and intensity of drought (Bose et al., 2020).

2.4.1 Climatic factors: Mean precipitation and mean temperature

The climatic data selected for the analysis were mean monthly precipitation and mean monthly temperature. Both the dataset were made available by FDHA: MeteoSwiss (2021) for the 3 meteorological stations located in the region of the city of Zurich. The 3 meteorological stations with main information are listed in table 2.

Table 2: Meteorological station where the data is taken from

Station	Abbreviation	altitude [m.a.s.l.]	latitude	longitude
Zurich Affoltern	REH	445	47.427594	8.517897
Zurich Fluntern	SMA	558	47.377858	8.565744
Zurich Kloten	KLO	428	47.479553	8.535911

Since the samples were collected within the city of Zurich and they were surrounded by the 3 stations, mean monthly precipitation and temperature from Affoltern, Fluntern and Kloten stations were integrated over the whole city of Zurich, in order to have mean monthly precipitation and temperature for the whole area.

Therefore, the mean monthly temperature and the mean monthly precipitation were assumed as a result of a single averaged value over the whole city. These values were then used to construct the climatic indices, which were used to be compared with the tree ring width (Bose et al., 2019).

2.4.2 Standardized precipitation evapotranspiration index (SPEI) and standardized precipitation index (SPI)

The SPEI, developed by Vicente-Serrano and colleagues (2010), and SPI, developed by McKee and colleagues (1993), were the 2 indices used in several studies by the scientific community to monitor drought patterns (Vicente-Serrano et al., 2010: Nedealcov et al., 2015: Tan et al., 2015: Li et al., 2012). As a matter of fact, the variation in precipitation pattern was discovered by the scientific community to be a strong predictor to detect drought distribution around the world (Potop et al., 2012). Therefore, the SPEI and SPI drought indices were built from mean precipitation, as a standard measure, in order to study and predict impacts of drought occurrence (Shukla et al., 2015). The SPI was approved by the World Meteorological Organization (WMO) as a valid standard index to monitor drought around the world (Chen, et al., 2013).

The SPI and SPEI used monthly precipitation values in order to build an index that ranges from extremely wet to extremely dry conditions (Wang et al., 2012). Negative SPI and SPEI values represented dry conditions, while positive values represented the wet condition and zero represented the middle way (Morid et al., 2006). The range of the SPI and SPEI values was in most of the cases between $SPI \leq -2$ (extremely dry) and $SPI \geq 2$ (extremely wet).

There was the possibility of some extreme and exceptional SPEI and/or SPI values that exceeded the ±2 threshold. These values represented exceptional dry or, respectively, wet conditions and it was detected mostly by short time scale SPEI and SPI, because of the calculation issues (see following explanations). On one hand, the exceptional values detected by both SPEI and SPI were solely caused by exceptional strong precipitation pattern fluctuation. On the other hand, the exceptional SPEI value only, was caused by exceptional precipitation pattern fluctuation combined with extreme temperature oscillations (Pei et al., 2020).

The SPI and SPEI values with the respective drought classification and levels are displayed in table 3.

Table 3: Level of drought and drought classification depending upon SPI and SPEI respective values

Level	Drought classification	SPEI and SPI value
0	Extremely wet (non-dry)	$index > 2$
0	Very wet (non-dry)	$2 \geq index > 1.5$
0	Moderately wet (non-dry)	$1.5 \geq index > 1$
0	Near normal (non-dry)	$1 \geq index > 0$
1	Mild dry	$0 \geq index > -1$
2	Moderately dry	$-1 \geq index > -1.5$
3	Severely dry	$-1.5 \geq index > -2$
4	Extremely dry	$index < -2$

According to McKee and colleagues (1993), SPI and SPEI values were calculated at multiple time scales, in order to have an optimal consideration about the period included in the drought monitoring and calculation. A long timescale meant that the calculation of the current drought took into account several months prior to the drought events. Respectively, a short timescale meant that the current drought considered few previous months in the calculation. On one hand, the long timescale was used to detect drought events, where temperature and precipitation had been exceptional for a long time before the month considered. On the other hand, short timescale detected short drought events, by considering months close to the one considered (Tan et al., 2015).

The SPEI was similar to the SPI, however, it used monthly precipitation and monthly mean temperature values and latitude, as input parameters in order to calculate the climate water balance (equation 1). The SPEI, differently from the SPI, considered the evapotranspiration changes caused by the variations of the temperature (Vicente-Serrano et al., 2014). Therefore, SPEI discovered drought patterns by considering multiple factors, which made it extremely useful in monitoring the drought under climate change (Li et al., 2012: Mehr et al., 2019: Tan et al., 2015: Diani et al., 2019).

In equation 2, the mean monthly temperature was used to estimate potential evapotranspiration through the Thornthwaite equation (Vincente-Serrano et al., 2011: Thornthwaite 1948). Finally, the climate water balance (CWB) was integrated at a monthly level (equation 3 and 4) and normalized over the whole period considered through a probability distribution function (equation 5 and 6). Through the Abramowitz and Stegun (1965) estimation (equation 8), the SPEI was calculated (equation 7). The calculation steps, which were described by Vicente-Serrano and colleagues (2010) were displayed in the following equations.

The CWB calculation is displayed in equation 1, where it is showed the difference between the monthly mean precipitation (P) and the estimated potential evapotranspiration (PET):

$$CWB_{month} = P_{month} - PET_{month} \tag{1}$$

The monthly PET was calculated in equation 2 through the Thornthwaite estimation (Thornthwaite, 1948) :

$$PET = 16K(\frac{10T}{I})^m \tag{2}$$

Where the monthly mean temperature in Celsius is represented by T, the heat index calculated as the sum of 12 monthly index values by I, the coefficient dependent on I is represented by m: $m = 6.75 * 10^{-7}I^3 - 7.71 * 10^{-7}I^2 + 1.79 * 10^{-2}I + 0.492$, and the correction coefficient calculated as a function of the latitude and month K (Tan et al., 2015). The monthly climate water balance values CWB_{month} was integrated at a different time scale, as in equation 3 and 4. The CWB varied among months (m), years (a), depending on the chosen time scale (t). The accumulated difference for monthly CWB (d) in a particular year (a) is regulated by the timescale t:

$$CWB^t_{a,m} = \sum_{d}^{t} D_{a-1,d} + \sum_{d}^{m} D_{m,d}, .m < t \tag{3}$$

$$CWB^t_{a,m} = \sum_{d}^{m} D_{a,d}, .if m > t \tag{4}$$

The CWB was then normalized for the whole period. The log-logistic distribution was used in equation 5, to normalize the CWB series in order to calculate the SPEI. The probability density function of a 3-parameter log-logistic distributed variable was calculated as:

$$f(x) = \frac{\beta}{\alpha} * \left(\frac{\chi - \gamma}{\alpha}\right)^{\beta-1} * \left[1 + \left(\frac{\chi - \gamma}{\alpha}\right)^{\beta}\right]^{-2} \tag{5}$$

Where the scale is represented by α, the shape by β and the origin for the CWB values by γ. As demonstrated by Singh and colleagues (1993), the parameters of the distribution were obtained. Therefore, the probability distribution function of the CWB series, following the log-logistic distribution, was calculated, as in equation 6:

$$F(x) = \left[1 + \left(\frac{\alpha}{\chi - \gamma}\right)^{\beta}\right]^{-1} \tag{6}$$

From the standardized values of F(x), the SPEI series was obtained through the estimation of Abramowitz and Stegun (1965), as in equation 7 and 8:

$$SPEI = W - \frac{C_0 + C_1W + C_2W^2}{1 + d_1W + d_2W^2 + d_3W^3} \tag{7}$$

C_0, C_1, C_2, d_0, d_1, d_2 are tabulated constants and they are equal to: $C_0 = 2.515517$, $C_1 = 0.8022853$,

$C_2 = 0.010328$, $d_1 = 1.432788$, $d_2 = 0.189269$, $d_3 = 0.001308$

$$W = \sqrt{-2ln(P)} for P \leq 0.5 \tag{8}$$

The probability of exceeding a definite CWB value of $P = 1 - F(x)$ is represented by P. (Vicente-Serrano et al., 2010: Tan et al., 2015).

Both SPEI and SPI values were calculated through the R software (R Development Core Team, 2018) with the function "spei" and "spi" under the package: "SPEI" (Vicente-Serrano et al., 2010); following the instruction of Cadro and Uzunovic (2013). SPEI and SPI timescale were arbitrarily chosen and calculated for 1 to 6 plus the 12, because it considered an estimation of the water available in a city (Potop et al., 2012). Since this master thesis considered an urban area with a discharge system for the rainfall and a soil typically asphalted (see figure 1), the timescale selected for both SPEI and SPI was coherent with the ability of the terrain to retain and store available water for trees. SPEI and SPI were then selected to evaluate the short-term drought in the city of Zurich because the city did not allow high water storage for trees pillage within the soil. Besides these timescales were typical to study trees growth under the effects of climate parameters because it considered trees physiological response to water content within the soil (Chen et al., 2013).

2.4.3 Evaluation of drought from monthly SPEI data

A drought event was defined by McKee and colleagues (1993) as a function of SPI values and it was approved by the World Meteorological Organization WMO. For instance, a period was catalogued as dry, when consecutive monthly SPI values remained below 0, with at least one month within this range, which values reached -1 or less (Tan et al., 2015).

According to Tan and colleagues (2015), both SPEI and SPI indices showed similarities in the results, since the calculations were analogues. However, this master thesis considered drought events within the city. Therefore, precipitation, temperature and evapotranspiration were significant for drought detection because it accounted for the drought severity which tended to raise the water demand for the evapotranspiration (Vicente-Serrano et al., 2010). Therefore, it was tested if SPEI and SPI data showed a monotonic trend, in order to define the number of similarities between the 2 indexes. This step helped in the recognition of the importance that mean monthly temperature and mean monthly evapotranspiration had on drought events.

In order to discover the relationship between the variables, SPEI and SPI were tested with the Mann-Kendall test for monotonic trend (Kendall, 1938) between SPEI and SPI data. The Mann-Kendall was chosen because it was a non-parametric test and it did not assume normally distributed data (Mondal et al., 2012: Soltani et al., 2013: Samuels, 2014). Therefore, a Mann-Kendall test for monotonic trend was run between SPEI and SPI over the timescale of 1, 2, 3, 4, 5, 6 and 12 and the 1981-2020 period. The Mann-Kendall test for the monotonic function was calculated through the R software (R Development CoreTeam, 2018) under the "Kendall" package (McLeod, 2015).

2.4.4 Cimatic indexes

SPEI and SPI were calculated over a 6 plus 1 time scale. The resolution of both SPEI and SPI was monthly. Therefore, a huge data set was created and analyzed. However, the size of the data set caused some difficulties which were solved by following the suggestions of Bose and colleagues (2020) and Tan and colleagues (2015).

In order to have a simplified overview of the multidimensional time scale SPEI and SPI, drought frequency and magnitude were evaluated through new indices built from SPEI and SPI (Tan et al., 2015: Bose et al., 2020). These new indices helped in the generalization of SPEI and SPI. These new indices were five and they are: The average SPEI over the vegetative periods (equation 9), the duration of drought (equation 10 and 11), the frequency of drought (equation 12), the severity of drought (equation 13) and the intensity of drought (equation 14). These drought measurement units were created by using the monthly values of SPEI and SPI as inputs and the resulting output was at an annual resolution (Adhyani et al 2017).

The average SPEI over the vegetative periods was calculated in equation 9 and it considered an arithmetic mean between the monthly SPEI values over a vegetative period in a year. Therefore, monthly SPEI values from March to August were averaged, to have a single yearly value.

$$V_{SPEI} = \sum_{March}^{August} SPEI * \frac{1}{6} \tag{9}$$

Duration and severity of drought served to build the intensity of drought. The frequency helped in the recognition in the special case, where the intensity was biased from too severe drought, and/or too long duration of drought (Tan et al., 2015).

The duration of a drought (d) was a measure that considers how long (in months) a drought occurred by considering the SPEI and SPI values (Cavus et al., 2020). It was represented by the count of months, in which respective values met the drought criteria explained in section "Evaluation of drought from monthly SPEI data" (table 3). The duration of drought is calculated in equation 10 and 11, which considered the highest count of consecutive drought months (m), and the results are displayed in table 27.

j = years from 1980 to 2020, i = SPEI's value from 1 to 12 (monthly), n = natural number from 1 to 12.

$$\exists!\ SPEI_{j,i} \leq -1 \Rightarrow\ SPEI_{j,i-1\ \vee\ i+1} < 0\ \Rightarrow\ SPEI_{j,i-2\ \vee\ i+2} < 0\ \Rightarrow\ ...\ \Rightarrow\ SPEI_{j,i-n\ \vee\ i+n} < 0\ \Rightarrow \tag{10}$$

$$\Rightarrow \sum_{j=1980}^{2020} \sum_{i=1}^{12} |SPEI_{j,i}| \tag{11}$$

Where $|SPEI_{j,i}|$ means set cardinality (i.e. number of elements in a set). On the other hand, the frequency of drought is represented by the counts of drought months (m) over the period at an annual resolution. Frequency detected the length of the drought over a year. On one hand, high-frequency values represented the drought

distributed over the whole year, on the other hand, low-frequency values, the drought interested in few months (Brito et al., 2017). The formula is represented by equation 12:

$$F_e = \frac{n_e}{N_e} \tag{12}$$

Where n_e was the number of consecutive months (m) with a drought occurrence and N_e was the period considered. Results are displayed in table 28.

The severity (equation 13) and intensity of drought (equation 14) were suited to evidence the strength and magnitude of drought over a period. The selection of the timescale for the SPEI and SPI calculation played a fundamental role in the results (Tan et al., 2015).

The severity evidenced the strength of a drought occurrence by comparing the SPEI and/or SPI values to the duration (d) of drought through a formula. The severity (S_e) of drought represented the overall drought strength for a drought event (Dalezios et al., 2000) by calculating the sum of all the SPEI and/or SPI values during the whole duration of a drought event (Tan et al., 2015). In the following formula (equation 13) it is displayed the calculation of the severity:

$$S_e = \left| \sum_{j=1}^{m} SPEI_j \right|_e \quad or \quad S_e = \left| \sum_{j=1}^{m} SPI_j \right|_e \tag{13}$$

Where the first month considered in the calculation is represented by j and the number of months considered by m. The indices values are represented by SPEI and respectively SPI.

The intensity of drought was used then to calculate the intensity (I_e) of the drought (equation 14). The (I_e) was calculated as the strength (severity) averaged over the duration of a drought event (Tan et al., 2015). On one hand, these measures generalized the SPEI and/or SPI values by creating a single measure that considered the strength and magnitude of drought over a specific period (Saravi et al., 2009: Lin et al., 2020). On the other hand, the frequency of drought measures helped in the detection of possible biased intensity by a too strong intensity or a too long duration. The formula for the calculation is displayed in the following formula (equation 14) (Tan et al., 2015):

$$I_e = \frac{S_e}{m} \tag{14}$$

This master thesis used the intensity of drought from different SPEI and SPI timescales, and checked the results with the frequency of drought because they provided a simplified overview and analysis of SPEI and SPI time resolution dependent for the detection of drought (e.g. short-term timescale: 1, 2, 3, 4, 5, 6; and annual resolution, the timescale of 12). Since the issue was to address extreme drought in the city of Zurich by considering both its duration and magnitude, the use of intensity was likely to be appropriate (tables 27, 28, 29 and 30).

2.5 Tree growth parameters

The assessment and analysis of tree growth was a fundamental task in dendrochronology (Cook and Kairiukstis, 1990). It allowed the detection of climatic factors, which affected the growth of the trees, and those signals were stored within the wood (Scweingrüber, 1988). The extreme change in climate factors, such as temperature, precipitation and evapotranspiration affected the growth of trees as well as the survival (Munalula et al., 2017). These climatic factors were responsible for the strengthening of drought occurrence diagnosed in 21^{st}, which was extraordinary and was found to be a strong predictor of tree growth disturbances. Therefore, the responses of trees and ecosystems under changing climate were a challenging but fundamental task (Saxe et al., 2000). Worse scenario following the increase in drought occurrence and magnitude comprehended, on one hand, the enhanced trees vulnerability, on the other hand, the complete loss of fitness and consequent trees death and forests die-off (Sánchez-Salguero et al., 2020). This was the main worry of GSZ because they wanted to foresee and prevent a high tree mortality rate in the next decades. This is caused by drought occurrence increase, which would lead to a loss of quality of life (Brodribb, 2020). Therefore, understanding the tree growth pattern in the last 40 years was an important task undertaken by this master thesis.

Samples were characterized by tree collected from GSZ. The samples corresponded to the trees that were cut down by urban foresters of the city of Zurich, because they were too damaged to recover. Once the trees were collected, they were brought to the WSL laboratory of Birmendorf and then they were prepared for the tree growth analysis. The further step consisted of the quantitative measure of the tree annual growth in order to place trees growth in a temporal dimension. As a matter of fact, the measure of the annual tree's growth allowed to date and compare trees depending on their age through a chronological perspective (Maxwell et al., 2011). The cross-dating of the tree growth chronologies was a fundamental step of the dendrochronology and it was calculated to compare and supervise the different measurements (Buras and Wilmkins, 2015). The final step consisted in the assessment of the ring width index because it allowed the creation of the unit less and normalized measurements of the ring width values. Ring width index (RWI) allowed to compare tree growth patterns between different tree species, and it allowed to reduce the disturbing effects of tree physiology and age (Bose et al., 2020: Bunn et al., 2018).

2.5.1 Tree samples

Trees samples consisted of dying trees that were cut down by the foresters of Zurich city because they were examined as too damaged to survive. GSZ prepared the samples in stem discs form, which were collected by the technicians and they were brought to the WSL laboratory of Birsmendorf. However, some tree discs were too large to be handled, therefore, they were cut in pieces in such a way, that the rings were visible. GSZ brought a total of 90 samples at the WSL laboratory at the beginning of September, mid-December 2020 and May 2021. Some samples were discarded after an attentive evaluation since they were too damaged to be measured.

The first step was represented by the collection of the samples and thereafter, they were catalogued, in order to produce an ordered dataset. Trees were catalogued depending on the year of death, species, type (urban

trees or park trees), birth date, plantation year (if it was given by GSZ) location (area, street and coordinates). Specific information are displayed in table 31, in the appendix. The samples provided were a small portion of the dead trees within the city, however, GSZ was not able to hand in every sample to the WSL laboratory.

2.5.2 Preparation of the samples

Once the discs were catalogued, they were left in a drying room for about 2 weeks to let them dry. In order to maintain the shape of the discs, the samples were pressed with heavy material (Niessner, 2013).

Discs were cleaned, and in some cases, they were cut with the circular saw in order to produce lines of tree disc. The lines allowed a better recognition of the tree rings. Therefore, they were sanded with the sanding machine in the carpentry with different sanding sizes: 60 µm, 80 µm, 100 µm, 120 µm, 150 µm, 240 µm. In addition, once the sanding process was finished, it was possible to manually sand with sanding paper, apply chalk to enhance the contrast of the rings, and so on. This work allowed the detection of the tree rings and the dating process was more accurate (Kariuki, 2002).

2.5.3 Tree ring width measurements and cross dating

Tree samples were brought to the WSL tree ring laboratory of Birsmendorf in order to measure the tree ring width. The width of a tree ring showed the amount of growth that had taken place for one year and that gave information about the growing conditions for that year (Schweingruber, 1988). Tree ring width dating was fundamental for dendrochronology because it allowed assessing the accuracy of the measure by matching the arrangement of rings among trees within a location (Maxwell et al., 2011). The technique of cross-dating allowed to match the different arrangement of tree ring width and it was the fundamental step to pursue a dendrochronology analysis (Cook and Kairiukstis, 1990: Fritts, 1976).

Cross dating was a mathematical calculation that allowed to recognizes climate and environmental drivers which affected the annual trees growth. Trees reacted to the environmental factors by increasing or reducing the growth (Visser, 2020). This growth pattern developed a frequent year-to-year fluctuation in radial ring growth across different trees within the same location (Maxell et al., 2011). An accurate cross dating allowed a precise interpretation of climatic and environmental drivers (such as drought), which signals were found in the annual tree ring growth (Maxwell et al., 2011: Jansma, 1995). Furthermore, the cross dating allowed the statistical detection and removal of measurements errors, caused both by random errors or by growth anomalies, such as missing rings and extremely thigh rings (Maxwell et al., 2011).

The "Gleichläufigkeit" cross-dating method was used because it considered a statistical approach to compare ring widths measurements. The "Gleichläufigkeit", as explained by Buras and Wilmking (2015), *is a frequently used measure in dendrochronology to calculate the percentage of common signs of year-to-year growth change between two series.* (Buras and Wilmkins, 2015). The "Gleichläufigkeit" in the TSAP-WIN software considered the slope intervals and checked whether the sum of the slope was equal in percentage (Rinn Tech, 2010). The "Gleichläufigkeit" was computed using the equation 15:

$$Glk = \sum(y_{ij} = x_{ij}) \ \ in \ \ \% \tag{15}$$

The Gleichäufigkeit was calculated within trees of the same species, in order to discover some similarities in growth patterns between the samples. To have better output results, the calculation was made in the R software (R Development Core Team, 2018) under the "dplR" package (Bunn and Korpela, 2020) through the "glk.legacy(x)" calculation (Buras and Wilmkins, 2015: Visser, 2020).

2.5.4 Standardization of tree ring width measurements

The objective of the master thesis was to quantify the magnitude of growth that city and park trees had during extreme drought, and respectively, compare this growth to the one during favourable conditions, between 1981 and 2020. Nevertheless, trees had different ages, different locations within the city, which affected the microclimate. Furthermore, different tree species allowed a limited comparison. Therefore, the raw ring width measurements (Rinn Tech, 2010) was converted into dimensionless ring-width indices (RWI) (Bose et al., 2020). According to Cook and Kairiukstis (1990), the decreasing growth trend with the increasing age of the trees and the high-frequency variation of trees growth was removed from the raw ring width, in order to have a unit-less index.

The raw ring-width chronology was de-trended by following linearly a negative exponential curve. The calculation is displayed in equation 16 and it was pursued in the "R" software (R Development Core Team, 2018) under the "dplR" package (library: "dplR") using the "detrend" function (Bunn et al., 2018).

$$y = Ae^{-Sx} + \epsilon \tag{16}$$

Where A, S and ϵ are constant dictated by the ring width data. Since the objective of the thesis was to discover tree species patterns during drought events and non-drought events, the de-trended ring width chronology was averaged within the same tree species. Therefore, every single RWI was averaged within the same tree species with the Tukey's biweight robust mean (Mosteller and Tukey, 1977: Shewchuck, 1997: Kafadar, 1983) with a "w" factor, or weight function of 6 (Bunn et al., 2018). The Tukey's biweight mean was an iterative process, which was computed through the following system of equations (equation 17), as suggested by Zhang (1996):

$$Tukey \begin{cases} if \mid x \mid \ \leq c \\ if \mid x \mid \ > c \end{cases} \quad \rho(x) \begin{cases} \frac{c^2}{6}(1-(1-(\frac{x}{c})^2)^3 \\ (\frac{c^2}{6}) \end{cases} \quad \psi(x) \begin{cases} x(1-(\frac{x}{c})^2)^2 \\ 0 \end{cases} \quad \omega(x) \begin{cases} (1-(\frac{x}{c})^2)^2 \\ 0 \end{cases} \tag{17}$$

Where the symmetric, positive-definite function with a unique minimum at zero is represented by $\rho(x)$, and it was chosen to be less increasing than square. The influence function, which measures the influence of a datum on the value of the parameter estimate is represented by $\psi(x) = \frac{d(\rho(x))}{dx}$. The weight function is represnted

by $\omega(x) = \frac{\psi(x)}{x}$. The elements of the formula are showed in equation 17. The averaged chronologies were calculated with the "R" software (R Development Core Team, 2018), using the "chron" function under the "dplR" package (Bunn et al., 2018). The method was chosen because the Tukey biweight mean statistics were not affected by outliers and because it allowed enhancing the statistical significance of the tree ring chronologies (Fowler and Boswijk, 2003).

2.6 Comparison between drought and tree growth indeces

As explained by Sanchez-Salguero and colleagues (2020), the climate change sharpened the frequency and the magnitude of the drought events. Drought events had a strong impact on tree growth, however, the trees responses to extreme drought events were challenging to disentangle because the drought events were diversified (Bose et al., 2020). Furthermore, urban trees were affected by multiple factors, which were not caused by climate, rather by human's influences. For instance, the strong drought events were responsible for loss of fitness, because trees did not resist the extreme deficit of water. However, it was also caused by a prolonged drought event, where the tree did not enter in resilience with climatic fluctuation and/or they had not enough time to recover (Zang et al., 2014: Bose et al., 2020).

The analysis of the tree growth responses during drought events in the city of Zurich in the last 40 years was pursued by considering the vegetative SPEI, the duration, frequency and magnitude of drought. The procedure considered the combination of tree ring width index (RWI) and the drought parameters: vegetative SPEI, duration, frequency, severity and intensity of drought (section "Meteorological data" and section "Tree growth parameters"). Therefore, first, the relationship between the RWI for each species with the SPEI and/or intensity of drought was computed. Then the 8 strongest drought events and the previous and following periods were analyzed, by following the guidelines of drought parameters. Consequently, the ring width measurements found in those drought periods were analyzed, wherefore the new ring width based indices were computed, such as the tolerance indexes. In summary, resistance, resilience and recovery to drought were calculated through formulas from the ring width index (RWI) by considering the drought events, the period before and after the drought events detected by the SPEI, the duration, the frequency, the severity and the intensity of drought (Bose et al., 2015: Zang et al., 2014).

2.6.1 Assessment of long-term drought events

To assess whether the trees followed a growth trend in response to the SPEI index, it was calculated an annual SPEI value based on the vegetative period of the trees. The months selected to average the SPEI in an annual value are March, April, May, June, July and August. Therefore, an annual value for the SPEI was computed for the integrated timescale from 1 to 6 and the 12. The second index used, was the intensity of drought, which calculation is explained in chapter "Climatic indexes".

Literature (Bose et al., 2020: Tan et al., 2015: Markonis et al., 2021: Hari et al., 2020) confirmed that the occurrence of drought events was increased in the last 2 decades in both frequency and magnitude concerning

previous ones. A trend was expected for SPEI data in the city of Zurich over the whole period 1981 - 2020. Therefore, the vegetative values of the SPEI and the intensity of drought, integrated over the timescale of 1 to 6 and 12 were used to evaluate the drought trend and the tree growth. The Mann-Kendall test was run for every tree species' ring width index and the vegetative SPEIs and intensity of drought. In this way, it was assessed the long-term relationship between trees growth and SPEI within the vegetative season or intensity of drought (Bose et al., 2020: Tan et al., 2015: Markonis et al., 2021: Hari et al., 2020). The best Mann-Kendall values were used to assess which timescale of SPEI was best suited to describe the tree ring width index for each tree species. Some tree species' ring width indexes did not show relation to any of the 7 vegetative SPEIs. Therefore, they are tested with the Mann - Kendall to the intensity of drought, to assess whether there was a relation not directly connected to the SPEIs. The null and alternative hypothesis will be as follow:
H_0: There is no monotonic trend between the two variables.
H_1: There is a monotonic trend between the two variables.
The Mann-Kendall test was calculated as follows in formula 18, 19 and 20 and the data was interpreted through table 4 (Wang et al., 2020). The first step to calculate the Mann-Kendall was to compute, as in equation 18:

$$S = \sum_{k-1}^{n-1} \sum_{j-k+1}^{1} sgn(x_j - x_k) \tag{18}$$

Where the chronologically ordered data is represented by x and the parametric timing of the observations by k and j.

If the further observations chronologically obtained had a tendency to be larger than the observations made before, they are represented by a positive S. On the contrary, if the observations made subsequently in time had the tendency to be smaller than observations made before, they are represented by a negative S. where g was the number of tied groups and t_p was the number of observations in the p^{th} group. (Pohlert, 2020: Gilbert, 1987).

Where the variance of S was computed, as in equation 19:

$$Var(S) = \frac{1}{18} * \left[n(n-1)(2n+5) - \sum_{p-1}^{g} t_p(t_p-1)(2t_p+5) \right] \tag{19}$$

where the number of tied groups is represented by g and the number of observations in the p^{th} group by t_p (Helsel, 2005).

The Mann-Kendall statistic was then calculated, as in equation 20:

$$Z_{MK} \begin{cases} \frac{S-1}{\sqrt{Var(S)}} \;\; if \;\; S > 0 \\ 0 \;\; if \;\; S = 0 \\ \frac{S+1}{\sqrt{Var(S)}} \;\; if \;\; S < 0 \end{cases} \tag{20}$$

A positive (negative) value of Z_{MK} indicated that the data tended to increase (decrease) with time (the strength of the relationship is showed in table 4).

The best tau values were selected and the corresponding SPEI's and intensity of drought's timescale was addressed to each tree species. For instance, this method allowed assessing whether the tree species showed a relation to short-term or long-term drought events (different SPEIs timescale) over the whole 40 years period.

The Mann-Kendall statistical test was computed with a "R" package "Zyp" (Library "zyp") with a trend-free pre-whitening, in order to avoid autocorrelation (Yue et al., 2002: Bayazit and Önöz, 2007). The correlation matrixes and the chart correlation were calculated in R using the package "PerformanceAnalytics" (library "PerformanceAnalytics") and the package "dplyr" (library "dplyr") (R Development Core Team, 2018).

Table 4: Mann-Kendall statistical test for monotonic function: τ statistic and interpretation

τ coefficient for direct relationship	τ coefficient for indirect relationship	Variable relationship
0.00 to 0.10	-0.00 to -0.10	Trivial
0.11 to 0.29	-0.11 to -0.29	Weak
0.30 to 0.49	-0.30 to -0.49	Moderate
0.50 to 0.99	-0.50 to -0.99	Strong
1.00	-1.00 to -0.10	Perfect

2.6.2 Assessment of annual drought events

This master thesis assessed the drought events considering the SPEI and the intensity of drought calculated through different SPEI timescales (subsection "Assessment of long-term trend"). Drought was defined as a period, where the SPEI's values were at the lowest (below 1) and the intensity of drought was at the highest (above 1) and it was checked through the frequency to avoid biases (Tan et al., 2015). This master thesis considered multiple SPEI timescales, in order to detect and study different time occurrences of drought events. Scientific studies (Chen, et al., 2013: Vicente-Serrano et al., 2010: Nedealcov et al., 2015: Potop et al., 2012: Tan et al., 2015: Li et al., 2012: Wang et al., 2012: Pei et al., 2020) tended to address timescale considered in this thesis as short-term timescale. Nevertheless, this thesis was pursued in a city, where the drought was considered severe, due to multiple stresses affecting the trees. Therefore, drought occurrence was detected by the SPEI and intensity of drought with short timescale: 1, 2, 3 (seasonal resolution); long-timescale: 4, 5, 6 (semester resolution) and annual timescale 12 (annual resolution).

It was researched the 8 driest years according to each vegetative SPEI and intensity with the integration over the 7 timescale (see table 30, 13, 14, 15, 16, 17, 18 and 19 reddish colours). The choice of eight years was mostly dictated by the data and by the fact that it allowed enough data for the statistical analysis.

As explained in section "Assessment of long-term trend", every tree species ring width index was compared to the SPEIs and intensity of drought values. Through the Mann - Kendall statistical test, the highest tau was selected, because it represented the best fit for the monotonic trend. This relation allowed recognizing which were the 8 driest years that best suited the ring width index of the selected tree species. As a matter of fact, the driest years depended upon the timescale of the SPEI and the intensity of the drought. For instance, the 19 tree species did not show the same driest years.

2.6.3 Assessment of the period during the drought events (PDDE)

The 8 driest years were selected, as in equation 21:

$$PDDE = \sum_{i=1}^{8} RWI_{D_{i^{th}}} \tag{21}$$

Where the RWI of a determined tree species during one of the 8 driest years is represented by RWI_{D_i}, while the rank (from 1 to 8) of the driest years by i^{th}.

2.6.4 Assessment of the period before the drought events (PBDE)

Once the drought years were defined, it was selected the periods preceding the drought events. It was selected the 3 years immediately before the drought years, which was detected as explained in section "Assessment of the period during the drought events (PDDE)" (Pretzsch et al., 2013: Bose et al., 2020: Zang et al., 2014). If the 3 years period contained a year, which coincides with a drought year, this year was removed from the analysis. Therefore, it was considered two years as a period preceding the drought events. This exceptional calculation allowed to exclude biased non - drought periods. As a matter of fact, drought values did not mix with non - drought values. The formula for the calculation of the periods before the drought events is displayed in equation 22:

$$PBDE = \sum_{i=1}^{8} \left(\sum_{j=1}^{3} RWI_{D_{i^{th},\ -j^{th}}} \right) \tag{22}$$

Where the RWI of a specific tree species during the driest years (from 1 to 8) is represented by $RWI_{D_{i^{th}}}$, while the rank of the years before or after the direst years (from 1 to 3) by j^{th}.

2.6.5 Assessment of the period after the drought events (PADE)

The same methodology of section "Assessment of period before the drought (PBDE)" was applied to detect the periods following the drought events. Differently from the periods preceding the drought events, the periods following the drought events considered 3 years after the occurrence of drought (Bose et al., 2020: Zang et al., 2014). In the case of coincidence between a drought year and a post-drought year, it was acted the same as section "Assessment of the period before the drought (PBDE)". The formula for the calculation of the periods during the drought events is displayed in equation 23:

$$PADE = \sum_{i=1}^{8} \left(\sum_{j=1}^{3} RWI_{D_{i^{th},\ j^{th}}} \right) \tag{23}$$

Where the RWI of a specific tree species during the driest years (from 1 to 8) is represented by $RWI_{D_{ith}}$, while the rank of the years before or after the direst years (from 1 to 3) by j^{th}.

2.6.6 Ring width indices and drought events

The ring width indices were considered in the analysis to detect the tree growth during drought events (PDDE), the 3 years periods preceding (PBDE) and following the drought events (PADE). The RWIs corresponding to the 8 drought events years were selected to have the tree growth during drought. Similarly, it was selected RWIs values in the other 2 periods, which corresponded to the PBDE and the PADE. Ideally, the drought years were dependent on the 8 driest years above listed, whereas the PBDE and PADE used 24 values each other. Nevertheless, there were some RWI values, which were referenced both within the PBDE and the PADE. Furthermore, some RWI data for the non - drought events periods were not available. For instance, if 2020 was recognized by the SPEI as a drought year, it was not possible to select the PADE.

2.7 Tolerance indices: resistance, resilience and recovery

To analyse the trees growth during drought events (PDDE), before the drought events (PBDE) and following the drought events (PADE), the 3 tolerance indexes: resistance, resilience and recovery were built, following the instructions of Lloret and colleagues (2011). The resistance (equation 24) was a quantitative measure between the annual growth during a drought year and the mean growth during the previous 3 years before drought. It assumed the capability of the trees to withstand the drought events and maintain a growth pattern under the pressure of drought (Bose et al., 2020). The recovery (equation 25) represented the quantitative measure between the mean growth during the 3 years following the drought events and the growth during the drought events. It considered the ability of the trees to compensate for the growth stress during drought events and carry on the growth pattern in the years following the traumatic events (Zang et al., 2014). In the end, resilience (equation 26) represented the quantitative measure between the mean tree's growth during the periods following the drought events (3 years interval) and the growth during the periods preceding the drought events. It assumed the capability of the trees to achieve the growth pattern as close as possible to the periods before the occurrence of the drought events (Fang et al., 2021). The formulas for the calculation are displayed:

$$Resistence = \frac{RWI_{PDDE}}{RWI_{PBDE}} \tag{24}$$

$$Recovery = \frac{RWI_{PADE}}{RWI_{PDDE}} \tag{25}$$

$$Resilience = \frac{RWI_{PADE}}{RWI_{PBDE}} \tag{26}$$

Where the ring width index is represented by RWI, the year of the drought by PDDE, the 3 years before the drought by PBDE and the 3 years periods following the drought by PADE.

The 3 tolerance indexes were constructed by a division between the tree growth during the specific periods. Values for resistance, resilience and recovery were constructed for each tree species, for each drought year (8 in total). This thesis tried to compare the temporal specific growth pattern. Therefore, it did consider the tolerance indexes calculated at an annual resolution because it was hard to be analysed. Thereafter, the average was computed within the indexes in order to get 2 values: the first for the period 1981-2000 and the second for the period 2001-2020.

Finally, the tolerance indexes resistance, resilience and recovery were compared within the same species (2 time periods, 1981-2000 and 2001-2020) and among the tree species. This latter step allowed this thesis to discover some relationship between inter-and intra-specific tree growth affected by drought events occurrence (Lloret et al., 2011). The tree species were in the end classified depending on their ability to resist the drought, recover from the drought and enter in resilience in the period following the drought.

2.8 Statistical analysis

The objectives of this master thesis were to discover which tree species had the best growth response to the drought, in order to allow the selection of the tree species, which best resisted, entered in resilience and recovered from the drought events.

The first statistical test comprehended the calculation of the tau value with the Mann - Kendall statistical test to search for monotonic trends between the vegetative SPEI and/or the intensity of drought and the ring width indexes. To allow an easier calculation through the R software, a correlation matrix was created (library "zyp", library "dplyr" and library "PerformanceAnalytics") (Kendall et al., 1945). The tau values, which represented the degree of the relation between the meteorological indexes and the tree ring width index, were modelled in a chart diagram to have a look at the relation (Becker et al., 1988). The tau values of the Mann - Kendall allowed the detection of the driest years depending on the amount of correlation with the timescale of the vegetative SPEI and/or the intensity of drought, and the ring width indexes, for different tree species (Bose et al., 2020: R Development Core Team, 2018). The Mann-Kendall statistical test for monotonic trend indicated the monotonic relationship among two dependent datasets and it was widely used in meteorology to test time series (Blain, 2013: Tripathi et al., 2014: Zhang et al., 2006: Kumar et al., 2009). The Mann - Kendall rank correlation coefficient consisted of a statistic measure to test the ordinal relationship between two variables (Tripathi et al., 2014): the increasing trend was characterized by a positive value, while decreasing trend was characterized by negative values (Sicard et al.,2010) and it ranged from $+1$ (strong positive dependency, to -1 (strong negative dependency) (Pohlert, 2020: Gilbert, 1987). The strength of the relationship and the interpretation based on the τ value are displayed in table 4.

After the driest years were selected for each tree species' ring width index, the 3 years periods PDDE, PBDE and PADE are selected. Ring width index data corresponding to one of these 3 classes (PDDE, PBDE and PADE) were used to model tree growth through box plots. It was modelled as a box plot for each tree species.

The dataset was checked for the presence of outliers because they affected strongly the further statistical analysis. Therefore, through the R software, it was checked for outliers and these data were controlled in the samples. When some uncertainties arised, the outliers' data was removed from the analysis (Osborne and Overbay, 2004). For instance, uncertainties originated from a false ring, unclear wood surface, inability to have a comparison within the same tree, and so on (Cook and Kairiukstis, 1990). The outliers were discovered in R through the function *boxplot()* and *mtext()* (R Development Core Team, 2018) and they were further tested with the Grubbs' statistical test (Grubbs, 1969: Urvoy and Autrusseau, 2014) or Dixon's statistical test (Rorabacher, 1991: Verma and Quiroz-Ruiz, 2006: Verma and Suarez, 2014). It was used Grubbs' statistical test to test whether a value was an outlier when the dataset showed more than 25 measurements, respectively Dixon's statistical test for a larger number of measurement within a dataset.

The 3 categories were tested with the analysis of the variance (ANOVA statistical test). The ANOVA test allowed comparing the 3 categories by assessing the internal variability to these groups with the variability among the categories (Kim, 2017: Sawyer, 2009). A one-way ANOVA statistical test (Ostertagova and Ostertag, 2013) was pursued on the 3 categories of data: tree growth during drought events, in the 3 years periods before and after them. If the analysis of the variance found significant variance, the Tukey's honest significance test (Tukey HSD statistical test) was used (Mohapatra and Mohapatra, 2021). The Tukey's honest significance test allowed multiple comparisons between the means which were significantly different among the 3 categories. The statistical test was calculated in R through the package "car" (library "car) (Barnette and McLean, 1998: R Development Core Team, 2018). These statistical tests gave indications about the number of differences that different tree species showed in disparate periods: PDDE, PBDE and PADE. Significant differences in tree growth during these 3 periods (PDDE, PBDE and PADE) allowed inferences about the growth pattern of the tree facing the drought events. The ANOVA test assumes that the variance was homogeneous, and that the data were normally distributed. Therefore, before the ANOVA statistical test, a Levene's test for the homogeneity of the variance was run in R software (Gastwirth et al., 2010: R Development Core Team, 2018). Furthermore, to test the normal distribution, it was run a Shapiro - Wilk test for the normality (Hanusz et al., 2016: R Development Core Team, 2018). If both tests confirmed the normal distribution and the homogeneity of the variance, the analysis of the variance was run (ANOVA). Otherwise, the data were tested with the Kruskal Wallis test, a non-parametric statistical test for testing whether samples originate from the same distribution (Ostertagova et al., 2014: Vargha and Delaney, 1998).

After the statistical comparison within the same tree species, the tolerance indexes resistance, resilience and recovery were calculated over 2 time periods (1981-2000 and 2001-2020) (Lloret et al., 2011). The resistance, resilience and recovery index were compared within and among the tree species in order to assess which ones had a suited growth response during the driest years, and or which ones best recovered from the drought events. The principal component analysis was used, to test statistically the number of significant differences between the tree species' growth patterns, indexed by the 3 tolerance indexes: resistance, resilience and recovery over the 2 time periods (Jolliffe and Cadima, 2016: Holand, 2019). A cluster analysis with the k-means method (Morisette and Chartier, 2013: Li and Wu, 2012) was then pursued to have statistically significant results about the similarities between tree species' tolerance indexes (Thrun, 2018: Kaufman and Rousseeuw, 1990:

Kassambara, 2017). It was tested with the silhouette cluster method to interpret and validate the consistency among the clustered data (Kaoungku et al., 2018). The silhouette method measured the number of similarities between the tree species and the classes, by comparing them to the other classes (or clusters) (Mamat et al., 2018). The silhouette statistic allowed selecting for the most suited number of clusters to classify the tree species depending on their resistance, resilience and recovery values. Thereafter, it was created a dendrogram to display the tree species classified within the clusters (MacEachren et al., 2010: Restrepo and Mesa, 2008). The cluster analysis was pursued in R using the "ward" statistical method. These calculations were done in R under the package "factoextra" throughout the "hclust()" function (R Development Core Team, 2018).

3 Results

3.1 Driest years

Table 5: The 8 driest years detected by the SPEI and intensity of drought. I = intensity of drought, while the number represents the timescale used to compute the SPEI.

$SPEI_1$	$SPEI_2$	$SPEI_3$	$SPEI_4$	$SPEI_5$	$SPEI_6$	$SPEI_{12}$	I_{SPEI1}	I_{SPEI2}	I_{SPEI3}	I_{SPEI4}	I_{SPEI5}	I_{SPEI6}	I_{SPEI12}
1985	1992	1992	1984	1992	1992	1984	1981	1994	1983	1988	1983	1983	2003
1992	1998	1998	1992	1997	1997	1992	1983	1995	1987	1993	1990	1990	2004
1997	2003	2003	1998	1998	1998	1997	1992	1999	1990	2003	1993	2003	2011
2003	2011	2011	2003	2003	2003	2011	1996	2003	1991	2005	1998	2008	2016
2011	2015	2017	2011	2011	2011	2017	2006	2011	2005	2006	2003	2011	2017
2015	2017	2018	2017	2017	2017	2018	2012	2012	2012	2015	2011	2015	2018
2018	2018	2019	2018	2018	2018	2019	2015	2015	2015	2016	2015	2016	2019
2020	2020	2020	2020	2020	2020	2020	2018	2018	2018	2018	2018	2018	2020

The research of the driest years during the period 1981-2020 is computed by considering SPEI values and the intensity of drought values. SPEI are averaged over the vegetative period, whereas the intensity of drought is calculated as explained in section "Climatic indexes". Despite the intensity of drought uses SPEI values for the calculation, the resulting drought values detected by the intensity of drought are different from the ones detected by the SPEI. As a matter of fact, it is noticeable from table 6 that the vegetative SPEI tend to be more homogeneous between the timescales. For instance, the selected drought years are similar among the 7 timescales. On the other hand, the intensity of drought shows more heterogeneity. As a matter of fact, the 8 driest years are much more dispersed over the whole 1981-2020 period. This is visible by the following tables, table 6 and table 5, which show the respective vegetative SPEI and intensity value for each SPEI's timescale, and the driest years selected. The reddish colours indicate the presence of drought events at an annual resolution for both vegetative SPEI and the intensity of drought. Furthermore, the vegetative SPEI values tend to variate less among the 7 timescales concerning the intensity of drought, as a matter of fact, the driest years are retrieved by the vegetative SPEI, independently of the timescale. On the other hand, intensity focuses on the drought years by considering the duration of the drought over the year and remove the non - drought years (they get the value of 0). The driest years selected by the vegetative SPEI and intensity of

drought are displayed in table 5. As it is noticeable, the 8 driest years differ depending on the choice of the vegetative SPEI timescale, which suggest a different drought computation. Vegetative SPEI and intensity of drought at short timescale (1, 2 and 3) detect best the short-term drought events, while the other time scale is best suited for the long-term drought (timescale of 4, 5 and 6) or the annual resolution (timescale of 12). Nevertheless, some drought years occur independently of the time scale: 1992, 1998, 2003, 2011, 2017, 2018 and 2020.

Table 6: SPEI averaged for the vegetative period (March, April, May, June, July and August) for each SPEI's timescale over the 1981-2020 period. Intensity of drought for each SPEI's timescale. The intensity of drought have been turned to negative values, to allow a proper comparison with the seasonal SPEI. In reddish colours are showed SPEI values considered dry, while in yellowish colors are represented the values around the 0 and above. In greenish colours are represented the non drought events years. Colours are linearly scaled to enhance the contrast among drought events and non drought events.

year	$SPEI_1$	$SPEI_2$	$SPEI_3$	$SPEI_4$	$SPEI_5$	$SPEI_6$	$SPEI_{12}$	I_{SPEI_1}	I_{SPEI_2}	I_{SPEI_3}	I_{SPEI_4}	I_{SPEI_5}	$ISPEI_6$	$I_{SPEI_{12}}$
1981	0.17	0.01	-0.09	-0.27	-0.35	-0.35	-0.11	-1.31	0	-0.57	0	-0.55	0	0
1982	-0.03	-0.05	-0.03	0.15	0.16	0.35	1.51	-0.91	-0.75	-0.68	-0.76	0	0	0
1983	-0.19	-0.29	-0.36	-0.24	-0.1	0.04	0.42	-1.25	-0.76	-1.35	-1.06	-1.21	-1.19	0
1984	-0.13	-0.25	-0.35	-0.46	-0.43	-0.49	-1.11	0	0	-0.65	-0.77	-0.92	-0.59	-0.87
1985	-0.27	-0.25	-0.24	-0.2	-0.2	-0.22	-0.04	-1.11	-1.04	-0.94	-0.94	-0.94	-0.9	-0.95
1986	0.43	0.69	0.92	1.09	1.36	1.38	0.57	-0.86	-0.87	-0.7	-0.59	0	0	0
1987	0.65	0.85	0.98	1.14	1.02	0.87	0.66	-0.67	0	-1.44	0	-0.69	-0.55	0
1988	0.64	0.95	1.11	1.17	1.21	1.12	1.23	0	0	0	-1.29	-0.99	0	0
1989	-0.16	-0.14	-0.26	-0.35	-0.44	-0.36	0.15	-0.95	-0.58	-0.74	0	0	0	0
1990	-0.2	-0.06	-0.01	0.06	-0.1	-0.12	-0.39	-1.03	-0.89	-1.53	-0.56	-1.18	-1.32	0
1991	-0.19	-0.32	-0.27	-0.21	-0.11	-0.02	0.23	-0.48	-1.08	-1.46	-0.89	-0.94	-0.79	0
1992	-0.28	-0.38	-0.51	-0.62	-0.62	-0.64	-1.14	-1.74	-0.77	-0.73	-0.61	-0.74	-0.81	-0.95
1993	0.19	0.19	0.17	-0.06	-0.01	0.15	0.31	-0.65	-0.88	-1.04	-1.09	-1.14	-0.79	0
1994	0.14	0.05	-0.01	0.2	0.4	0.48	0.94	-1.22	-1.32	-0.87	-0.54	-0.52	-0.77	0
1995	0.6	0.78	0.95	1.25	1.42	1.44	1.13	-1.08	-1.56	-0.69	0	0	0	0
1996	-0.02	-0.06	-0.22	-0.26	-0.28	-0.52	-0.48	-1.59	-0.69	-0.66	-0.66	-0.69	-0.72	0
1997	-0.42	-0.27	-0.32	-0.44	-0.58	-0.56	-0.26	-0.75	-0.76	-0.89	-1.03	-0.78	-0.84	-0.4
1998	-0.23	-0.59	-0.74	-0.71	-0.81	-0.8	-0.92	-0.92	-1	-0.74	-0.9	-1.17	-0.75	-0.82
1999	0.58	0.89	1.12	1.29	1.47	1.55	1.4	0	-1.21	0	0	0	0	0
2000	0.2	0.32	0.34	0.32	0.44	0.49	0.98	-0.56	-0.78	-0.65	0	0	0	0
2001	0.94	1.17	1.45	1.61	1.68	1.73	1.5	0	0	0	0	0	0	0
2002	0.2	0.22	0.03	-0.11	-0.09	-0.17	0.57	0	-0.56	-0.68	-0.77	0	0	0
2003	-1.04	-1.35	-1.47	-1.66	-1.5	-1.3	-0.26	-1.01	-1.12	-1.24	-1.23	-1.47	-1.48	-1.18
2004	-0.12	-0.23	0	0.06	0.05	0.11	-0.45	-1.09	-0.9	0	-0.66	-0.5	0	-1.21
2005	0.05	0.19	0.05	-0.11	-0.35	-0.38	-0.74	-0.64	-1.04	-1.55	-1.3	-0.98	-0.98	-0.79
2006	0.47	0.63	0.47	0.59	0.79	0.92	0.49	-1.64	-1.02	-1.33	-1.48	-1.03	-0.93	0
2007	0.28	0.41	0.29	0.05	-0.21	-0.5	-0.71	-0.75	-1.01	-0.88	-0.96	-1.02	-0.95	-0.97
2008	0.41	0.34	0.28	0.28	0.28	0.27	0.36	-1.03	-0.96	-1.14	-0.98	-1.01	-1.35	0
2009	-0.17	-0.16	-0.14	-0.23	-0.42	-0.43	0.11	-0.79	-0.76	-0.65	-0.37	0	-0.59	-0.53
2010	0.11	0.03	-0.07	-0.08	-0.02	-0.1	-0.34	-0.54	0	0	-0.48	0	0	0
2011	-0.64	-1.02	-1.07	-1.3	-1.47	-1.63	-1.23	-1.15	-1.73	-1.19	-1.08	-1.07	-1.25	-1.16
2012	-0.02	-0.15	-0.13	-0.05	-0.31	-0.48	-0.76	-1.32	-1.33	-1.53	-0.85	-0.69	-0.8	-1.07
2013	0.01	-0.02	-0.03	0.2	0.46	0.6	1.27	-0.86	-1	-0.69	-0.86	0	0	0
2014	-0.12	-0.08	-0.11	-0.31	-0.38	-0.35	-0.42	-0.45	-0.56	-0.62	-0.71	-0.67	-0.53	-0.48
2015	-0.27	-0.33	-0.27	-0.2	-0.13	-0.11	-0.2	-1.26	-1.51	-1.68	-1.62	-1.48	-1.32	-1.1
2016	0.09	0.37	0.8	0.93	0.88	0.7	-0.54	-0.96	-0.98	-0.96	-1.16	-0.8	-1.25	-1.22
2017	-0.24	-0.47	-0.53	-0.81	-0.92	-0.92	-0.93	-1.16	-0.56	-0.75	-0.77	-0.83	-1	-1.27
2018	-0.73	-1.09	-1.22	-1.2	-1.09	-1.09	-1.22	-1.31	-1.16	-1.33	-1.4	-1.4	-1.43	-1.24
2019	-0.13	-0.31	-0.48	-0.37	-0.35	-0.47	-1.36	0	-0.5	0	0	0	0	-1.27
2020	-0.71	-0.73	-0.92	-1.06	-1.26	-1.27	-1.25	-0.92	-0.89	-0.9	-1.03	-1.06	-1.1	-1.31

3.2 long-term relation between ring width indexes and the drought events

The below figure (figure 2 or figure 11, 12, 13, 14, 15, 16, 17 and 18, 19, 20, 21, 22, 23, 24 in the appendix, for the whole calculation) represents, on one hand, the Mann - Kendall tau values within a correlation matrix. In the diagonal are represented the tree species and the 7 best vegetative SPEI timescales ($SPEI_1$, $SPEI_2$, $SPEI_3$, $SPEI_4$, $SPEI_5$, $SPEI_6$, $SPEI_{12}$). On the other hand it represents the intensity of drought values, which are best correlated to the ring width indexes of certain tree species. Under the diagonal (bottom right region) there are the graphs of the regressions for all the correlations calculated. This correlation matrix shows the similarities between tree species and SPEI, but it also shows the similarities between the SPEI and the similarities between the tree species. The upper side (upper left region) shows the Mann - Kendall tau value with the confidence interval for the p-value, represented by the red asterisks. The table shows the regression fitted to a linear function.

As it is visible from the upper right side of the correlation matrix (figure 2), SPEI values with different timescales have a high degree of correlation (visible by the tau value for the Mann - Kendall statistical test and the significance or p-value represented by the red asterisks). As a matter of fact, as explained in the previous chapter, SPEI, which is integrated over different timescale, tends to discriminate similar drought years over the whole 1981-2020 periods.

The correlation matrix also shows the correlation between the tree species' ring width indexes, which can be indicative of a similar growth pattern between the trees species. The high tau value of the Mann - Kendall statistical test between tree species is indicative of a similar tree growth pattern, which suggests a similar responses to climatic drivers.

In general, the correlation matrix is used to assess whether tree species follow the climatic indexes SPEI (and intensity of drought) and, which SPEI's timescale would be best suited to describe the tree species' ring width indexes.

Four tree species do not show any similarities to SPEI. The tree species analyzed are *Acer platanoides and rufinerve*, *Aesculus hippocastanum*, *Prunus umineko* and *Platanus x hispanica*. On one hand, *Aesculus hippocastanum* and *Platanus x hispanica* is limited by the amount of data, as a matter of fact, both the tree species are relatively young, and they do not allow a proper comparison over a reliable period. On the other hand, *Acer platanoides and rufinerve* and *Prunus umineko* show enough data for the Mann - Kendall test statistic, however, it is found no monotonic trend between the tree species' ring width indexes and the SPEI. They are tested with the Mann - Kendall test statistic for monotonic trends with the intensity of drought. *Acer platanoides and rufinerve* shows similarities to intensity of drought calculated with short-term SPEI, while *Prunus umineko* shows high tau values for intensity of drought with short-term and annual SPEI's timescale.

Fraxinus excelsior on one hand, shows similarities to SPEI calculated with the timescale of 6, on the other hand, it does not show similarities with both other SPEI's long-term timescale and short-term timescale. *Pyrus communis* does show similarities with both short-term and long-term SPEI's timescale, however, no relationship is found for specific SPEI's timescale of 1 and 12 (annual).

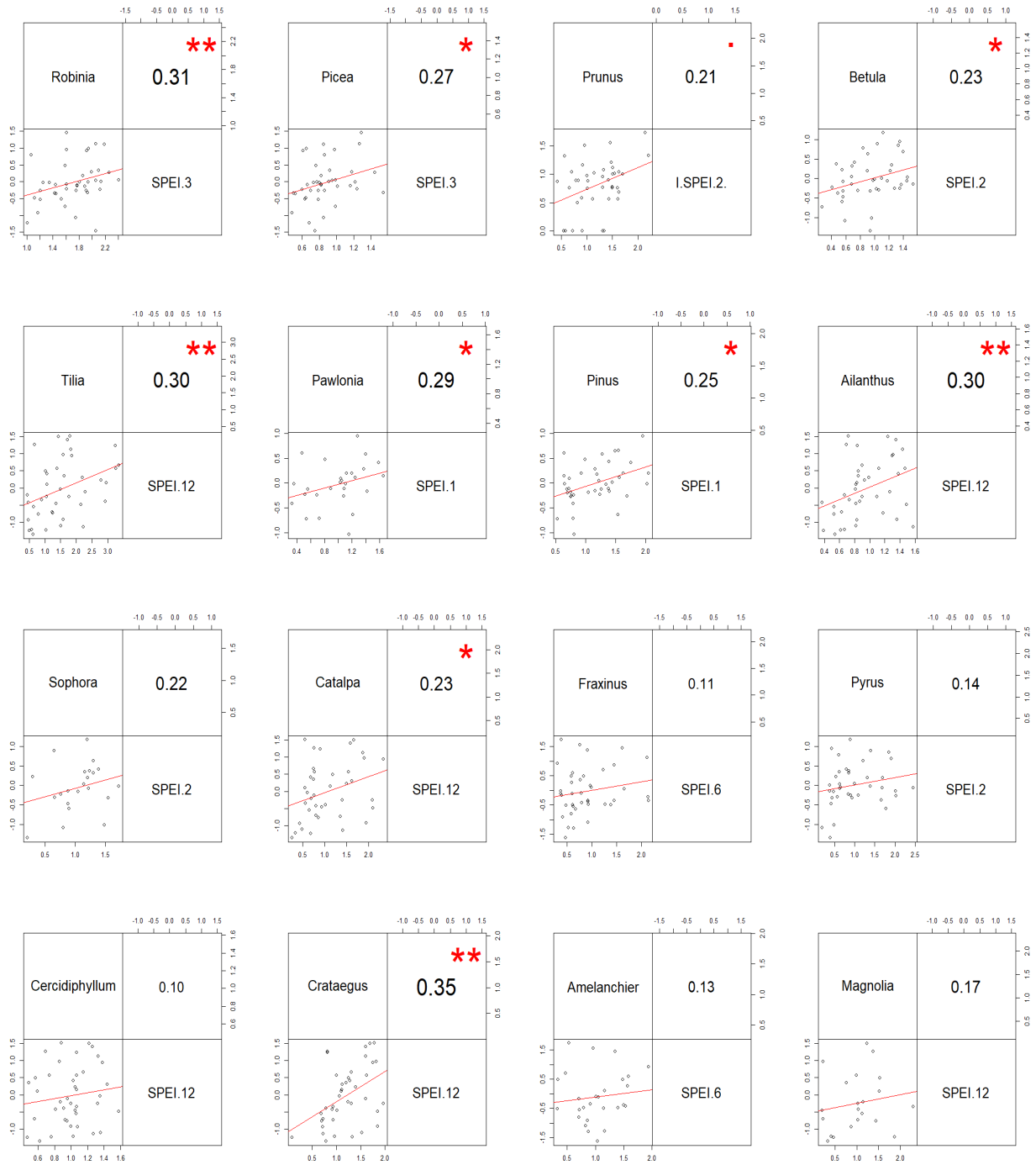

Figure 2: Correlation matrix between trees species ring width indexes and the best correlated averaged SPEIs or intensity of drought with the specific timescale (number). In the diagonal from bottom left to top right there are the respective tree species and SPEIs or intensity of drought with the timescale. In the left side there are the Mann-Kendall τ values with the respective p-values (red asterisks) p-values (0.001, 0.01, 0.05, 0.1, 1) <=> symbols("***", "**", "*", ".", "). In the right side there are the graphs with the linear regression fit to display graphically the relation between tree species and SPEIs.

Picea omorika shows similarities to short-term SPEI's timescale. The Mann - Kendall tau values range from 0.25 to 0.30 with the confidence intervals (p-values) smaller than 0.05.

Crataegus levigata and lavellei, *Cercidiphyllum japonicum*, *Magnolia kobus* and *Amelanchier lamarckii* shows similarities to long-term SPEI's timescale. The Mann - Kendall statistical test values range from 0.15 to 0.35 with the confidence intervals (p-values) smaller than 0.05.

All the other tree species, *Robinia pseudoacacia*, *Betula pendula*, *Catalpa bignonioides*, *Sophora japonica*, *Tilia europea*, *Paulownia tormentosa*, *Ailanthus altissima* and *Pinus sylvestris* shows the presence of a monotonic trend with all the SPEI's timescale. Mann - Kendall tau values range from 0.15 to 0.35 with confidence intervals below the 0.05 (p-values).

In general, 8 out of 17 species, removing *Aesculus hippocastanum* and *Platanus x hispanica* from the analysis, because they did not show enough data, show the presence of a weak monotonic trend with the SPEI's timescale at short-term, long-term and annual. Such results, suggest that tree species' ring width indexes can be partly described by the climatic variation over the 1981-2020 period within the city. the growth of *Robinia pseudoacacia*, *Betula pendula*, *Catalpa bignonioides*, *Sophora japonica*, *Tilia europea*, *Paulownia tormentosa*, *Ailanthus altissima* and *Pinus sylvestris* shows weak response to drought indexes regardless of the timescale of the SPEI. This result suggests that such trees are sensible to precipitation and temperature pattern change within the city.

On one hand, *Picea omorika* shows the response to short-term SPEI's timescale. This latter suggests that *Picea omorika* growth is sensible to the strongest drought events, which lasted for few months during a year. On the other hand, *Crataegus levigata and lavellei*, *Cercidiphyllum japonicum*, *Magnolia kobus* and *Amelanchier lamarckii* show sensitivity to long period of precipitation and temperature anomalies.

Specifically, *Robinia pseudoacacia* shows the highest Mann - Kendall tau value of 0.31 for SPEI with a timescale of 3 ($p - value < 0.01$). *Picea omorika* shows the highest Mann - Kendall tau value of 0.27 for SPEI with a timescale of 3 ($p - value < 0.05$). *Prunus umineko* shows the highest Mann - Kendall tau value of 0.37 for intensity of drought with a SPEI with a timescale of 2 ($p - value < 0.01$). *Betula pendula* shows the highest Mann - Kendall tau value of 0.23 for SPEI with a timescale of 3 ($p - value < 0.05$). *Tilia europea* shows the highest Mann - Kendall tau value of 0.3 for SPEI with a timescale of 12 ($p - value < 0.01$). *Paulownia tormentosa* shows the highest Mann - Kendall tau value of 0.29 for SPEI with a timescale of 1 ($p - value < 0.05$). *Pinus sylvestris* shows the highest Mann - Kendall tau value of 0.25 for SPEI with a timescale of 1 ($p - value < 0.05$). *Ailanthus altissima* shows the highest Mann - Kendall tau value of 0.3 for SPEI with a timescale of 12 ($p - value < 0.01$). *Sophora japonica* shows the highest Mann - Kendall tau value of 0.22 for SPEI with a timescale of 2 ($p - value > 0.05$, the trees are younger than 40 years). *Catalpa bignonioides* shows the highest Mann - Kendall tau value of 0.23 for SPEI with a timescale of 12 ($p - value < 0.05$). *Fraxinus excelsior* shows the highest Mann - Kendall tau value of 0.11 for SPEI with a timescale of 6 ($p - value > 0.05$, only one sample for comparison). *Pyrus communis* shows the highest Mann - Kendall tau value of 0.16 for SPEI with a timescale of 3 and 6 ($p - value > 0.05$, only one sample for comparison). *Cercidiphyllum japonicum* shows the highest Mann - Kendall tau value of 0.13 for SPEI with a timescale of 12 ($p - value > 0.05$, only

one sample for comparison). *Acer platanoides and rufinerve* shows the highest Mann - Kendall tau value of 0.22 for intensity of drought with a SPEI with a timescale of 2 ($p - value < 0.05$). *Crataegus levigata and lavellei* shows the highest Mann - Kendall tau value of 0.35 for SPEI with a timescale of 12 ($p - value < 0.01$). *Catalpa bignonioides* shows the highest Mann - Kendall tau value of 0.23 for SPEI with a timescale of 12 ($p - value < 0.05$). *Amelanchier lamarckii* shows the highest Mann - Kendall tau value of 0.23 for SPEI with a timescale of 6 ($p - value > 0.05$, four samples were damaged by a illness not directly connected to the drought). *Magnolia kobus* shows the highest Mann - Kendall tau value of 0.17 for SPEI with a timescale of 12 ($p - value > 0.05$, the trees are younger than 40 years). *Aesculus hippocastanum* and *Platanus x hispanica* do not have enough data to allow a proper correlation matrix calculation.

Table 7: Relationship between drought events and tree species' RWI. Short term drought: SPEI with a timescale of 1, 2 and 3. Long term drought: SPEI with a timescale of 4, 5 and 6. Annual drought: SPEI with a timescale of 12. Values are based on Mann - Kendall statistics for vegetative SPEI and intensity of drought. Values are addressed with strong, moderate, weak and no. Values are not taken from table 4, but they are adjusted for the simplification.

Tree species' RWI	Short term drought	Long term drought	Annual drought
Robinia pseudoacacia	strong	moderate	moderate
Picea omorika	strong	weak	no
Prunus umineko	no	weak	no
Betula pendula	moderate	moderate	moderate
Tilia europea	strong	moderate	strong
Paulownia tormentosa	strong	moderate	strong
Pinus sylvestris	moderate	weak	moderate
Ailanthus altissima	weak	weak	strong
Sophora japonica	weak	moderate	weak
Catalpa bignonioides	moderate	weak	moderate
Fraxinus excelsior	no	weak	no
Pyrus communis	weak	weak	no
Cercidiphyllum japonicum	no	weak	weak
Acer platanoides and rufinerve	no	no	no
Crataegus levigata and lavellei	weak	weak	strong
Amelanchier lamarckii	weak	weak	no
Magnolia kobus	weak	weak	weak
Platanus x hispanica	no enough data	no enough data	no enough data
Aesculus hippocastanum	no enough data	no enough data	no enough data

3.3 Ring width index and the most severe drought events

Figure 3 shows the tree ring width index in the 3 periods: PDDE, PBDE and PADE respectively. The axis range is kept constant to all the boxplots, therefore, it is possible to observe within a tree species and among the tree species. In general, as it is observable by table 8 and 9, the F - value is significative for 14 tree species out of 19. As a matter of fact, *Prunus umineko*, *Fraxinus excelsior*, *Amelanchier lamarckii*, *Platanus hispanica* and *Aesculus hippocastanum* do not show a significant p-value for the F - statistics. In particular, *Platanus hispanica* and *Aesculus hippocastanum* are not included in the analysis, because they do not have enough data for comparison.

Sophora japonica is the tree species with the highest F - value, which means the it has the highest variation among the 3 categories: PDDE, PBDE and PADE, with a significant p-value. It is followed by *Picea omorika*, which shows high variability among the categories, with a significant p-value. *Tilia europea*, *Betula pendula*, *Robinia pseudoacacia*, *Pyrus communis*, *Magnolia kobus*, *Paulownia tormentosa*, *Catalpa bignonioides*, *Crataegus levigata and lavellei*, *Cercidiphyllum japonicum*, *Acer platanoides and rufinerve*, *Pinus sylvestris* and *Ailanthus altissima* tree species have a F - statistics which ranges from 3 to 4 and they all show a significant p-value. That means these tree species show variability among the 3 categories and the difference is significant. Based on the F - statistics, it is possible to infer that 14 out of 19 tree species show differences in tree ring growth depending on the selection of the period: Drought years, the 3 years period before and after the drought events.

Looking at the t-value for no difference between the means, it is possible to infer differences in tree growth between drought years (PDDE) and non - drought years (PBDE and PADE). All the tree species show significant p-value for the differences between growth during drought and non - drought, except for *Pyrus communis*. In general, the t-value for the comparison between drought and non - drought years are at the highest, which suggests the highest variation in tree growth patterns during drought events. Furthermore, the t-value indicates that some tree species show higher differences in tree ring growth in PDDE with respect to PBDE and PADE, in comparison to other tree species. These species are listed in decreasing t-value: *Robinia pseudoacacia*, *Prunus umineko*, *Picea omorika*, *Cercidiphyllum japonicum*, *Ailanthus altissima*, *Amelanchier lamarckii*, *Sophora japonica*, *Paulownia tormentosa*, *Crataegus levigata and lavellei*, *Betula pendula*, *Acer platanoides and rufinerve*, *Fraxinus excelsior*, *Pinus sylvestris*, *Catalpa bignonioides*, *Tilia europea* and *Magnolia kobus*. Therefore, it is possible to infer that *Robinia pseudoacacia*, *Prunus umineko*, *Picea omorika* and *Cercidiphyllum japonicum* are the 4 tree species with the highest variability in growth during PDDE compared to PBDE and PADE.

Figure 3: Displayed the ring width index in the y-axis, for the selected tree species, depending on the selected drought periods (x-axis). The drought periods are divided in 3 groups. The ring width index during the drought years, or the tree species growth responses to drought events. The ring width index before the drought events, or the 3 years periods before the drought years (2 if the third year coincide with another drought year). The ring width index after the drought periods, or the 3 years average after the drought years (2 if the third year coincide with another drought year). Drought years are selected with the highest Mann - Kendall statistical value for each tree species' ring width index with the SPEI or intensity of drought.

Looking at the t-value for the PBDE, it is possible to infer the differences in tree growth between the PBDE compared to PDDE and PADE. As it is visible from table 8 and 9, there are fewer tree species with significant p-value with respect to PDDE. As a matter of fact, *Prunus umineko*, *Betula pendula*, *Paulownia tormentosa*, *Ailanthus altissima*, *Fraxinus excelsior*, *Acer platanoides and rufinerve*, *Amelanchier lamarckii* and *Magnolia kobus* do not have a significant p-value. On one hand, this would allow inference about differences in tree growth between the PBDE and the others 2 categories. On the other hand, the other tree species showed a significant p-value, which indicates that differences in tree growth between the PBDE compared to PDDE and PADE. However, the t-values are lower with respect to tree growth during PDDE compared with the other 2 categories. This latter result indicates that, in general, the difference between drought events and non - drought events periods (PDDE versus PBDE and PADE) is stronger with respect than the mixed categories (e.g. PBDE compared to PDDE and PADE). The tree species are listed by decreasing t-values: *Sophora japonica*, *Robinia pseudoacacia*, *Cercidiphyllum japonicum*, *Catalpa bignonioides*, *Picea omorika*, *Pyrus communis*, *Tilia europea*, *Crataegus levigata and lavellei* and *Pinus sylvestris*.

Except for *Amelanchier lamarckii*, all the other 16 tree species show a significant p-value for the t-test statistic, which means differences in tree growth between the PADE in comparison to the PDDE and PBDE. All the tree species show t-values between 2 and 3, except for *Sophora japonica* and *Catalpa bignonioides*, which show higher variation in tree growth during the PADE with respect than growth during PDDE and PBDE.

To sum up, on one side, *Robinia pseudoacacia*, *Prunus umineko*, *Picea omorika* and *Cercidiphyllum japonicum* seem to be the tree species which growth is strongly affected by the PDDE in comparison to the growth during PBDE and PADE. On the other side, *Catalpa bignonioides*, *Tilia europea* and *Magnolia kobus* seem to have a growth pattern during the PDDE with fewer differences in comparison to the PBDE and PADE.

Sophora japonica, *Robinia pseudoacacia*, *Cercidiphyllum japonicum*, *Catalpa bignonioides*, *Picea omorika*, *Pyrus communis*, *Tilia europea*, *Crataegus levigata and lavellei* and *Pinus sylvestris* seem to be the tree species, which growth pattern has been stronger affected by the PDDE and the PADE, with respect than the growth in the PBDE.

Sophora japonica and *Catalpa bignonioides* seem to be the tree species, which have significant differences in tree growth during PADE with respect than the PDDE and PBDE.

Table 8: Table statistic for ANOVA (Kruskall - Wallis) statistical test. Comparison among ring width index of each tree species during the 3 different drought periods: drought events, after drought events and before drought events. First 10 tree species.

Robinia	Estimate	std. E.	t-value	p-value	Residuals std. E.	Adj. R^2	F-stat.	p-value
PDDE (Intercept)	1.43	0.12	12.38	$9.7 * 10^{-14}$	0.33	0.15	3.91	0.03
PADE	0.40	0.15	2.69	0.01				
PBDE	0.33	0.14	2.27	0.03				
Picea	Estimate	std. E.	t-value	p-value	Residuals std. E.	Adj. R^2	F-stat.	p-value
PDDE (Intercept)	0.72	0.08	9.48	$8.22 * 10^{-11}$	0.22	0.20	5.26	0.01
PADE	0.23	0.10	2.35	0.025				
PBDE	0.30	0.094	2.273	$3 * 10^{-3}$				
Prunus	Estimate	std. E.	t-value	p-value	Residuals std. E.	Adj. R^2	F-stat.	p-value
PDDE (Intercept)	1.15	0.11	10.33	$1.01 * 10^{-11}$	0.27	0.08	2.48	0.10
PADE	0.23	0.13	1.55	0.13				
PBDE	0.29	0.13	2.23	0.033				
Betula	Estimate	std. E.	t-value	p-value	Residuals std. E.	Adj. R^2	F-stat.	p-value
PDDE (Intercept)	0.62	0.11	5.57	$2.59 * 10^{-6}$	0.31	0.14	3.98	0.027
PADE	0.25	0.14	1.82	0.078				
PBDE	0.38	0.13	2.82	$7.73 * 10^{-3}$				
Tilia	Estimate	std. E.	t-value	p-value	Residuals std. E.	Adj. R^2	F-stat.	p-value
PDDE (Intercept)	0.901	0.29	3.15	$3.91 * 10^{-3}$	0.76	0.18	4.27	0.024
PADE	0.82	0.36	2.28	0.031				
PBDE	1.03	0.36	2.86	$7.94 * 10^{-3}$				
Paulownia	Estimate	std. E.	t-value	p-value	Residuals std. E.	Adj. R^2	F-stat.	p-value
PDDE (Intercept)	0.77	0.13	5.75	$4.07 * 10^{-6}$	0.30	0.14	3.47	0.046
PADE	0.18	0.16	1.14	0.26				
PBDE	0.39	0.16	2.48	0.020				
Pinus	Estimate	std. E.	t-value	p-value	Residuals std. E.	Adj. R^2	F-stat.	p-value
PDDE (Intercept)	0.74	0.17	4.25	$1.16 * 10^{-4}$	0.43	0.084	3.03	0.059
PADE	0.42	0.20	2.08	0.044				
PBDE	0.48	0.20	2.44	0.020				
Ailanthus	Estimate	std. E.	t-value	p-value	Residuals std. E.	Adj. R^2	F-stat.	p-value
PDDE (Intercept)	0.74	0.12	6.39	$1.49 * 10^{-7}$	0.30	0.090	3.02	0.060
PADE	0.20	0.14	1.50	0.14				
PBDE	0.33	0.14	2.43	0.020				
Sophora	Estimate	std. E.	t-value	p-value	Residuals std. E.	Adj. R^2	F-stat.	p-value
PDDE (Intercept)	0.69	0.12	5.76	$1.49 * 10^{-5}$	0.27	0.36	6.90	$5.58*^{-3}$
PADE	0.45	0.15	3.03	$6.90 * 10^{-3}$				
PBDE	0.54	0.15	3.58	$2.0 * 10^{-3}$				
Catalpa	Estimate	std. E.	t-value	p-value	Residuals std. E.	Adj. R^2	F-stat.	p-value
PDDE (Intercept)	0.76	0.22	3.51	$1.53 * 10^{-3}$	0.53	0.14	3.47	0.045
PADE	0.65	0.26	2.47	0.020				
PBDE	0.54	0.15	3.58	0.027				

Table 9: Table statistic for ANOVA (Kruskall - Wallis) statistical test. Comparison among ring width index of each tree species during the 3 different drought periods: drought events, after drought events and before drought events. Last 9 tree species.

Pyrus	Estimate	std. E.	t-value	p-value	Residuals std. E.	Adj. R^2	F-stat.	p-value
PDDE (Intercept)	0.39	0.22	1.72	0.096	0.50	0.16	3.97	0.030
PADE	0.61	0.26	2.35	0.026				
PBDE	0.72	0.26	2.78	$9.22 * 10^{-3}$				
Fraxinus	Estimate	std. E.	t-value	p-value	Residuals std. E.	Adj. R^2	F-stat.	p-value
PDDE (Intercept)	0.61	0.11	5.33	$9.08 * 10^{-6}$	0.32	0.085	2.50	0.090
PADE	0.25	0.15	1.70	0.1				
PBDE	0.32	0.15	2.18	0.037				
Cercidiphyllum	Estimate	std. E.	t-value	p-value	Residuals std. E.	Adj. R^2	F-stat.	p-value
PDDE (Intercept)	0.83	0.096	8.58	$2.54 * 10^{-9}$	0.24	0.14	3.36	0.049
PADE	0.30	0.12	2.53	0.017				
PBDE	0.25	0.12	2.11	0.044				
Acer	Estimate	std. E.	t-value	p-value	Residuals std. E.	Adj. R^2	F-stat.	p-value
PDDE (Intercept)	1.52	0.11	14.28	$2.21 * 10^{-14}$	0.57	0.12	3.06	0.062
PADE	0.26	0.19	1.39	0.18				
PBDE	0.41	0.18	2.27	0.031				
Crataegus	Estimate	std. E.	t-value	p-value	Residuals std. E.	Adj. R^2	F-stat.	p-value
PDDE (Intercept)	0.87	0.15	5.70	$3.2 * 10^{-6}$	0.40	0.13	3.42	0.046
PADE	0.41	0.19	2.16	0.039				
PBDE	0.47	0.19	2.53	0.017				
Amelanchier	Estimate	std. E.	t-value	p-value	Residuals std. E.	Adj. R^2	F-stat.	p-value
PDDE (Intercept)	0.89	0.15	5.95	$2.42 * 10^{-6}$	0.40	$7.38 * 10^{-3}$	1.11	0.34
PADE	0.28	0.19	1.47	0.15				
PBDE	0.21	0.19	1.08	0.29				
Magnolia	Estimate	std. E.	t-value	p-value	Residuals std. E.	Adj. R^2	F-stat.	p-value
PDDE (Intercept)	0.51	0.23	2.20	0.048	0.26	0.37	3.52	0.063
PADE	0.54	0.31	1.73	0.11				
PBDE	0.80	0.30	2.64	0.022				
Platanus	Estimate	std. E.	t-value	p-value	Residuals std. E.	Adj. R^2	F-stat.	p-value
PDDE (Intercept)	0.84	0.30	2.76	0.022	0.61	-0.046	0.76	0.50
PADE	0.46	0.43	1.07	0.31				
PBDE	0.46	0.43	1.07	0.31				
Aesculus	Estimate	std. E.	t-value	p-value	Residuals std. E.	Adj. R^2	F-stat.	p-value
PDDE (Intercept)	1.17	0.30	3.92	$7.78 * 10^{-3}$	0.52	-0.020	0.92	0.45
PADE	0.42	0.47	0.89	0.41				
PBDE	0.19	0.39	0.47	0.65				

Figures 5 and 4 show the differences between the categories (95% family-wise confidence level) singularly: PDDE, PBDE and PADE. For instance, the Tukey honest significance test allows assessing whether there is a significant difference between the tree growth among the 3 periods within the same tree species. Figure 5 and 4 show these comparisons for each species: tree growth during the PDDE versus PBDE (top bars), the tree growth during the PDDE versus the PADE (middle bars) and the tree growth during the PBDE versus the PADE (bottom bars). If the bars cross the 0 value, it means that the differences are not significant ($p - value > 0.05$).

Table 10: Trees reaction to drought events according to the Tolerance indexes: resistance, resilience and recovery. Very high, high, moderate, low and very low.

Tree species	PDDE vs. PBDE, PADE	PADE vs. PDDE, PBDE	PBDE vs. PDDE, PADE
Robinia pseudoacacia	very high	moderate	moderate
Picea omorika	very high	moderate	moderate
Prunus umineko	very high	low	moderate
Betula pendula	high	low	moderate
Tilia europea	moderate	moderate	moderate
Paulownia tormentosa	high	low	moderate
Fraxinus excelsior	high	low	low
Pinus sylvestris	high	low	moderate
Ailanthus altissima	high	low	moderate
Sophora japonica	high	moderate	moderate
Catalpa bignonioides	moderate	moderate	moderate
Pyrus communis	low	moderate	moderate
Cercidiphyllum japonicum	very high	moderate	low
Acer rufinerve and lavellei	very high	low	moderate
Crataegus levigata and lavellei	high	low	moderate
Amelanchier lamarckii	high	low	low
Magnolia kobus	low	low	moderate
Platanus hispanica	too few data	too few data	too few data
Aesculus hippocastanum	too few data	too few data	too few data

In general, 12 out of 19 tree species show a significant lower tree growth during the PDDE concerning the PBDE. *Prunus umineko*, *Fraxinus excelsior*, *Catalpa bignonioides Amelanchier lamarckii* and *Cercidiphyllum japonicum*, *Platanus hispanica* and *Aesculus hippocastanum* do not show differences in the tree growth between the PDDE and PBDE. Therefore, these tree species show a comparable growth pattern during the PDDE compared to PBDE. On that account, it is possible to infer that these latter tree species show low drought signals or they do not show drought events signals.

On one hand, 3 out of 19 species show a significant lower tree growth during the PDDE concerning the PADE. The concerned species are *Sophora japonica*, *Catalpa bignonioides* and *Cercidiphyllum japonicum*, on the other hand, the other tree species show low or do not show significant differences between the tree growth during PDDE and PADE. Therefore, these tree species show a comparable tree growth pattern during the PDDE and PADE. Consequently, it can be inferred that these latter tree species do not show drought events signals and they can maintain the growth pattern during the PDDE at a comparable level to the PADE. Otherwise, these

tree species are not able to restore completely the growth in the PADE and they maintain a similar growth pattern in comparison to the PDDE.

No tree species show a significant difference between tree growth in the PBDE compared to PADE. Therefore, it is possible to infer that the tree species considered do show a reaction to the drought events by restoring in PADE, a growth pattern, which is comparable to one of the PBDE.

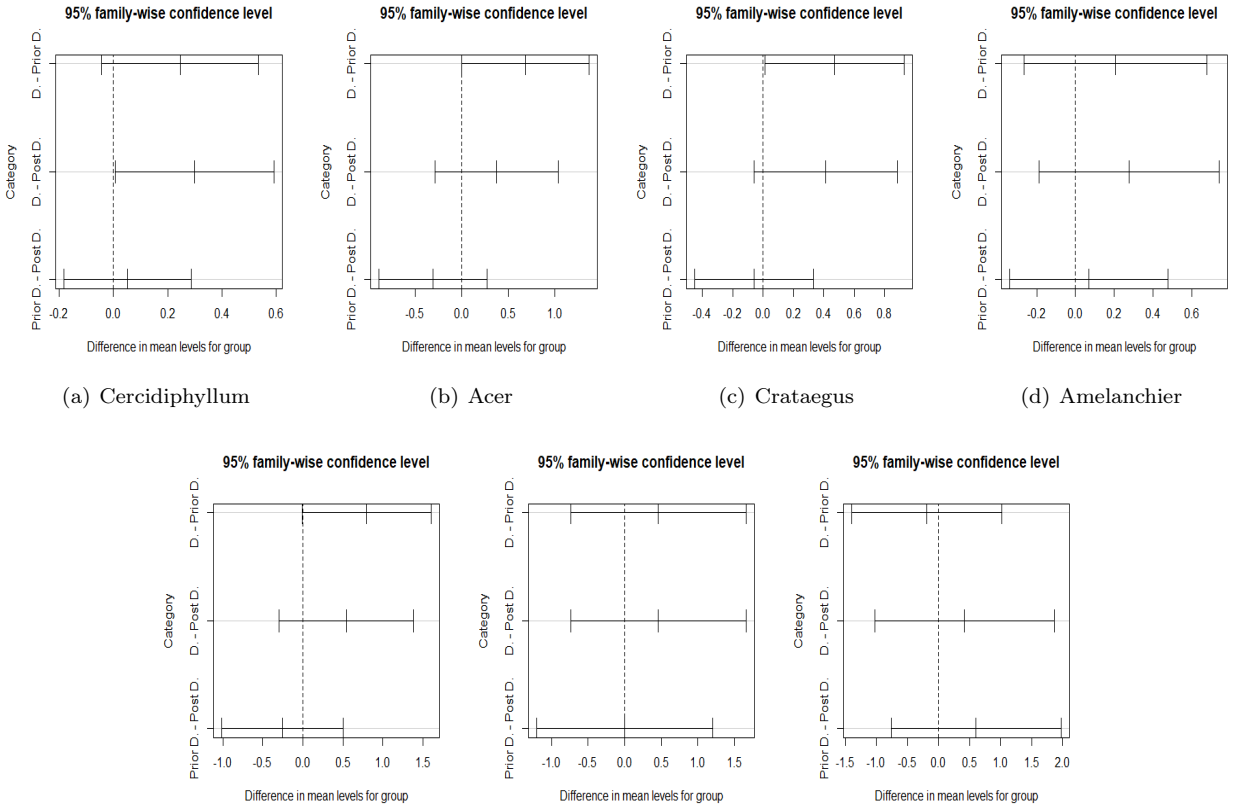

(a) Cercidiphyllum (b) Acer (c) Crataegus (d) Amelanchier

(e) Magnolia (f) Platanus (g) Aesculus

Figure 4: Tukey honest significance test (Tukey HSD) for all the selected species at 95% family - wise confidence interval. In the y-axis there is the comparison between the categories: tree ring width index in PDDE (D.) versus PBDE (Prior - D.), tree ring width index in PDDE (D.) versus PADE (Post - D.) and tree ring width index in PBDE (Prior - D.) versus PADE (Post - D.). In the x-axis is displayed the difference in mean levels of group. D. is for Drought. First 7 tree species

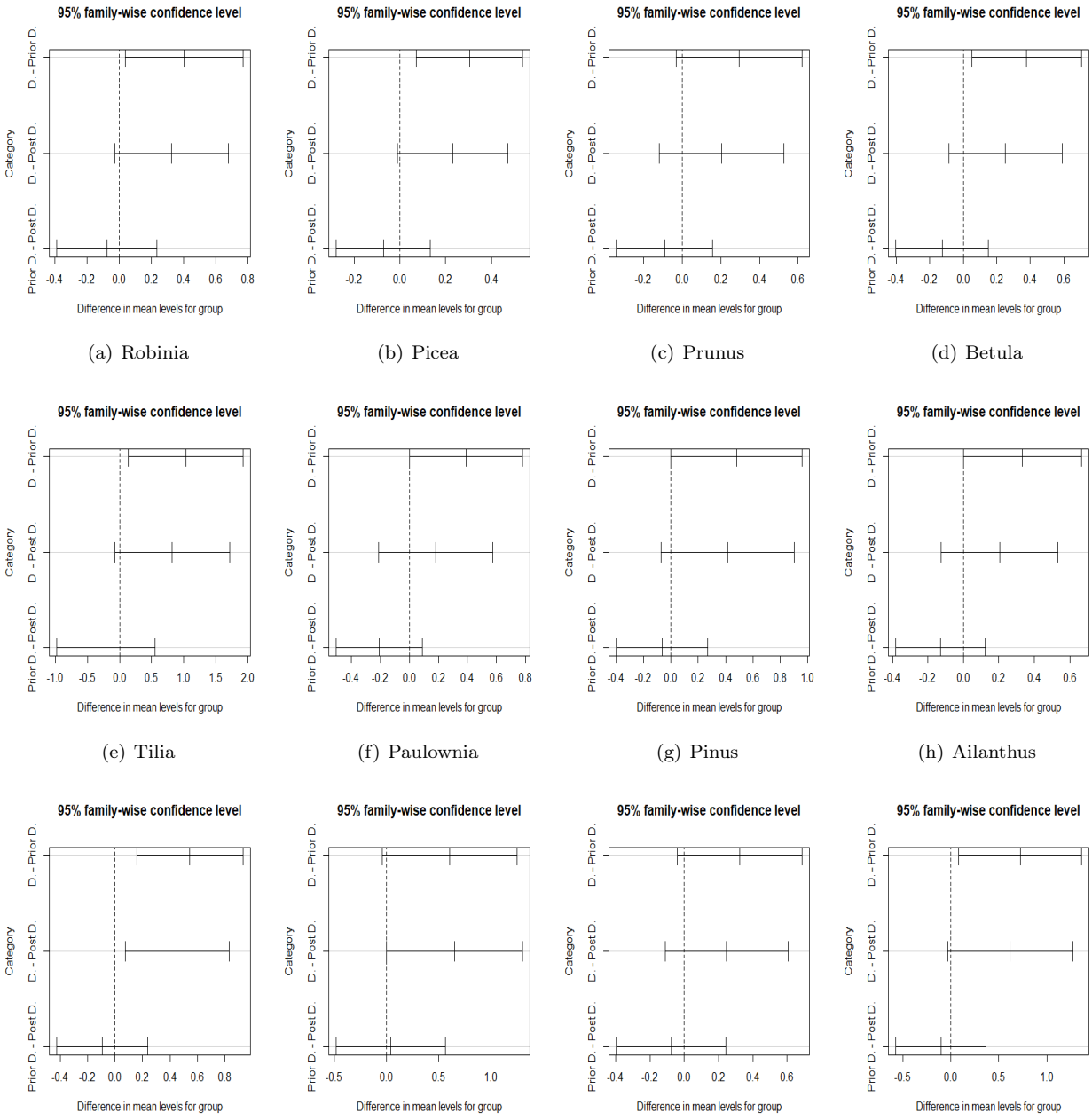

(a) Robinia (b) Picea (c) Prunus (d) Betula

(e) Tilia (f) Paulownia (g) Pinus (h) Ailanthus

(i) Sophora (j) Catalpa (k) Fraxinus (l) Pyrus

Figure 5: Tukey honest significance test (Tukey HSD) for all the selected species at 95% family - wise confidence interval. In the y-axis there is the comparison between the categories: tree ring width index in PDDE (D.) versus PBDE (Prior - D.), tree ring width index in PDDE (D.) versus PADE (Post - D.) and tree ring width index in PBDE (Prior - D.) versus PADE (Post - D.). In the x-axis is displayed the difference in mean levels of group. D. is for Drought. Last 12 tree species

To have a tree species classification, it could be sum up as following:

On one hand, *Sophora japonica* shows a significant difference in tree growth during PDDE in comparison to the PBDE and PADE. It shows no significant difference between the tree growth during the PBDE and PADE. On the other hand, *Amelanchier lamarckii* shows no significant difference among the 3 categories.

Robinia pseudoacacia, *Picea omorika*, *Tilia europea*, *Catalpa bignonioides*, *Pyrus communis* and *Crataegus levigata and lavellei* behave similarly among the 3 periods: PDDE, PBDE and PADE. For instance, they show significant ($p - value < 0.05$) lower tree growth during the PDDE with respect than the PBDE. Furthermore, they show a significant difference in tree growth during the PDDE and in the PADE. The difference of this latter is lower but still significant. However, it is not found significant differences in tree growth during the PBDE versus the PADE. Therefore, on one hand, *Robinia pseudoacacia*, *Picea omorika*, *Tilia europea*, *Catalpa bignonioides*, *Pyrus communis* and *Crataegus levigata and lavellei* seem to react to the drought by reducing tree growth in a significant amount in comparison to the PBDE. On the other hand, they seem to restore a similar growth pattern to the one of PBDE, in the PADE.

Table 11: Trees reaction to drought events. Yes, means that the trees show differences in growth patter among the different periods considered (PDDE, PBDE and PADE). No, means that the trees do not show differences in growth pattern. low means that the trees show small differences in growth pattern. The table is based on the Tukey HSD results (table 5 and 4). Displayed the differences among the 3 drought periods: PDDE versus PBDE; PDDE versus PADE and PBDE versus PADE.

Tree species	PDDE vs. PBDE	PDDE vs. PADE	PBDE vs. PADE
Robinia pseudoacacia	yes	low	no
Picea omorika	yes	low	no
Prunus umineko	low	low	no
Betula pendula	yes	low	no
Tilia europea	yes	low	no
Paulownia tormentosa	yes	low	no
Fraxinus excelsior	low	low	no
Pinus sylvestris	yes	low	no
Ailanthus altissima	yes	low	no
Sophora japonica	yes	yes	no
Catalpa bignonioides	low	yes	no
Pyrus communis	yes	low	no
Cercidiphyllum japonicum	low	yes	no
Acer rufinerve and lavellei	yes	low	no
Crataegus levigata and lavellei	yes	low	no
Amelanchier lamarckii	low	low	no
Magnolia kobus	yes	low	no
Platanus hispanica	too few data	too few data	too few data
Aesculus hippocastanum	too few data	too few data	too few data

Betula pendula, *Paulownia tormentosa*, *Ailanthus altissima*, *Magnolia kobus* and *Acer rufinerve and lavellei* show similar behaviours among the three periods: PDDE, PBDE and PADE. As a matter of fact, a significant lower tree ring growth during the PDDE was found, with respect to the PBDE. However, it shows no significant

differences between tree growth during PDDE and the tree growth in the PADE. Furthermore, it shows no significant difference between tree growth in the PBDE concerning the PADE. Therefore, *Betula pendula*, *Paulownia tormentosa*, *Ailanthus altissima*, *Magnolia kobus* and *Acer rufinerve and lavellei* seem to react to the drought events by reducing the growth in comparison to previous pattern. However, they seem unable to restore previous growth patterns in the PADE.

On one hand, *Prunus umineko* and *Fraxinus excelsior* show a low significant difference between tree growth during PDDE in comparison to the PBDE. On the other hand, they do not show any significant differences between the other 2 categories. *Prunus sylvestris* and *Fraxinus excelsior* seem to react to the drought events by reducing slightly tree growth.

Catalpa bignonioides and *Cercidiphyllum japonicum* show significant differences between tree growth during PDDE and the PADE. Furthermore, they show a low significant difference between tree growth during PDDE and the PBDE and no significant difference to the last category. *Catalpa bignonioides* and *Cercidiphyllum japonicum* seem to react to the drought events by slightly reducing tree growth. In addition, they seem to have a growth increase in the PADE.

Table 11 summarizes the Tukey honest significance test interpreted for each tree species. Trees species can be described for the different reactions to drought events. Depending on the Tukey honest significance test values for the relationship between the 3 time periods, it is possible to describe the tree species' reactions into 2 main groups (excluding the ones that do not allow a proper analysis because of the lack of data): Tree species, which tolerates the drought events by slightly reducing the growth and can restore a similar growth pattern in the PADE. However, they do not seem able to cope with the drought events. As a matter of fact, the growth pattern in the PADE increase in comparison to the growth during PDDE but it remains lower than the PBDE. the species are: *Robinia pseudoacacia*, *Picea omorika*, *Tilia europea*, *Sophora japonica*, *Catalpa bignonioides*, *Pyrus communis*, *Cercidiphyllum japonicum* and *Crataegus levigata and lavellei*.

The second group comprehends *Prunus umineko*, *Betula pendula*, *Paulownia tormentosa*, *Pinus sylvestris*, *Ailanthus altissima*, *Fraxinus excelsior* and *Magnolia kobus*. These tree species seem to suffer drought events. As a matter of fact, they do not tolerate the drought events and they show low or no increase in the tree growth in the PADE. Therefore, they do not seem to restore and cope with drought events.

3.4 Tolerance index: resistance, resilience and recovery for each tree species

The tolerance indexes are displayed in figure 6, 7 and 8 or in figure 25 in the appendix. As explained in the section "Methods", they represent an index between tree growth during PDDE and the tree growth in the PBDE (resistance), the growth in the PADE and the PBDE (resilience) and the tree growth in the PADE and the tree growth during PDDE (recovery).

As it is visible in figure 6, resistance lays under the threshold of 1 for almost every tree species, which is a sign that almost all the tree species during drought events have a reduction in tree growth. *Ailanthus altissima*, *Amelanchier lamarckii*, *Prunus umineko*, *Tilia europea* and *Cercidiphyllum japonicum* are the most

resistant tree species, because they have the highest tolerance index. On the other side, *Sophora japonica Pyrus communis*, *Magnolia kobus*, *Picea omorika* and *Betula pendula* are the less resistant tree species.

The most resilient tree species are *Amelanchier lamarckii*, *Fraxinus excelsior*, *Betula pendula* and *Prunus umineko*, which are listed among the most resistant. *Magnolia kobus*, *Crataegus levigata and lavellei* and *Picea omorika* seem to have the lowest resilience, which indicates that trees could not reach past growth pattern in 3 years following the drought events.

The recovery index shows more variations among the tree species in comparison to resistance and resilience indexes. *Crataegus levigata and lavellei*, *Ailanthus altissima*, *Cercidiphyllum japonicum* and *Magnolia kobus* seem to be the trees that recover less. On the other hand, *Sophora japonica*, *Fraxinus excelsior*, *Paulownia tormentosa* and *Betula pendula* seem to be the tree species with the highest recovery. Therefore, this is a sign that these latter trees have a growth in the periods following the drought events, which is considerably higher than during the drought events.

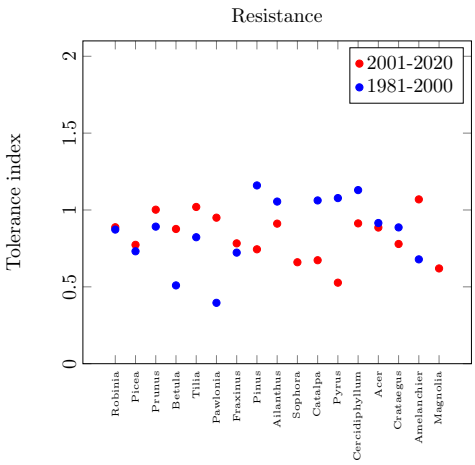

Figure 6: Displayed the average tolerance index resistance, for all the tree species, during the two time periods

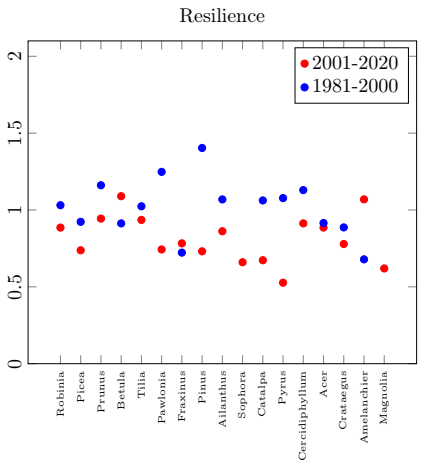

Figure 7: Displayed the average tolerance index resilience, for all the tree species, during the two time periods

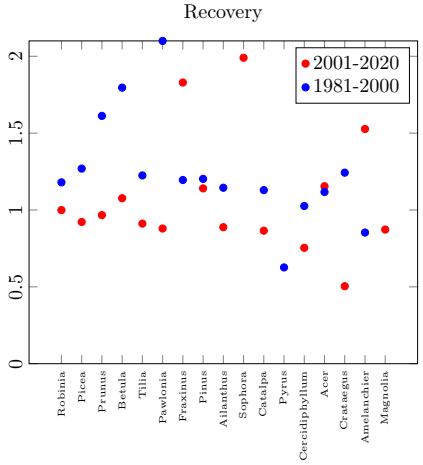

Figure 8: Displayed the average tolerance index recovery, for all the tree species, during the two time periods

Betula pendula, *Picea omorika*, *Fraxinus excelsior*, *Acer platanoides and rufinerve* and *Ailanthus altissima* are the tree species, which show low variations in the tolerance indexes between 1981-2000 and 2001-2020.

Figure 10 shows the tree species classified depending on the 3 tolerance indexes. It is possible to discriminate among the tree species depending on the amount of variance that each one has in resistance, resilience and recovery. What is noticeable from Figure 6, 7 and 8, on one hand, the 5 tree species with high recovery indexes, tend to show low resistance indexes. Therefore, tree species, which during PDDE face a strong reduction in tree growth, compensate in the PADE. On the other hand, *Robinia pseudoacacia*, *Sophora japonica*, *Amelanchier*

lamarckii and *Cercidiphyllum japonicum* are the tree species with relatively low recovery, but they show a moderate resistance and resilience index.

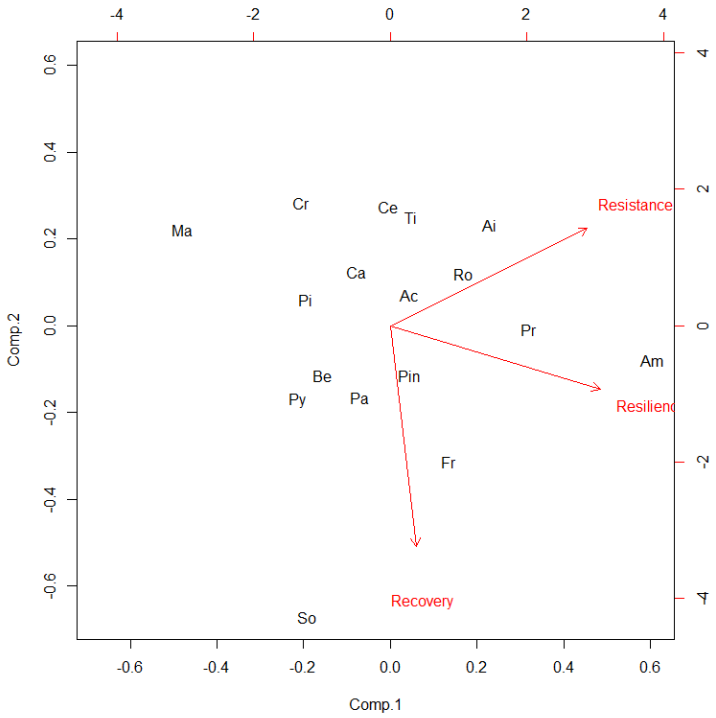

Figure 9: 2 dimensional principal component analysis for the tolerance indexes: resistance, resilience and recovery. Ac = Acer, Ai = Ailanthus, Am = Amelanchier, Be = Betula, Ca = Catalpa, Ce = Cercidiphyllum, Cr = Crataegus, Fr = Fraxinus, Ma = Magnolia, Pa = Paulownia, Pi = Picea, Pin = Pinus, Pr = Prunus, Py = Pyrus, Ro = Robinia, So = Sophora, Ti = Tilia

In general, resistance has little variation between the 1981-2000 and 2001-2020 periods for almost all the tree species. Furthermore, there is no trend in tree species' resistance between the 2 periods. While resilience and recovery tend to show a different pattern, the values for the 1981-2000 period are higher than the ones for 2001-2020 (exception made for Betula, Amelanchier, Fraxinus and Pyrus). This means that resilience and recovery decrease from 1981-2000 to 2001-2020.

Figure 9 shows trees species behaviours in respect to resistance, resilience and recovery indexes. *Magnolia kobus*, *Amelanchier lamarckii*, *Sophora japonica* and *Fraxinus excelsior* show extreme tolerance index values. For instance, *Magnolia kobus* is characterized by extremely low resilience, on the other side, *Amelanchier lamarckii* is characterized by extremely high resilience. *Sophora japonica* show extremely high recovery value and *Fraxinus excelsior* show high recovery and resilience value.

To sum up, looking at figure 10, it is possible to classify the tree species under 4 different groups. *Sophora japonica* is strongly discriminated against, because it has the highest recovery value and the lowest resistance

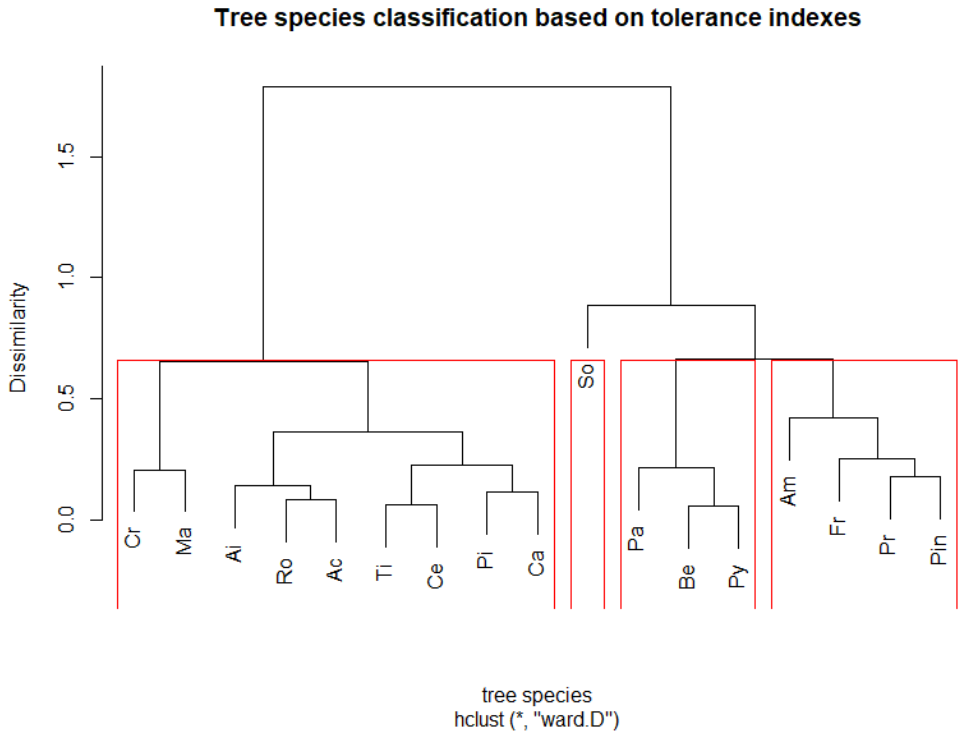

Figure 10: Dendrogram for each tree species based on tolerance indexes. Ac = Acer, Ai = Ailanthus, Am = Amelanchier, Be = Betula, Ca = Catalpa, Ce = Cercidiphyllum, Cr = Crataegus, Fr = Fraxinus, Ma = Magnolia, Pa = Paulownia, Pi = Picea, Pin = Pinus, Pr = Prunus, Py = Pyrus, Ro = Robinia, So = Sophora, Ti = Tilia

value. Therefore, it is possible to states that *Sophora japonica* shows an uncommon growth pattern during PDDE, the PBDE and the PADE concerning the other tree species.

Betula pendula, *Pyrus communis* and *Paulownia tormentosa* represents another cluster. Similar to *Sophora japonica*, these tree species show strong recovery values and weak resistances values.

Amelanchier lamarckii, *Fraxinus excelsior*, *Pinus rufinerve* and *Prunus umineko* tend to show relatively strong recovery and resilience values and moderate resistance values.

The remaining tree species, *Crataegus levigata and lavellei*, *Magnolia kobus*, *Ailanthus altissima*, *Tilia altissima*, *Cercidiphyllum japonicum*, *Robinia pseudoacacia*, *Acer platanoides and rufinerve*, *Picea omorika* and *Catalpa bignoinioides* are the tree species in the last class. This latter class seems to have similar values of resistance, resilience and recovery: They show moderate resistance, resilience and recovery values. However, this last class compared to the other 3, shows the lowest internal variation. As a matter of fact, these tree species are discriminated against because they possess no extreme values for specific tolerance indexes.

Table 12: Difference in the tree species' RWI during the 3 period of the drought events (PDDE, PBDE and PADE). Values are based on ANOVA statistics. Values are addressed with very high, high, moderate, low and very low. Values are taken arbitrarily to have an adjustment for the simplification. Trees are divided among the 4 categories (red lines) and they are ordered from the highest responses to the indexes to the lowest. * *Ailanthus altissima* and *Robinia pseudoacacia* are considered outliers of the group, since they show good responses to the tolerance indexes.

Tree species' RWI	Resistance	Resilience	Recovery
Amelanchier lamarckii	very high	very high	low
Prunus umineko	high	high	low
Fraxinus excelsior	low	high	high
Pinus sylvestris	low	moderate	moderate
Sophora japonica	low	low	very high
Paulownia tormentosa	low	low	moderate
Betula pendula	low	low	moderate
Pyrus communis	low	low	moderate
*Ailanthus altissima**	high	moderate	low
*Robinia pseudoacacia**	moderate	moderate	low
Acer platanoides and rufinerve	moderate	low	low
Tilia europea	moderate	low	low
Cercidiphyllum japonicum	low	low	low
Catalpa bignonioides	low	low	low
Picea omorika	low	low	low
Crataegus levigata and lavellei	low	low	very low
Magnolia kobus	very low	very low	very low
Platanus x hispanica	no enough data	no enough data	no enough data
Aesculus hippocastanum	no enough data	no enough data	no enough data

The tree species which showed evident responses to the drought events were the tree species with the highest tolerance indexes, and they are: *Amelanchier lamarckii*, *Prunus umineko*, *Fraxinus excelsior*, *Pinus sylvestris*, *Sophora japonica*, *Ailanthus altissima* and *Robinia pseudoacacia*.

4 Discussion

This master thesis attempts to study urban trees in order to discover the reaction to drought events and whether such reaction is quantifiable (Lloret et al., 2011). Trees are measured at the WSL laboratory of Birsmendorf through apposite equipment (Rinn Tech, 2010) and thereafter, the ring width is indexed, following the study of Bose and colleagues (2020). Raw ring widths are removed with the trended and all the measures are averaged for each tree species through the Tukey biweight mean method (Bunn et al., 2018: Mosteller and Tukey, 1977: Shewchuck, 1997: Kafadar, 1983). Such a method allows to control the decreasing growth trend with increasing age of the trees, and it allows to remove the high-frequency variation of trees growth (Cook and Kairiukstis, 1990).

Afterwards, the ring width indexes are compared to the climatic indexes, in order to discover the relationship between the city climate and tree growth (Vicente-Serrano et al., 2010: Nedealcov et al., 2015: Tan et al., 2015:

Li et al., 2012). Tree growth is then analysed at the specific years when drought events occurred. this latter step is pursued by considering the 8 driest years in the last 40 years (1981 - 2020) and the 3 years periods preceding and following the drought events (Chen, et al., 2013: Bose et al., 2020: Li et al., 2012: Wang et al., 2012: Pei et al.,2020). The tree ring widths during the 3 different periods are before considered within the same species. The ANOVA statistical test for difference in the mean of the tree ring widths during the 3 different periods is run and then it is followed by Tukey's honest significant test. Such a way allows having significant statistics to assess trees reaction to the PDDE, PBDE and PADE.

In the end, following the instruction of Lloret and colleagues (2011), Fang and colleagues (2021), Zang and colleagues (2014), Serra-Maluquer and colleagues (2018), Bohner and colleagues (2021), Schwarz and colleagues (2020) and Vila-Cabrera and colleagues (2019) the 3 tolerance indexes: resistance, resilience and recovery are built. Tolerance indexes would allow a better comparison and classification of the tree species' ring width index and it would allow distinguishing among tree species, which ones are best suited to thrive under future drought events (Fang et al., 2021: Zang et al., 2014).

4.1 Driest years selection

The SPEI and SPI indexes are developed respectively by Vicente-Serrano and colleagues in 2010 and McKee and colleagues (1993). They are very common indexes used in the literature to monitor the drought pattern (Vicente-Serrano et al., 2010: Nedealcov et al., 2015: Tan et al., 2015: Li et al., 2012). SPEI and SPI are tested with the Mann - Kendall test for the presence of a monotonic trend, in order to discover if they are comparable in the region of Zurich. After such statistics, it is decided to consider only SPEI values. The SPEI estimates the climate water balance from precipitation data, and it estimates the potential evapotranspiration through the Thornthwaite equation (Vincente-Serrano et al., 2011: Thornthwaite 1948). Then, it creates a probability distribution function (Gaussian), wherewith the insertion of the timescale, it is possible to estimate the weight of the previous months in the actual drought value (Potop et al., 2012). Such considerations result fundamental, especially in regions where the impact of the climate (precipitation and temperature) affect the tree physiology (Chen et al., 2013). SPEI is appositely chosen for such master thesis because it considers tree growth patterns and its versatility in the research for both short-term and long-term drought events (Li et al., 2012: Mehr et al., 2019: Tan C. et al., 2015: Diani et al., 2019). For instance, the choice of the index with monthly resolution and the possibility to be calculated over the integration of timescale seems to fit the purpose of the master thesis. For instance, the SPEI output has a monthly resolution. Therefore, considering 7 SPEI timescale at a monthly resolution would generate a huge dataset. Therefore, this thesis tried to generalize SPEI data by following 2 approaches (Bose et al., 2015: Tan et al., 2015). The first one considers the average of the SPEI value over the vegetative period at an annual resolution. The months of March, April, May, June, July and August are selected. This method is similar to the one in the study of Bose and colleagues (2015) and Zang and colleagues (2014). The difference lay on the average, as a matter of fact, this master thesis attempts to reduce the data by averaging the SPEI values, whereas such studies consider the whole dataset. On the other hand, the second approach considers the construction of an additional index, the intensity of drought,

which will be further discussed.

The first approach generates homogeneous SPEI values over the whole 1981 - 2020 period. For instance, the choice of the 8 driest years is comparable among the different SPEI's timescale. Such congruity among the timescale is probably dictated by the average, which tends to homogenise the results. However, there are some issues, which is considered. The average tends to preserve the general pattern, but some details might be hidden by the average itself. For instance, extremely drought months might be dampened by the other non - drought months. Secondly, the SPEI's average considers both dry and moist months, which means that such a method selects the driest period within the 7 months selected. Therefore, the 8 driest years consider mainly the drought events, which occurred on all the months considered vegetative (or in the majority of them). That explains the homogeneity in the different SPEI values independently of the timescale and the similarity in the driest years selected by the different SPEI's timescale.

On the other hand, the intensity of drought, as explained by Tan and colleagues (2015) indexes the data to a 0 - 2 range. However, this approach relies on SPEI data for the computation of the severity and divide the final result by the duration. Therefore, there are no fixed rules on how to manage the strength that severity and duration have on the final intensity calculations (Saravi et al., 2009: Lin et al., 2020). The introduction of the computation of the frequency of drought events is helpful in such a context (Brito et al., 2015) because it allows checking the intensity results for biased results. For instance, the intensity of drought is strongly affected by the severity and the duration considered (Cavus et al., 2020). As a matter of fact, short-duration values combined with strong severity values within a year would generate a strong intensity of drought index (Tan et al., 2015). Therefore, an integration of intensity of drought index over 7 different SPEI timescale create many variations in the identification of the driest years and, in addition, it hides the non - drought events periods (Adhyani et al., 2017). Furthermore, the approach of the intensity of drought is suited in regions with strong drought impact (Bae et al., 2018: Lin et al., 2020), which might not be the case of Zurich city, because it lays in a temperate climate zone. Zurich's climate is characterised by the winds from westerly directions, which often bring precipitation (1054 mm on average). In general, the approach of the intensity of drought to detect the driest years is helpful (Tan et al., 2015: Adhyani et al., 2017:Bae et al., 2018: Lin et al., 2020).

In the end, the 8 driest years are selected for each SPEI's timescale and intensity of drought. The above-explained remark suggests that SPEI could be more reliable in evaluating the driest years. For instance, most of the drought events detected by the SPEI are comparable with the literature (Pretzsch et al., 2013: Bose et al., 2020: Zang et al., 2014: Chen, et al., 2013: Vicente-Serrano et al., 2010: Nedealcov et al., 2015: Potop et al., 2012: Tan et al., 2015: Li et al., 2012: Wang et al., 2012: Pei et al., 2020). Therefore, in the search for monotonic trends between the ring width index of the tree species, it is preferred the Mann - Kendall statistic compared with SPEI rather than the intensity of drought. The intensity of drought is used if the monotonic trend between tree ring width index and SPEI is found insignificant.

4.2 Long-term relationship between drought events and tree growth

The long-term relationship between tree ring width index and climate is explored through the Mann - Kendall statistical test to search for a monotonic trend (Blain, 2013: Tripathi et al., 2014: Zhang et al., 2006: Kumar et al., 2009). This master thesis discovered that the reaction to short-term or long-term drought events can be typical for each tree species. As a matter of fact, different tree species discovered different best Mann - Kendall tau values depending on SPEI's timescale. A correlation matrix is built in order to observe and present the results of the amount of relationship between the climatic indexes and the tree ring width index. Such an approach finds confirmation in the literature, where it is researched the long-term correlation between SPEI's value and tree ring width index (Bose et al., 2020: Zang et al., Tan et al., 2015). However, this master thesis attempts to calculate the relationship through the Mann - Kendall statistical test (Zang et al., 2014: Adhyani et al., 2017: Bae et al., 2018: Lin et al., 2020: Tan et al., 2015) rather than the Pearson's correlation coefficient (Bose et al., 2020). Such an approach allows evidence of which SPEI's timescale best describe the tree ring width. However, this procedure does not allow to check for monotonic trend between the intensity of drought and the tree ring width, because the intensity of drought shows many 0 during the non - drought years (Zang et al., 2014: Adhyani et al., 2017: Bae et al., 2018: Lin et al., 2020: Tan et al., 2015). Therefore, the intensity of drought is only considered if no relationship between tree species' ring with index and SPEI's are found. This could be a limitation for the master thesis, because, as above explained, SPEI's values are averaged and homogenise the resulting tau values. For instance, it is possible to extract the highest tau value for each tree species' ring width index, however, some tau values are similar among each other, therefore, the selection of the best tau statistic for discriminating the SPEI's timescale might be inaccurate. For instance, the study of Bose and colleagues (2020) considered the 8 best correlated (though Pearson's correlation coefficient) among the whole SPEI dataset (without averaging). This latter might have a stronger impact on the final Mann - Kendall statistic results. However, this thesis attempts to detect the best tau coefficient by following this novel approach, since the results are checked and there is a good outcome.

At each tree species' ring width index is assigned a best correlated SPEI's timescale average, and, in general, it is possible to assess whether tree species are more sensitive to short (timescale of 1, 2 and 3) or long-term (timescale of 4, 5 and 6, plus the annual 12) SPEI.

The best correlated SPEI's average is selected for each tree species' ring width index and it will be used to assess the 8 driest years, the periods prior to the drought events and the periods following the drought events.

4.3 Tree growth and the drought events

The 8 driest years are selected from the 7 SPEI's timescale and intensity of drought events. Therefore, from the driest years, 3 time periods are selected: PDDE, PBDE and PADE. The correspondent tree species' ring width indexes are assigned to the 3 periods. The objective of the thesis is to evaluate the differences in tree species' growth during such periods and discover if some tree species show a common pattern. Therefore, it is attempted to create a classification depending on the tree species reactions to the drought events, the 3 years

preceding and following the drought events.

This master thesis discovered that the 17 tree species selected show a reaction to the drought events. For instance, all the tree species have a significant reduction in tree ring width index during the 8 driest years concerning the PBDE (DeSoto et al., 2020). Tree ring width index measures allow detection of the growth reducing the effect of drought events on trees (Camarero et al., 2018). This effect is probably driven by the inability of the tree to face the water shortage by improving the hydraulic system at an annual timescale (Choat et al., 2018). Furthermore, if the drought events manifest at the beginning of the growing season, it reduces the vegetative period of the trees and leads to a reduction in tree growth (Lobo-do-Vale et al., 2019). Another key point to consider is the number of drought events, which are considered in this master thesis. As a matter of fact, 8 driest years are selected depending on the SPEI's definition of drought events. For instance, the study of Serra-Maluquer and colleagues (2018) considers 3 driest years. Despite they represent the years with the lowest precipitation and highest temperature, they show differences among the 2 variables. As a matter of fact, the last 20 years show an increase in magnitude and frequency of the drought events (Pretzsch et al., 2013: Bose et al.,2020: Zang et al., 2014: Chen, et al., 2013: Vicente-Serrano et al., 2010: Nedealcov et al., 2015: Potop et al., 2012: Tan et al., 2015: Li et al., 2012: Wang et al., 2012: Pei et al., 2020). This latter implication can be decisive if the legacy effect is considered (Navarro-Cerrillo et al., 2018: Anderegg et al., 2020). As a matter of fact, the increase in drought events magnitude and frequency in the last 20 years lead to a strong progressive reduction in tree growth patterns among the species (Kolus et al., 2019). This master thesis can not disentangle between global tree growth reduction during the succession of drought events and the specific effects that a drought year had on tree growth. Furthermore, it can not quantify the effect of the cumulative drought stress on tree growth patterns (Vilà-Cabrera and Jump, 2019). However, tree species have different vulnerabilities in facing drought events, which is strongly dependent on the conditions before the drought events, such as dry winter or heatwave during the early vegetative season (Lobo-do-Vale et al., 2019). For instance, cumulative drought events in a relatively short time have a stronger impact on tree growth, concerning one single strong event (Anderegg et al., 2020).

On the other side, tree species do not show a common pattern when the tree growth during PDDE is compared to the PADE. As a matter of fact, the tree species show variability in the growth pattern in the PADE both among and within the species. This latter suggests tree species have different reactions in the PADE. A crucial point can be the choice of the periods, which is set to 3 years (Bose et al., 2020: Tan et al., 2015). For instance, the study of DeSoto and colleagues (2020) considered a larger period to compute the PBDE and PADE. As a matter of fact, tree physiological feedback to decreasing precipitation are quite common and generalized among the trees, however, the quantification of such responses depend strongly on the tree species (McDowell et al., 2008). Tree reactions, facing strong drought events, can vary considerably among tree species (Ryan, 2011). For instance, some tree species drop the leaves in order to maintain available water within the tree to avoid excessive evapotranspiration and to pursue living activities. In contrast, they compensate for such loss by regulating the rooting system (McDowell et al, 2008). In addition, some tree species, in order to maintain the living activities with contained water stress, reduce the growth because the cell division and expansion are defected (Hsiao, 1973). Therefore, trees have physiological responses to the

drought events which vary among the species and the strongest of the drought events (Ditmarova et al., 2010). Furthermore, the cumulative effect of consecutive drought events can be decisive in evaluating the tree specific growth responses (Anderegg et al., 2020). The timings and the reactions that trees have in the period following the drought events are not included in this thesis. Therefore, further studies can be useful in understanding the tree physiological responses to drought events and the role of the timing in these responses for each tree species (Ryan, 2011). For instance, drought events can also trigger other effects on tree species, such as weakening of the trees that increase the vulnerability to disease and parasites (McDowell et al., 2008: Whyte et al., 2016).

In general, tree species show a common pattern between tree growth in the PBDE compared to the tree growth in the PADE. As a matter of fact, almost all the tree species do not show a significant difference in tree growth among the two periods. As explained before, this is probably a sign that trees are restoring from the drought events in the PADE (DeSoto et al., 2020). However, this master thesis can not disentangle the different tree physiological responses (Ryan, 2011). This study can quantify the growth pattern in the PADE and discover which tree species tend to have delayed growth responses to the drought events (Anderegg et al., 2020). Even there, the choice of the periods can play a fundamental role in understanding the timing of tree specific responses (Bose et al., 2020: DeSoto et al., 2020). More studies are needed to disentangle the types and the timing of tree physiological responses to drought events and the PADE because it is a crucial point to gain perspective and quantify the trees' reactions. Furthermore, the cumulative effect of the drought events on trees is monitored, because it can play a fundamental role in future urban environment planning (Navarro-Cerrillo et al., 2018: Anderegg et al., 2020).

4.4 Tolerance indexes

According to the literature (Lloret et al., 2011: Fang et al., 2021: Zang et al., 2014: Serra-Maluquer et al., 2018: Bohner et al., 2021: Schwarz et al., 2020: Vila-Cabrera et al., 2019) 3 tolerance indexes are created: resistance, resilience and recovery. These indexes are constructed from the tree ring width index measurements. The measures are selected depending on the drought events years considered and the 3 indexes are created for each tree species by averaging the measures over the 8 driest years. The tolerance indexes allow a classification of the tree species, where similar tree responses during the drought events and in the periods preceding and following the event are clustered.

This master thesis discovered 4 different classifications. The first class is represented by the *Sophora japonica*, which show an extremely low resistance value and extremely strong recovery value and an average resilience value.

The second class is represented by tree species, which show similar responses to the previous tree species: *Pyrus communis*, *Pawlonia tormentosa* and *Betula pendula*. Differently from *Sophora japonica*, these tree species do not show such a high recovery index. besides, recovery values for these 3 tree species are among the highest in comparison to the other tree species.

The third class comprehends *Fraxinus excelsior*, *Prunus umineko*, *Pinus rufinerve* and *Amelanchier lamarckii*, which are characterized by high resistance and resilience value and weak recovery values.

The fourth class shows *Crataegus levigata and lavellei*, *Magnolia kobus*, *Ailanthus altissima*, *Robinia pseudoacacia*, *Acer platanoides and rufinerve*, *Tilia europea*, *Cercidiphyllum japonicum*, *Picea omorika* and *Catalpa bignoides*. This latter class seems to have similar values of resistance, resilience and recovery: They show moderate resistance, resilience and recovery values.

According to literature (Madrigal-González et al., 2017: Navarro-Cerrillo et al., 2018: DeSoto et al., 2020), resilience and recovery are fundamental parameters to estimate the ability of trees to thrive under drought events occurrences. For instance, the studies demonstrate that trees with higher resilience during previous, not deadly drought events have a reduced mortality risk in comparison to fewer resilient trees (DeSoto et al., 2020). Nevertheless, Madrigal-González and colleagues (2017) discover a high resilience rate in trees, which are not characterized by a low survival rate. This latter is an indicator of a high recovery of the trees growing in the period following the drought events. Based on the data of this master thesis it is possible to confirm that trees experience a loss in both resilience and recovery in the last 2 decades. This is probably a sign that all the trees species suffered the drought events and the PADE is not enough to allow a proper recovery and resiliency. This is visible in the results, on one hand, the resilience values are similar among all the tree species and there is a decreasing trend for almost all the tree species between the 1981-2000 and 2001-2020 periods. On the other hand, the recovery, differently from the study of Madrigal-González and colleagues (2017), does not compensate for the growth loss. For instance, this master thesis considers the evolution of the tree's resilience among the whole 1981-2000 and 2001-2020 periods. The consideration of disjointed resilience values for each severe drought could help in the comprehension of resilience and recovery variations with increasing drought events occurrences (Serra-Maluquer et al., 2018). Despite the calculation of a trend in the evolution of resilience and recovery is possible, it would be difficult to be compared among the 17 species. Nevertheless, Anderegg et al., (2020), Camarero et al., (2018) and Serra-Maluquer et al., (2018) discover that the consideration of short-term or long-term resilience capacity varies among the trees. As a matter of fact, the impact of subsequent drought events is greater than one single strong initial event (Anderegg et al., 2020). Similar results are found by Serra-Maluquer and colleagues (2018); they discovered a reduction in resistance, resilience and recovery in trees after a succession of drought events. As a matter of fact, successive drought events do not allow the trees to recover properly to resist and enter in resilience with the subsequent drought events. In addition, trees, which experience reduction in tolerance indexes do not regain health and they remain more prone to generate new spaces for pest and disease outbreaks (Whyte et al., 2016). Therefore, that could explain the trees growth reduction found in this thesis and the decrease in resilience and recovery indexes from 1981-2000 to 2001-2020. For instance, the last decades show the lowest resilience and recovery values concerning 1981-2000 in all the tree species considered. This latter indicates a general trees growth loss in the decades with stronger and more frequent drought events because the trees are not able to cope and restore in a short time after a drought events.

However, in addition to the temporal aspect, it is considered the effects of the tree size (and age) when considering trees growth under drought events occurrence. As a matter of fact, Bohner and Diez (2021) and Serra-Maluquer and colleagues (2018) discover differences in trees growth response during drought events, which is dependent on the size of the trees. For instance, larger trees tend to lose resistance and resilience

(Serra-Maluquer et al., 2018), because of the higher water demand (Bohner and Diez, 2021). This master thesis is not able to consider the effect of the size of the trees, this could lead to biased results.

Another important condition that is considered is the status of the trees. Camarero and colleagues (2018) and Navarro-Cerillo (2018) highlight the importance of the impacts that drought events exert on declining and/or non-declining trees. The drought events exert growth reduction regardless of the tree status, however, it impacts strongly the recovery in both the long-term and short-term (Camarero et al., 2018). For instance, the loss of growth resilience and recovery is found to be stronger in a declining tree, in addition, successive drought events occurrence sharp the growth reduction (Navarro-Cerrillo et al., 2018). This thesis considers declining trees because they are the ones GSZ is allowed to cut. Therefore, this could explain the general pattern of growth reduction during drought events, regardless of the tree species considered. As a matter of fact, as highlighted by Bohner and Diez (2021), there is little variation among the tree species in the growth reduction and resistance during the occurrence of the drought. However, they find high variability among tree species in their recovery and resilience in the years following the drought events (Bohner and Diez, 2021).

The location of the trees (parks or streets) could have influences in the growth during drought events occurrence. Vilà-Cabrera and colleagues (2019), Cavin and Jump (2017) and Bohner and Diez (2021) highlight these differences in their studies. As a matter of fact, they discover that trees in rear edges and trees in the species' continuous range have different growth reactions to drought events. Bohner and Diez (2021) discover that trees in dense forests have lower resistance and a higher recovery rate in the years following the drought events. Similarly, Cavin and Jump (2017) discover that trees in the core's species range show high sensitivity and little resistance to drought events. Whereas trees in rear edges show high resistance and few signs of growth reduction attributable to the drought events (Vilà-Cabrera et al., 2019). The high resistance of trees on the rear edge is a sign that the trees die-off caused by drought events is not ubiquitous and it is not characterized by an abrupt and diffuse event, rather the range shifts are heterogeneous and characterized by a reduction in the trees' density before (Cavin and Jump, 2017). This thesis considers trees in the city, which can be located in the street, where the density of individuals is low, and/or in the park, where the density of trees will be higher. Such differentiation in location can impact differently the resistance and recovery rate during and following the drought events. As a matter of fact, the study of Hagedorn and colleagues (2016) demonstrate that after severe drought events, trees tend to provide before assimilates to the underground components. Trees tend to restore before the root system and after that, they initialize the recovery of the growth of the tree. Therefore, resilience and recovery values are not exclusive indicators of trees reaction to the drought events. Also on this occasion, the location of trees can be an important factor. For instance, trees growing on the roads have a higher damage risk to the root system, as the soil tends to be asphalted and compacted. Therefore, the underground space that the trees have at disposal for the rooting system is fundamental to allow proper restoring and functioning of the underground components. Thereafter, the trees set up the recovery and resilience of the growth above ground.

5 Conclusion

This master thesis attempt to discover which urban tree species have the best possibilities to survive under the future climatic scenario. Climate is expected to be warmer and dryer in the next decades, therefore, the aim is to discover which tree species best reacted to past anomalous years. Dendrochronology allows the study of past trees reactions to drought events and it allows the creation of quantitative measures. 8 driest years are selected through SPEI and indexes calculated by SPEI and the 3 years periods before and after the drought events are selected. Ring width indexes for different tree species are then compared to the drought events. It is statistically assessed the difference ring width indexes during the different periods (PDDE, PBDE and PADE). In the end, the tolerance indexes resistance, resilience and recovery are built in order to classify the trees reaction to the drought events.

It is discovered a significant difference in tree species ring width indexes depending on the periods selected. Trees in the city, in general, show responses to the drought events by reducing the growth during the PDDE and they try to restore previous growth patterns in PADE. This demonstrates that trees after drought events events have reactions in order to tolerate the drought events and survive in the PADE. If trees cope with drought events is hard to define, because many factors are not included in the analysis. Looking at the statistics, it is possible to state that the trees cope with drought events since the growth in the PADE is comparable to the growth in the PBDE. The tolerance indexes resistance, resilience and recovery give a better comparison among the tree species about the reaction to the drought events. Generally, resistance values lie behind the 1, which indicates that trees reduce the growth during the PDDE in comparison to the PBDE. However, resistance does not show a defined pattern between the 2001-2020 period in comparison to 1981-2000. This is probably explained by the fact that the 1981-2000 period show fewer, not consecutive drought events than the 2001-2020 period, therefore, trees are not highly stressed. Recovery tends to show higher values for the 1981-2000 period in comparison to the 2001-2020 period. This is probably an indicator of a loss in the trees' ability to recover from drought events after consecutive events. Resilience values are relatively high compared to literature, which indicates that trees cope with drought events. Also there, resilience values for the 1981-2000 period are higher than the 2001-2020 period, demonstrating a trees' loss in health. The construction of the tolerance indexes allows also to classify the tree species for similar reactions to drought events because resistance, resilience and recovery consider the tree's growth (indexed) in the different periods. In the end, the tree species are classified into 4 classes with the principal component and cluster analysis.

To conclude, this master thesis discovered trees reactions to the 8 strongest drought events in urban trees. Trees responses are classified into 4 classes, which can be generalized as follow: *Sophora japonica*, which show extremely low resistance value and extremely strong recovery value.

The second class is represented by tree species, which show a similar response to the previous tree species, but less sharp: *Pyrus communis*, *Pawlonia tormentosa* and *Betula pendula*.

The third class comprehends *Fraxinus excelsior*, *Prunus umineko*, *Pinus rufinerve* and *Amelanchier lamarckii*, which are characterized by high resistance and resilience value and weak recovery values.

The fourth class shows *Crataegus levigata and lavellei*, *Magnolia kobus*, *Ailanthus altissima*, *Robinia pseudoacacia*, *Acer platanoides and rufinerve*, *Tilia europea*, *Cercidiphyllum japonicum*, *Picea omorika* and *Catalpa bignoides*. This latter class seems to have similar values of resistance, resilience and recovery: They show moderate resistance, resilience and recovery values.

The tree species which show good responses to the drought events are the tree species with the highest tolerance indexes, and they are: *Amelanchier lamarckii*, *Prunus umineko*, *Fraxinus excelsior*, *Pinus sylvestris*, *Sophora japonica*, *Ailanthus altissima* and *Robinia pseudoacacia*. They are ordered depending on the strength of the tolerance indexes. *Prunus umineko* and *Fraxinus excelsior* show low differences in tree growth during PDDE in comparison to PBDE and PDDE in comparison to PADE. In addition, they show no differences in tree growth during PBDE in comparison to PADE. Therefore, these 2 tree species are considered among the most appropriate to survive the drought events in urban environment. However, this thesis does not consider enough aspects to determine which tree species is best suited to be planted in an urban area in the future. Some species can be generalized, but some reactions is studied deeply by considering biological aspects, soil types, the status of the trees, size of the trees, timing, and so on. Furthermore, it is considered that some tree species do not have enough samples to allow a generalization at a species level. Results for *Aesculus hippocastanum*, *Catalpa bignonioides*, *Sophora japonica*, *Cercidiphyllum japonicum*, *Paulownia tormentosa*, *Amelanchier lamarckii*, *Pinus sylvestris* and *Fraxinus excelsior* can not be considered attainable. Results for *Crataegus levigata and lavellei*, *Magnolia kobus* and *Picea omorika* should also be considered carefully.

Further studies are required to assess with reliability the tree's reactions to the drought events within the city.

6 Literature

1. Adhyani N.L., June T., Sopaheluwakan A., 2017, Exposure to Drought: Duration, Severity and Intensity (Java, Bali and Nusa Tenggara). IOP Conf. Ser.: Earth Environ. Sci. Vol. 58, pp. 11-14.

2. Abramowitz M., Stegun I.A., 1965, Handbook of Mathematical Functions: With Formulas, Graphs, and Mathematical Tables. Dover Publications: Mineola.

3. Anderegg W.R.L., Trugman A., Badgley G., Konings A.G., Shaw J., 2020, Divergent forest sensitivity to repeated extreme drought events. Nature Climate Change. Vol. 10. pp. 1-20.

4. Bae S., Lee S.-H., Yoo S.-H., Kim T.„ 2018, Analysis of Drought Intensity and Trends Using the Modified SPEI in South Korea from 1981 to 2010. Water. Vol. 10, Issue 327.

5. Barnette J.J., McLean J.E., 1998, The Tukey Honestly Significant Difference Procedure and Its Control of the Type I Error-Rate. Paper presented at the Annual Meeting of the Mid-South Educational Research Association (27th, New Orleans, LA, November 4-6, 1998). Reports Research (143) Speeches/Meeting Papers (150).

6. Barzagli F., Mani F., 2019, The increased anthropogenic gas emissions in the atmosphere and the rising of the Earth's temperature: are there actions to mitigate the global warming? Substantia. An International Journal of the History of Chemistry, Vol. 3, No. 1, pp. 101-111.

7. Batllori E., Lloret F., Aakala T., Anderegg W.R.L., et al., 2020, Forest and woodland replacement patterns following drought-related mortality. PNAS. Vol. 117. No. 47. pp. 29720-29729.

8. Bayaziz M., Önoz B., 2007, To prewhiten or not to prewhiten in trend analysis? Hydrological Sciences Journal. Vol. 52, Issue 4, pp. 611-624.

9. Becker R.A., Chambers J.M., Wilks A.R., 1988, The New S Language. Wadsworth and Brooks/Cole.

10. Blain G., 2013, The Mann-Kendall test: The need to consider the interaction between serial correlation and trend. Maringá. V. 35, No. 4, pp. 393-402.

11. Bohner T., Diez J., 2021, Tree resistance and recovery from drought mediated by multiple abiotic and biotic processes across a large geographic gradient. Science of the Total Environment. Vol. 789. No. 147744. pp. 1-10.

12. Bolte A., Ammer C., Lof M., Madsen P., Nabuurs G.-J., Schall P., Spathelf P., Rock J., 2009, Adaptive forest management in central Europe: climate change impacts, strategies and integrative concept. Scandinavian Journal of Forest Research, Vol. 24, pp. 473–482.

13. Bose A.K., Gessler A., Bolte A., Bottero A., Buras A., Cailleret M., Camarero J.J., Haeni M., Heres A.-M., Hevia A., Lévesque M., Linares J.C., Vilalta J.M., Matias L., Menzel A., Sánchez-Salguero R., Saurer M., Vennetier M., Ziche D., Rigling A., 2019, Growth and resilience responses of Scots pine to extreme drought events across Europe depend on predrought growth conditions. Glob Change Biol. Vol. 00, pp. 1–17.

14. Brito S.S.B., Cunha A.P.M.A., Cunningham C.C., Alvalá R.C., Marengo J.A., Carvalho M.A., 2017, Frequency, duration and severity of drought in the Semiarid Northeast Brazil region. Int. J. Climatol.

15. Brodribb T.J., 2020, Learning from a century of drought events. Nature Ecology and Evolution. Vol. 4. pp. 1007–1008.

16. Brunner M.I., Liechti K., Zappa M., Extremeness of recent drought events in Switzerland: dependence on variable and return period choice. Nat. Hazards Earth Syst. Sci., Vol. 19, pp. 2311–2323.

17. Bunn A., Korpela M., Biondi F., Campelo F., Merian P., Qeadan F., Zang C., 2018, dplR: Dendrochronology program library in R. R package version 1.6.4.

18. Bunn A., Korpela M., 2020, Crossdating in dplR. Processed with dplR 1.7.1 in R version 3.6.2 (2019-12-12). pp. 1-12.

19. Buras, A. and Wilmking, M. (2015) Correcting the calculation of Gleichläufigkeit, Dendrochronologia 34, 29-30.

20. Cadro S., Uzunovic M., HOW TO USE: Package 'SPEI' For BASIC CALCULATIONS, 2013.

21. Camarero J., Gazol A., Sanguesa-Barreda G., Cantero A., Sanchez-Salguero R., Sanchez-Miranda A., Granda E., Serra-Maluquer, Ibanez R., 2018, Forest Growth Responses to Drought at Short- and Long-Term Scales in Spain: Squeezing the Stress Memory from Tree Rings. Front. Ecol. Evol. Vol. 6. No. 9. pp. 1-11.

22. Cavin L., Jump A., Highest drought sensitivity and lowest resistance to growth suppression are found in the range core of the tree Fagus sylvatica L. not the equatorial range edge. Global Change Biology. Vol. 23. pp. 362–379.

23. Cavus Y., Aksoy H., 2020, Critical drought severity/intensity-duration-frequency curves based on precipitation deficit. Vol. 584, pp. 1-14.

24. Chen J., MacEachren A.M., Peuquet D.J., 2009, Constructing Overview + Detail Dendrogram-Matrix Views. IEEE TRANSACTIONS ON VISUALIZATION AND COMPUTER GRAPHICS. VOL. 15. NO. 6. pp. 889-896.

25. Chen T., van der Werf G.R., de Jeu R.A.M., Wang, G., Dolman, A.J., 2013, A global analysis of the impact of drought on net primary productivity. Hydrol. Earth Syst. Sci., Vol. 17, pp. 3885–3894.

26. Choat B., Brodribb T.J., Brodersen C.R., Duursma R.A., Lopez R., Medlyn B.E., 2018, Triggers of tree mortality under drought. NATURE. Vol. 558. pp. 531-541.

27. Churkina G., Running S., 1998, Contrasting climatic controls on the estimated productivity of global terrestrial biomes. Ecosystems, Vol. 1, pp. 206–215.

28. Clark J., Iverson L., Woodall C.W., Allen C.D., Bell D.M., Bragg D.C., D'Amato A.W., Davis F.W., Hersh M.H., Ibanez I., Jackson S.T., Matthews S., Pederson N., Peters M., Schwartz M.W., Waring K.M., Zimmermann N.E., 2016, The impacts of increasing drought on forest dynamics, structure, and biodiversity in the United States. Global Change Biology, pp. 1-24.

29. Cook, E.R., Kairiukstis, L.A., 1990. Methods of Dendrochronology: Applications in the Environmental Science. Kluwer Academic Publishers, Doredrecht, 394 pp.

30. Dai A., Zhao T., Chen J., 2018, Climate Change and Drought: a Precipitation and Evaporation Perspective. Current Climate Change Reports.

31. Dalezios N.R., Athanasios L., Vasiliades L., Liakopoulos E., 2000, Severity-duration-frequency analysis of drought events and wet periods in Greece. Hydrological Sciences-Journal-des Sciences Hydrologiques, Vol. 45, No. 5, pp. 751-769.

32. Danandeh Mehr A., Şorman Ü.A., Kahya E., Afshar M.H., 2019, Climate change impacts on meteorological drought using SPI and SPEI: case study of Ankara, Turkey. Hydrological Sciences Journal/Journal des Sciences Hydrologiques, Vol. 65, No.2.

33. DeSoto L., Cailleret M., Sterck F., Jansen S., et al., 2020, Low growth resilience to drought is related to future mortality risk in trees. NATURE COMMUNICATIONS. Vol. 11. No. 545. pp. 1-10.

34. Diani K., Kacimi I., Zemzami M., Tabyaoui H., Haghighi A.T., 2019, Evaluation of meteorological drought using the Standardized Precipitation Index (SPI) in the High Ziz River basin, Morocco. Limnol. Rev. Vol. 19, Issue 3, pp. 125–135.

35. Ditmarová L., Kurjak D., Palmroth S., Kmet' J., Strelcová K., 2010, Physiological responses of Norway spruce (Picea abies) seedlings to drought stress. Tree Physiol. Vol. 30. pp. 205–213.

36. Fachplanung Hitzeminderung, 2020. Stadt Zürich (Hrsg.). Zürich.

37. Fang O., Zhang Q.-B., Vitasse Y., Zweifel R., Cherubini P., 2021, The frequency and severity of past drought events shape the drought sensitivity of juniper trees on the Tibetan plateau. Forest Ecology and Management, Vol. 486, No. 118968, pp. 1-7.

38. Flexas J., and Medrano H., 2002, Drought-inhibition of photosynthesis in C3 plants: Stomatal and non-stomatal limitations revisited. Annals of Botany, Vol. 89, No.2, pp. 183–189.

39. Federal Department of the Environment, Transport, Energy and Communications Federal Office for the Environment, 2020, Data, indicators, maps. Retrieved 20.12.2020. from: https://www.bafu.admin.ch/bafu/en/home.htm

40. Federal Department of the Environment, Transport, Energy and Communications Federal Office for the Environment, 2020, Publications, media. Retrieved 20.12.2020. from: https://www.bafu.admin.ch/bafu/en/home.html.

41. Federal Office of Meteorology and Climatology MeteoSwiss, 2020, Measurement values. Retrieved 20.12.2020. from: https://www.meteoswiss.admin.ch/home/measurement-values.html?param=messwerte-niederschlag-10min&table=true&chart=month&sortDirection=&station=KLO.

42. Federal Office of Meteorology and Climatology Federal Statistic Office, 2020, Look for statistics. retrieved 20.12.2020 from: https://www.bfs.admin.ch/bfs/en/home/statistics/territory-environment.html.

43. Fowler A and Boswijk G., 2003,. "Chronology stripping as a tool for enhancing the statistical quality of tree-ring chronologies." Tree-Ring Research, Vol. 9, No. 2, pp. 53–62.

44. Fritts, H.C., 1976. Tree Rings and Climate. Academic Press, New York, pp. 567.

45. Fritts H.C., 2001, Tree Rings and Climate. The Blackburn. Press.

46. Gastwirth J.L., Gel Y.R., Miao W., 2010, The Impact of Levene's Test of Equality of Variances on Statistical Theory and Practice. Statistical Science. Vol. 24. No. 3. pp. 343–360.

47. Gedalof, Z., Smith, D.J., 2001. Dendroclimatic response of mountain hemlock (Tsuga mertensiana) in Pacific North America. Canadian Journal of Forest Research. Vol. 31, pp. 322–332.

48. Gilbert R.O., 1987, Statistical Methods for Environmental Pollution Monitoring, Wiley, NY.

49. Grubbs F.E., 1969, Procedures for Detecting Outlying Observations in Samples. Technometrics, Vol. 11. No. 1. pp. 1-21.

50. Hagedorn F., Joseph J., Peter M., Luster J., Pritsch K., et al., 2016, Recovery of trees from drought depends on belowground sink control. NATURE PLANTS. Vol. 2. pp. 1-5.

51. Haines A., Klingmller K., Pozzer A., Burnett R.T., Lelieveld J., Ramanathan V., 2019, Effects of fossil fuel and total anthropogenic emission removal on public health and climate. Proceedings of the National

Academy of Sciences of the United States of America. Vol. 116, No. 15, pp. 7192-7197.

52. Hanusz Z., Tarasinska J., Zielinski W., 2014, SHAPIRO–WILK TEST WITH KNOWN MEAN. Statistical Journal. Vol. 14. No. 1. pp. 89–100.

53. Hari V., Rakovec O., Markonis Y., Hanel M., Kumar R., 2020,IIncreased future occurrences of the exceptional 2018–2019 Central European drought under global warming. Springer Nature journal, scientific report. pp. 1-10.

54. Holand S.M., 2019, PRINCIPAL COMPONENTS ANALYSIS (PCA). pp. 1-12.

55. Hsiao T.C., 1973, Plant responses to water stress. Annu. Rev. Plant Physiol. Plant Mol. Biol. Vol. 24. pp. 519–570.

56. Huang M., Wang X., Keenan T.F., Piao S., 2018, Drought timing influences the legacy of tree growth recovery. Glob Change Biol., pp. 1–14.

57. Jansma, E., 1995, RemembeRINGs; The development and application of local and regional tree-ring chronologies of oak for the purposes of archaeological and historical research in the Netherlands, Nederlandse Archeologische Rapporten 19, Rijksdienst voor het Oudheidkundig Bodemonderzoek, Amersfoort.

58. Jolliffe I.T., Cadima J., 2016, Principal component analysis: a review and recent developments. s.Phil. Trans. R. Soc. A. Vol. 374. pp. 1-16.

59. Kafadar K., he Efficiency of the Biweight as a Robust Estimator of Location. JOURNAL OF RESEARCH ofthe Notional Bureau of Standards. Vol. 88, No. 2.

60. Kaoungku N., Suksut K., Chanklan R., Kerdprasop K., Kerdprasop N.,2018, The Silhouette Width Criterion for Clustering and Association Mining to Select Image Features. International Journal of Machine Learning and Computing, Vol. 8. No. 1. pp. 69-73.

61. Kariuki M., 2002, Height estimation in complete stem analysis using annual radial growth measurements. Forestry, Vol. 75, No. 1, pp. 63.74.

62. Kassambara A., 2017, Practical Guide To Cluster Analysis in R. Unsupervised Machine Learning. Published by STHDA. pp. 1-187.

63. Kaufman L., Rousseeuw P.J., 1990, Finding Groups in Data. An Introduction to Cluster Analysis. A JOHN WILEY AND SONS, INC., PUBLICATION. pp. 1-355.

64. Kendall, M., 1938, A New Measure of Rank Correlation. Biometrika. Vol. 30, No. 1–2), pp. 81–89.

65. Kendall M.G., 1945, The treatment of ties in rank problems. Biometrika. Vol. 33 pp. 239–251.

66. Kew S.F., Philip S.Y., Hauser M., Hobbins M., Wanders N., van Oldenborgh G.J., van der Wiel K., Veldkamp T.I.E., Kimutai J., Funk C., Otto F.E.L., 2019, Impact of precipitation and increasing temperatures on drought in eastern Africa. Earth Syst. Dynam. Discuss. pp. 1-29.

67. Kim T.K., 2005, Understanding one-way ANOVA using conceptual figures. Korean Journal of Anesthesiology. Vol. 70. No. 1. pp. 22-26.

68. Kim T.-W., Jehanzaib, 2020, Drought Risk Analysis, Forecasting and Assessment under Climate Change. Water, Vol. 12, No. 1862, pp. 2-7.

69. Kolus H.R., Huntzinger D.N., Schwalm C.R., Fisher J.B., McKay N., Fang Y., Michalak A.M., Schaefer K., Wei Y., Poulter B., Mao J., Parazoo N.C., Shi X., 2019, Land carbon models underestimate the severity and duration of drought's impact on plant productivity. Scientific reports. Vol. 9. No. 2758. pp. 1-10.

70. Kumar S., Merwade V., Kam J., Thurner K., 2009, Streamflow trends in Indiana: Effects of long-term persistence, precipitation and subsurface drains. J. Hydrol. Vol. 374, pp. 171–183.

71. Li W. G., YI X., Hou M. T., Chen H. L., Chen Z. L., 2012, Standardized precipitation evapotranspiration index shows drought trends in China. Chinese Journal of Eco-Agriculture, Vol. 20, No. 5, pp. 643-649.

72. Lin H., Wang J., Li F., Xie Y., Jiang C., Sun L., 2020, Drought Trends and the Extreme Drought Frequency and Characteristics under Climate Change Based on SPI and HI in the Upper and Middle Reaches of the Huai River Basin, China. Water, Vol. 12, No. 1100, pp. 1-19.

73. Lloret F., Keeling E.G., Sala A., 2011, Components of tree resilience: effects of successive low-growth episodes in old ponderosa pine forests. Oikos, Vol. 120, pp. 1909–1920-

74. Lobo-do-Vale R., Besson C.K., Caldeira M.C., Chaves M.M., Pereira J.S., 2019, Drought reduces tree growing season length but increases nitrogen resorption efficiency in a Mediterranean ecosystem. Biogeosciences. Vol. 16. pp. 1265–1279.

75. Luyssaert S., Ciais P., Piao S., Schulze E.-D., Jung M., Zahele S., Schelhaas M.J., Reichstein M., Churkina G., Papale D., Abril G., Beer C., Grace J., Loustau D., Matteucci G., Magnanis F., Nabuurs G.J., Verbeeck H., Sulkava M., van der Werf G.R., Janssens I.A., Carboeurope-IP Synthesis team, 2010, The European carbon balance. Part 3: forsts. Global Change Biology, Vol. 16, pp. 1429–1450.

76. Madrigal-Gonzalez J., Herrero A., Ruiz-Benito P., Zavala M.A., 2017, Resilience to drought in a dry forest: Insights from demographic rates. / Forest Ecology and Management. Vol. 389. pp. 167-175.

77. Mamat A.R., Mohamed F.S., Mohamed M.F., Rawi N.M, Awang M.I., 2018, Silhouette index for determining optimal k-means clustering on images in different color models. International Journal of Engineering and Technology. Vol. 7. pp. 105-109.

78. Maxwell R.S., Wixom J.A., Hessl A.E., 2011, A comparison of two techniques for measuring and crossdating tree rings. Dendrochronologia. Vol. 29, pp. 237–243.

79. Markonis Y., Kumar R., Hanel M., Rakovec O., Máca P., AghaKouchack A., 2021, The rise of compound warm-season drought events in Europe. , Sci. Adv., pp. 1-7.

80. McKee T.B., Doesken N.J., Kleist J., 1993, The relationship of drought frequency and duration to time scales. In Proceedings of the Eighth Conference on Applied Climatology. pp. 179–184.

81. McDowell N.G., 2011. Mechanisms linking drought, hydraulics, carbon metabolism, and vegetation mortality. Plant Physiol. Vol. 155. pp. 1051–1059.

82. McDowell N., Pockman W.T., Allen, C.D., et al. 2008, Mechanisms of plant survival and mortality during drought: why do some plants survive while others succumb to drought? New Phytol. Vol. 178.

pp. 719–739.

83. McLeod A.I., 2015, Kendall rank correlation and Mann-Kendall trend test. V. 2.2.

84. Mesa H., Restrepo G., 2008, 2008, On dendrograms and topologies. MATCH Commun. Math. Comput. Chem. Vol. 60. pp. 371-384.

85. Mondal A., Kundu S., MukhoPADEhyay A., 2012, Rainfall trend analysis by Mann-Kendall test: A case study of North-Eastern part of Cuttack district, Orissa. International Journal of Geology, Earth and Environmental Sciences. Vol. 2, No. 1, pp. 70-78.

86. Morid S., Smakhtin V., Moghaddasi M., 2006, Comparison of seven meteorological indices for drought monitoring in Iran. Int. J. Climatol. Vol. 26, pp. 971–985.

87. Morissette L., Chartier S., 2013, The k-means clustering technique: General considerations and implementation in Mathematica. Tutorials in Quantitative Methods for Psychology. Vol. 9. No. 1. pp. 15-24.

88. Mosteller F. and Tukey J.W., 1977, Data Analysis and Regression: a second course in statistics. Addison-Wesley.

89. Munalula F., Seifert T., Meincken M., 2017, The Expected Effects of Climate Change on Tree Growth and Wood Quality in Southern Africa. Springer Science Reviews.

90. Myhre G., Shindell D., Bréon F.-M., Collins W., Fuglestvedt J., Huang J., Koch D., Lamarque J.-F, Lee D., Mendoza B., Nakajima T., Robock A., Stephens G., Takemura T., Zhang H., 2013, Anthropogenic and Natural Radiative Forcing Supplementary Material. In: Climate Change 2013: The Physical Science Basis. Contribution of Working Group I to the Fifth Assessment Report of the Intergovernmental Panel on Climate Change (Stocker T.F., Qin D., Plattner G.-K., Tignor M., Allen S.K., Boschung J., Nauels A., Xia Y., Bex V., Midgley P.M.).

91. Nanda A., Mohapatra B.B., Mahapatra A.P.K., Mahapatra A.P.K., Mahapatra A.P.K., 2021, Multiple comparison test by Tukey's honestly significant difference (HSD): Do the confident level control type I error. International Journal of Statistics and Applied Mathematics. Vol. 6. No. 1. pp. 59-65.

92. Navarro-Cerrillo R.M., Rodriguez-Vallejo C., Silveiro E., Hortal A., Palacios-Rodríguez G., Duque-Lazo J., Camarero J.J., 2018, Cumulative Drought Stress Leads to a Loss of Growth Resilience and Explains Higher Mortality in Planted than in Naturally Regenerated Pinus pinaster Stands. Forests. Vol. 9. No. 358. pp. 1-18.

93. Nedealcov M., Răileanu V., Sîrbu R., Cojocari R., 2015, THE USE OF STANDARDIZED INDICATORS (SPI AND SPEI) IN PREDICTING drought events OVER THE REPUBLIC OF MOLDOVA TERRITORY. PESD, Vol. 9, No. 2. pp. 149-158.

94. Niessner A., 2013, Stem growth dynamics of Picea glauca (Moench) Voss in interior Alaska. Master thesis. pp. 1-95.

95. North M., Manley P.N., 2012, Managing Sierra Nevada Forests. United States Department of Agriculture. Forest Service. pp. 1-197.

96. Osborne J. W., Overbay A., 2004. The power of outliers (and why researchers should ALWAYS check for them). Practical Assessment, Research and Evaluation, Vol. 9. No. 6.

97. Ostertagová E., Ostertag O., 2013, Methodology and Application of One-way ANOVA. American Journal of Mechanical Engineering, Vol. 1. No. 7. pp. 256-261.

98. Ostertagová E., Ostertag O., Kováč J., 2014, Methodology and Application of the Kruskal-Wallis Test. Applied Mechanics and Materials. Vol. 611. pp 115-120.

99. Parlow E., Fehrenbach U., Scherer D., 2014, Klimaanalyse der Stadt Zrich (KLAZ). Regio Basiliensis, Vol. 55, No. 3, pp. 143-164.

100. Pei Z., Fang S., Wang L., Yang W., 2020, Comparative Analysis of Drought Indicated by the SPI and SPEI at Various Timescales in Inner Mongolia, China. Water, Vol. 12, pp. 1-20.

101. Pohlert T., 2020, Non-Parametric Trend Tests and Change-Point Detection. pp. 1-18.

102. Potop, V. Evolution of drought severity and its impact on corn in the Republic of Moldova, 2011. Theor. Appl. Climatol. Vol. 105, pp. 469–483.

103. Potop V., Mozny M., Soukup J., 2012, Drought evolution at various time scales in the lowland regions and their impact on vegetable crops in the Czech Republic. Agric. Forest Meteorol. Vol. 156, pp. 121–133.

104. Pretzsch H., Schutze G., Uhl E., 2013, Resistance of European tree species to drought stress in mixed versus pure forests: evidence of stress release by inter-specific facilitation. Plant Biology, Vol. 15, pp. 483–495.

105. R Development Core Team. (2018). R: A language and environment for statistical computing. Vienna, Austria: R Foundation for Statistical Computing.

106. Reddy A.R., Chaitanya K.V., Vivekanandan M., 2004, Drought induced responses of photosynthesis and antioxidant metabolism in higher plants. Journal of Plant Physiology, Vol. 161, No. 11, pp. 1189–1202.

107. Richman M.B., Leslie L.M., 2015, Uniqueness and Causes of the California Drought. Procedia Computer Science, Vol. 61, p. 428 – 435.

108. Rinn Tech, 2010. TSAP-WIN: Time Series Analysis and Presentation Dendrochonology and Related Applications.

109. Rorabacher D.B., 1991, Statistical Treatment for Rejection of Deviant Values: Critical Values of Dixon's "Q" Parameter and Related Subrange Ratios at the 95% Confidence Level. Anal. Chem. Vol. 63. pp. 139-146.

110. Saxe H., Cannell M.G.R., Johnsen O., Ryan M.G., Vourlitis G., 2001, Tree and forest functioning in response to global warming. New Phytologist. Vol. 149, pp. 369–400.

111. Samuels P., Gilchrist M., 2014, Pearson Correlation. pp. 1-4.

112. Sánchez-Salguero R., Colangelo M., Matias L., Ripullone F., Camarero J.J., 2020, Shifts in Growth Responses to Climate and Exceeded Drought-Vulnerability Thresholds Characterize Dieback in Two

Mediterranean Deciduous Oaks. Vol. 11, No. 714, pp 1-19.

113. Saravi M.M., Safdari A.A., Malekian A., 2009, Intensity-Duration-Frequency and spatial analysis of drought events using the Standardized Precipitation Index. Hydrol. Earth Syst. Sci. Discuss., Vol. 6, pp. 1347–1383.

114. Sawyer S., 2009, Analysis of Variance: The Fundamental Concepts. The Journal of Manual and Manipulative Therapy. Vol. 17. No. 2. pp. 27-38.

115. Serra-Maluquer X., Mencuccini M., Martinez-Vilalta J., 2018, Changes in tree resistance, recovery and resilience across three successive extreme drought events in the northeast Iberian Peninsula. Oecologia. Vol. 187. pp. 343–354.

116. Schr C., Vidale P., Luthi D., Frei C., Haberli C., Liniger M., Appenzeller C., 2004, The role of increasing temperature variability in European summer heatwaves. Nature, Vol. 427, pp. 332–336.

117. Schober P., Boer C., Schwarte L.A., 2018, Correlation Coefficients: Appropriate Use and Interpretation. ANESTHESIA AND ANALGESIA. Vol. 126, No. 5, pp. 1763-1768.

118. Schwarz J., Skiadaresis G., Kohler M., Kunz J., Schnabel F., Vitali V., Bauhus J., 2020, Quantifying Growth Responses of Trees to Drought—a Critique of Commonly Used Resilience Indices and Recommendations for Future Studies. Current Forestry Reports. Vol. 6. pp. 185–200.

119. Schweingruber, F. H. (1988) Tree rings: basics and applications of dendrochronology, Kluwer Academic Publishers, Dordrecht, Netherlands, p. 276.

120. Sedgwick P., 2012, Pearson's correlation coefficient. BMJ. Vol. 345, No. 4483, pp. 1-2.

121. Sicard P., Mangin A., Hebel P., Mallea P., 2010, Detection and estimation trends linked to air quality and mortality on French Riviera over the 1990–2005 period. Sci. Total Environ. Vol. 408, pp. 1943–1950.

122. Shewchuk, J. R. (1997) Adaptive Precision Floating-Point Arithmetic and Fast Robust Geometric Predicates. Discrete and Computational Geometry. Vol. 18, No. 3, pp. 305-363.

123. Shukla Shraddhanand, Steinemann Anne, Iacobellis Sam F., Cayan Daniel R., 2015, Annual Drought in California: Association with Monthly Precipitation and Climate Phases. Journal of Applied Meteorology and Climatology, Vol. 54, No. 11, pp. 2273-2281.

124. Singh V.P., Guo H., Yu F.X., 1993, Parameter estimation for 3-parameter log-logistic distribution. Pome. Stoch. Hydrol. Hydraul. Vol. 7, pp. 163–177.

125. Soltani M., Rousta I., Modir Taheri S.S., 2013. Using Mann-Kendall and Time series Techniques for Statistical Analysis of Long-Term Precipitation in Gorgan Weather Station. World Applied Science Journal. Vol. 28, No. 7, pp. 902-908.

126. Summary for Policymakers. In: Global Warming of 1.5°C. An IPCC Special Report on the impacts of global warming of 1.5°C above pre-industrial levels and related global greenhouse gas emission pathways, in the context of strengthening the global response to the threat of climate change, sustainable development, and efforts to eradicate poverty (Masson-Delmotte V., Zhai P., PörtnerH.-O., Roberts D., Skea J., Shukla P.R., Pirani A., Moufouma-Okia W., Péan C., Pidcock R., Connors S., Matthews J.B.R., Chen Y., Zhou X., Gomis M.I., Lonnoy E., Maycock T., Tignor M., Waterfield T.). World Meteorological Organization, Geneva, Switzerland, pp. 1-32.

127. Tan C., Yang J., Li M., 2015, Temporal-Spatial Variation of Drought Indicated by SPI and SPEI in Ningxia Hui Autonomous Region, China. Atmosphere. Vol. 6. pp. 1399-1421.

128. Thornthwaite C.W., 1948, An approach toward a rational classification of climate. Geogr. Rev. Vol. 38, pp. 55–94.

129. Thrun M.C., 2018, , Projection-Based Clustering through Self-Organization and Swarm Intelligence. pp 21-32.

130. Urvoy M., Autrusseau F., 2014, Application of Grubbs' Test for Outliers to the Detection of Watermarks. IH and MMSEC' 14, June 11–13, 2014, Salzburg, Austria.

131. Vargha A., Delaney H., 1998, The Kruskal-Wallis Test and Stochastic Homogeneity. Journal of Educational and Behavioral Statistics. Vol. 23. No. 2. pp. 170-192.

132. Verma M.P., Suarez A. M.C., 2014, DixonTest.CriticalValues: A Computer Code to Calculate Critical Values for the Dixon Statistical Data Treatment Approach. Journal of Statistical Software. Vol. 57, No. 2. pp. 1-12.

133. Verma S.P., Quiroz-Ruiz A., 2006, Critical values for six Dixon tests for outliers in normal samples up to sizes 100, and applications in science and engineering. Revista Mexicana de Ciencias Geológicas, Vol. 23, No. 2, pp. 133-161.

134. Vicente-Serrano S.M., Begueria S., Lopez-Moreno J.I., 2010, A Multiscalar Drought Index Sensitive to Global Warming: The Standardized Precipitation Evapotranspiration Index. Journal of Climate, Vol. 23, No.7, pp. 1696-1718.

135. Vicente-Serrano S.M., Lopez-Moreno J.-I., Beguería S., Lorenzo-Lacruz J., Sanchez-Lorenzo A., García-Ruiz J.M., Azorin-Molina C., Morán-Tejeda E., Revuelto J., Trigo R., 2014, Evidence of increasing drought severity caused by temperature rise in southern Europe. Environ. Res. Lett. Vol. 9, pp. 1–9.

136. Vila-Cabrera A., Jump A.S., 2019, Greater growth stability of trees in marginal habitats suggests a patchy pattern of population loss and retention in response to increased drought at the rear edge. Ecology Letters. Vol. 22. pp. 1439–1448.

137. Visser, R.M. (2020) On the similarity of tree-ring patterns: Assessing the influence of semi-synchronous growth changes on the Gleichläufigkeit for big tree-ring data sets,Archaeometry, 63, 204-215.

138. Wang F., Shao W., Yu H., Kan G., He X., Zhang D., Ren M., Wang G., 2020, Re-evaluation of the Power of the Mann-Kendall Test for Detecting Monotonic Trends in Hydrometeorological Time Series. Earth Sci. Vol. 8, No. 14, pp. 1-12.

139. Wang S.Y., Zheng G.F., Yang J., Li X., 2012, Application of three drought evaluation indices in Ningxia. J. Desert Res. Vol. 32, pp. 517–524.

140. Whyte G., Howard K., Hardy G.E.St.J., Burgess T.I., 2016, The Tree Decline Recovery Seesaw; a conceptual model of the decline and recovery of drought stressed plantation trees. Forest Ecology and Management. Vol. 370. pp. 102–113.

141. Wu H., Li Y., 2012, A Clustering Method Based on K-Means Algorithm. Physics Procedia. Vol. 25. pp. 1104–1109.

142. Yudav R., Tripathi S.K., Pranuthi G., Dubey S.K., 2014, Trend analysis by Mann-Kendall test for precipitation and temperature for thirteen districts of Uttarakhand. Journal of Agrometeorology. Vol. 16, No. 2, pp. 164-171.

143. Yue S., Wang C.Y., 2002, Applicability of prewhitening to eliminate the influence of serial correlation on the Mann–Kendall test. Water Resour. Res. Vol. 38, pp. 1-7.

144. Zang C., Hartl-Meier C., Dittmar C., Rothe A., Menzel A., 2014, Patterns of drought tolerance in major European temperate forest trees: climatic drivers and levels of variability. Global Change Biology, Vol. 20, pp. 3767–3779.

145. Zhang Q., Liu, C.L., Xu C.Y., Xu Y.P., Jiang, T., 2006, Observed trends of annual maximum water level and streamflow during past 130 years in the Yangtze River Basin, China. J. Hydrol. Vol. 324, pp. 255–265.

7 Appendix

Table 13: SPEI with a timescale of 1 over the 1981-2020 period. In red are showed SPEI values below -1, whilein yellow are represented the values below 0 and above -1. 0 values coloured mean that the value isapproximated but within the range

$SPEI_1$												
year	Jan	Feb	Mar	Apr	May	Jun	Jul	Aug	Sep	Oct	Nov	Dec
1981	0.81	-1.03	0.95	-1.21	0.06	-1.31	0.77	0	1.89	2.12	-0.49	1.82
1982	1.59	-1.68	-0.02	-0.49	-1.44	1	0.4	1.47	-1.13	0.98	-0.07	0.6
1983	0.4	0.56	0.22	0.35	1.01	-0.74	-1.68	-1.34	0.85	-1.08	0.66	-0.99
1984	0.83	0.47	-0.85	0	-0.16	-0.62	-0.68	-0.66	2.08	-0.48	-0.11	-0.45
1985	0.35	0.28	-0.41	0.8	0.18	0.24	-1.08	-0.36	-1.24	-1.76	1.34	-0.49
1986	1.6	0.04	0.44	1.97	0.7	0	0.06	1.29	-1.48	-0.28	-0.82	0.12
1987	-0.4	1.08	0.46	-0.24	0.97	1.93	-0.09	0.24	1.28	-1.05	-0.22	-0.75
1988	-0.21	-0.1	2.11	-0.17	0.24	0.41	0.63	1.21	0.04	0.57	-0.3	0.78
1989	-1.67	0.73	-0.77	1.16	-1.32	-0.58	1.01	-0.29	-0.35	0.38	-0.93	-0.52
1990	-0.79	2.03	-0.93	-0.08	-0.57	1.41	-0.7	-1.37	0.83	0.81	1.47	-0.27
1991	-0.15	-1.41	-0.15	-0.2	0.71	1.65	-1.21	-2.15	0.03	-1.09	1.04	-0.33
1992	-1.32	0.32	0.64	0.41	-1.74	0.36	-0.19	-0.78	-0.65	1.72	1.89	0.21
1993	-1.35	-1.41	-0.41	-0.24	-0.3	-0.2	2.39	0.15	-0.04	0.55	-0.22	0.84
1994	0.93	-0.44	0.01	0.72	1.78	-0.89	-1.55	0.25	0.7	-0.23	-1.15	1.17
1995	1.49	1.11	1.1	0.32	1.36	0.67	-0.7	1	0.43	-2.03	-0.12	1.38
1996	-1.59	0	-0.3	-0.75	0.58	-0.53	0.79	0.42	-0.38	0.41	0.98	0.06
1997	-1.59	0.74	-1.92	0.14	-1.35	1.17	0.87	-0.45	-1.38	-0.1	-1.06	1.12
1998	0.5	-0.94	0.03	0.03	-1.84	0.23	-0.56	-1.06	1.54	1.24	1.34	-1.2
1999	-0.28	2.18	-0.31	0.54	1.95	1.29	-0.48	0.35	0.71	-0.72	0.87	1.24
2000	-0.93	1.74	0.42	-0.75	0.03	-1.21	1.65	0.45	0.79	-0.36	-0.1	-1.21
2001	0.94	-0.63	2.16	1.4	-0.46	1.33	0.29	-0.01	1.85	-0.35	0.64	-0.82
2002	-0.93	0.61	-0.33	-0.21	1.38	-0.94	-0.43	1.06	0.88	0.97	1.8	-0.24
2003	0.11	-0.85	-1.52	-0.67	-0.6	-2.1	-0.34	-1.14	-0.87	1.54	-0.14	-1.07
2004	1.78	-0.77	0.11	-0.94	0.86	0.42	0.26	-1.13	-0.44	0.94	-1.4	-0.78
2005	-0.94	-0.23	-0.43	1.03	-0.06	-0.51	0.2	1.38	-1.25	-0.04	-1.26	-0.03
2006	-0.99	0.42	1.76	1.91	0.71	-1.64	-1.63	1.84	0.32	-0.8	-0.94	-0.84
2007	-0.54	0.26	0.99	-1.97	0.03	-0.2	1.18	2.08	-0.17	-1.51	-0.55	0.61
2008	-0.25	-1.03	0.76	1.96	-1.35	-0.72	0.19	1.16	0.87	1.34	-1.05	-0.18
2009	-0.58	0.17	1.25	-1.56	-0.69	0.61	0.84	-1.22	-0.42	-0.74	0.96	0.97
2010	-0.72	-0.27	-0.08	-1.09	0.74	0.17	0.45	0.47	0.14	-0.74	0.14	0.77
2011	-0.37	-1.55	-1.74	-1.53	-0.77	-0.93	1.29	-0.47	-0.34	-0.23	-1.95	1.57
2012	0.58	-1.88	-2.36	-0.53	-0.51	1.14	0.88	0.8	0.46	0.79	0.56	1.56
2013	-0.12	0.36	0.32	0.49	1.54	-0.62	-1.01	-0.93	0.3	0.7	1.12	-1.03
2014	-0.46	0.33	-1.53	-0.04	-0.06	-0.17	1.11	0.28	-0.41	-0.33	0.13	-0.71
2015	0.6	-0.67	0.34	1.08	0.69	0.07	-1.67	-1.38	-1.04	-0.93	-0.54	-2.04
2016	1.74	0.75	-0.73	0.61	1.1	1.51	0.71	-1.14	-1.44	-0.29	0.66	-2.05
2017	0.55	-0.41	-0.48	0.63	-1.19	-1.13	0.42	-0.59	0.69	-1.29	0.43	0.78
2018	1.27	-0.3	0.34	-1.82	-0.74	-1.35	-1.31	0.11	-0.37	-0.96	-1.53	1.67
2019	0.06	-0.99	0.13	-0.49	0.66	-0.89	-0.61	0.31	-0.02	0.85	-0.45	-0.57
2020	-1.22	1.33	-0.65	-1.42	-0.69	0.33	-1.21	0.51	-1.83	0.41	-1.33	-0.07

Table 14: SPEI with a timescale of 2 over the 1981-2020 period. In red are showed SPEI values below -1, whilein yellow are represented the values below 0 and above -1. 0 values coloured mean that the value isapproximated but within the range

$SPEI_2$												
year	Jan	Feb	Mar	Apr	May	Jun	Jul	Aug	Sep	Oct	Nov	Dec
1981	0.09	0.1	0.23	-0.2	-0.75	-0.89	-0.4	0.49	1.57	2.32	1.38	1.19
1982	2.05	0.79	-1.01	-0.37	-1.36	-0.26	0.9	1.22	0.53	0.12	0.66	0.26
1983	0.71	0.6	0.31	0.4	0.93	0.22	-1.57	-1.83	-0.5	-0.15	-0.26	-0.26
1984	-0.02	0.9	-0.43	-0.39	-0.09	-0.56	-0.93	-0.91	1.52	1.55	-0.42	-0.55
1985	-0.06	0.36	-0.29	0.42	0.66	0.29	-0.71	-1.03	-1.07	-2.33	-0.07	0.81
1986	1.02	1.42	0.2	1.47	1.73	0.48	-0.09	0.84	0.17	-1.16	-0.77	-0.67
1987	-0.19	0.39	0.81	0.14	0.56	1.95	1.53	0	0.99	0.33	-0.95	-0.85
1988	-0.76	-0.4	1.94	1.62	0.08	0.45	0.6	1.16	0.82	0.4	0.22	0.25
1989	-0.52	-1.05	-0.19	0.56	-0.11	-1.38	0.24	0.51	-0.6	0.03	-0.32	-1.19
1990	-1.03	1.26	1.01	-0.5	-0.44	0.77	0.5	-1.25	-0.54	1.03	1.46	1.08
1991	-0.32	-1.1	-0.98	-0.2	0.39	1.62	0.37	-1.86	-1.58	-0.87	0.09	0.57
1992	-1.3	-1.08	0.51	0.67	-1.05	-1.07	-0.02	-0.64	-1.07	0.98	2.1	1.79
1993	-0.83	-2.18	-1.17	-0.38	-0.35	-0.36	1.77	1.92	-0.11	0.34	0.26	0.36
1994	1.18	0.53	-0.39	0.54	1.62	0.76	-1.56	-1.08	0.48	0.31	-0.96	0.02
1995	1.68	1.78	1.28	0.91	1.15	1.32	-0.15	0.07	0.87	-1.39	-1.73	0.94
1996	0.22	-1.57	-0.38	-0.76	-0.05	0.03	0.1	0.74	-0.1	0.04	0.94	0.77
1997	-1.17	-0.96	-0.76	-0.72	-0.9	-0.02	1.37	0.3	-1.18	-0.95	-0.8	0.03
1998	1.12	-0.19	-0.62	0.07	-1.37	-1.26	-0.36	-1.02	0.47	1.71	1.58	0.37
1999	-1.21	1.69	1.39	0.27	1.65	2.01	0.55	-0.22	0.56	-0.01	0.18	1.47
2000	0.46	0.79	1.26	-0.27	-0.45	-0.84	0.4	1.43	0.7	0.31	-0.32	-1.07
2001	-0.08	0.45	1.9	2.08	0.7	0.76	1.12	0.12	1.51	1.34	0.24	-0.16
2002	-1.42	-0.49	-0.02	-0.31	0.89	0.39	-0.94	0.31	1.22	1.16	1.75	1.48
2003	-0.09	-0.53	-1.57	-1.33	-0.85	-1.89	-1.47	-0.92	-1.38	0.74	1.04	-1
2004	0.91	1.33	-0.47	-0.67	0.04	0.85	0.34	-0.52	-1.18	0.42	-0.14	-1.65
2005	-1.38	-1.13	-0.6	0.58	0.67	-0.41	-0.3	1.02	0.37	-0.82	-0.88	-1.08
2006	-0.76	-0.71	1.63	1.99	1.69	-0.67	-1.89	0.08	1.6	-0.41	-1.27	-1.4
2007	-1.11	-0.43	0.79	-0.96	-1.34	-0.13	0.62	2.22	1.64	-1.38	-1.58	-0.08
2008	0.32	-0.98	0.02	1.57	0.61	-1.49	-0.44	0.83	1.3	1.37	0.44	-1.05
2009	-0.58	-0.53	1.02	-0.16	-1.51	-0.02	0.91	-0.14	-1.23	-0.89	0.25	1.34
2010	0.33	-0.97	-0.37	-0.96	-0.16	0.62	0.3	0.52	0.25	-0.5	-0.43	0.57
2011	0.37	-1.38	-2.04	-2.49	-1.54	-1.21	0.25	0.64	-0.71	-0.44	-1.54	-0.07
2012	1.46	-0.59	-2.5	-1.53	-0.69	0.56	1.36	1.04	0.72	0.8	0.88	1.52
2013	1.15	0.01	0.27	0.54	1.35	0.72	-1.12	-1.24	-0.65	0.64	1.18	0.21
2014	-1.21	-0.31	-0.89	-0.73	-0.05	-0.17	0.59	0.9	-0.23	-0.56	-0.14	-0.54
2015	-0.03	0.07	-0.22	0.91	1.15	0.52	-1.21	-1.84	-1.59	-1.44	-1.08	-1.89
2016	0.3	1.82	-0.15	0.15	1.13	1.71	1.58	-0.2	-1.6	-1.15	0.29	-1.02
2017	-1.21	0.15	-0.73	0.27	-0.42	-1.64	-0.53	-0.11	-0.12	-0.47	-0.62	0.79
2018	1.36	0.95	-0.06	-1.47	-1.72	-1.47	-1.61	-0.97	-0.32	-1.04	-1.82	0.36
2019	1.32	-0.66	-0.56	-0.27	0.17	-0.16	-1.01	-0.33	0.02	0.57	0.36	-0.89
2020	-1.43	0.03	0.38	-1.7	-1.41	-0.25	-0.75	-0.67	-0.72	-0.76	-0.56	-1.16

Table 15: SPEI with a timescale of 3 over the 1981-2020 period. In red are showed SPEI values below -1, while in yellow are represented the values below 0 and above -1. 0 values coloured mean that the value is approximated but within the range

$SPEI_3$												
year	Jan	Feb	Mar	Apr	May	Jun	Jul	Aug	Sep	Oct	Nov	Dec
1981	-0.4	-0.57	0.54	-0.65	-0.17	-1.33	-0.3	-0.39	1.66	2.44	1.86	1.94
1982	1.87	1.82	0.36	-0.97	-1.23	-0.51	-0.02	1.57	0.61	0.99	0.03	0.87
1983	0.37	0.86	0.34	0.4	0.77	0.31	-1.04	-1.86	-1.44	-1.06	0.24	-0.91
1984	0.24	0.09	0.07	-0.29	-0.42	-0.49	-0.94	-1.11	0.75	1.07	1.2	-0.72
1985	-0.36	-0.06	-0.16	0.31	0.35	0.59	-0.54	-0.82	-1.4	-1.8	-0.68	-0.41
1986	1.63	0.95	1.11	1.33	1.46	1.43	0.39	0.64	0.11	-0.07	-1.36	-0.69
1987	-0.91	0.37	0.35	0.42	0.58	1.63	1.82	1.39	0.66	0.24	0.12	-1.44
1988	-0.95	-0.97	1.71	1.48	1.46	0.23	0.72	1.15	0.98	0.97	0.13	0.62
1989	-0.83	-0.19	-1.19	0.61	-0.42	-0.48	-0.54	0.02	0.2	-0.33	-0.48	-0.67
1990	-1.53	0.77	0.37	0.67	-0.74	0.55	0.18	-0.26	-0.86	0	1.42	1.26
1991	0.79	-1.17	-0.94	-0.76	0.21	1.31	0.8	-0.72	-1.77	-1.89	0.02	-0.15
1992	-0.34	-1.21	-0.43	0.56	-0.62	-0.67	-1.03	-0.42	-0.92	0.29	1.61	2.01
1993	0.98	-1.67	-1.67	-0.9	-0.49	-0.46	1.43	1.55	1.7	0.2	0.13	0.68
1994	0.81	0.97	0.17	0.2	1.26	0.93	-0.47	-1.36	-0.77	0.23	-0.36	-0.05
1995	1.02	2.02	1.77	1.08	1.29	1.22	0.76	0.38	0.15	-0.47	-1.12	-0.49
1996	-0.13	0.07	-1.28	-0.75	-0.21	-0.41	0.48	0.25	0.4	0.12	0.55	0.87
1997	-0.31	-0.79	-1.53	-0.4	-1.39	0	0.49	0.94	-0.36	-1.1	-1.33	0.04
1998	0.25	0.73	-0.3	-0.39	-1.22	-1.01	-1.37	-0.81	-0.07	1.11	1.79	1.08
1999	0.05	0.89	1.03	1.26	1.22	1.95	1.71	0.61	0.05	0.03	0.45	0.87
2000	0.81	1.41	0.6	0.55	-0.23	-1.07	0.43	0.53	1.58	0.36	0.16	-1.12
2001	-0.36	-0.56	2.06	1.99	1.79	1.28	0.79	0.92	1.34	1.13	1.27	-0.28
2002	-0.78	-1.11	-0.67	-0.16	0.56	0.16	0	-0.33	0.64	1.51	1.66	1.56
2003	1.3	-0.68	-1.17	-1.42	-1.26	-1.78	-1.7	-1.72	-1.22	-0.19	0.49	0.49
2004	0.55	0.53	0.87	-0.94	0.02	0.2	0.86	-0.28	-0.75	-0.49	-0.38	-0.65
2005	-1.96	-1.6	-1.1	0.3	0.35	0.2	-0.27	0.52	0.36	0.25	-1.34	-0.89
2006	-1.54	-0.65	1.05	2.01	1.98	0.63	-1.61	-0.87	0.11	1	-0.84	-1.81
2007	-1.58	-1.07	0.26	-0.79	-0.66	-1.21	0.62	1.85	1.95	0.67	-1.37	-1.08
2008	-0.32	-0.31	-0.27	1.25	0.75	0.03	-1.14	0.23	1.09	1.77	0.71	0.28
2009	-1.31	-0.63	0.48	-0.23	-0.58	-0.9	0.47	0.16	-0.42	-1.45	-0.05	0.75
2010	0.77	0.05	-0.83	-0.99	-0.22	-0.1	0.76	0.46	0.42	-0.25	-0.31	0.08
2011	0.19	-0.47	-1.7	-2.28	-1.92	-1.69	-0.18	-0.05	0.33	-0.78	-1.42	-0.13
2012	0.21	0.91	-1.44	-1.83	-1.31	0.14	0.97	1.51	1.06	1.01	0.83	1.51
2013	1.23	1.22	0	0.45	1.13	0.78	-0.09	-1.37	-1.11	-0.17	1	0.67
2014	-0.19	-1.12	-1.05	-0.6	-0.58	-0.21	0.54	0.6	0.55	-0.42	-0.36	-0.6
2015	-0.17	-0.53	0.06	0.53	0.98	0.92	-0.79	-1.59	-2	-1.82	-1.41	-2.5
2016	-0.33	0.57	1.02	0.27	0.65	1.69	1.92	0.82	-0.8	-1.56	-0.45	-1.02
2017	-0.63	-1.54	-0.34	-0.05	-0.58	-1.01	-1.12	-0.76	0.14	-0.87	-0.12	-0.08
2018	1.37	1.23	0.67	-1.34	-1.41	-1.99	-1.91	-1.46	-1.11	-0.85	-1.66	-0.25
2019	0.25	0.98	-0.53	-0.69	0.14	-0.43	-0.58	-0.81	-0.43	0.5	0.21	-0.02
2020	-1.51	-0.45	-0.49	-0.7	-1.5	-0.98	-1.05	-0.46	-1.27	-0.41	-1.33	-0.61

Table 16: SPEI with a timescale of 4 over the 1981-2020 period. In red are showed SPEI values below -1, while in yellow are represented the values below 0 and above -1. 0 values coloured mean that the value is approximated but within the range

$SPEI_4$												
year	Jan	Feb	Mar	Apr	May	Jun	Jul	Aug	Sep	Oct	Nov	Dec
1981	0.51	-0.89	0.08	-0.22	-0.48	-0.84	-0.91	-0.32	0.82	2.42	1.89	2.21
1982	2.17	1.42	1.47	0.05	-1.5	-0.5	-0.29	0.74	1.08	0.94	0.8	0.25
1983	0.9	0.61	0.64	0.47	0.77	0.29	-0.84	-1.43	-1.61	-1.63	-0.61	-0.26
1984	-0.34	0.43	-0.5	0.1	-0.32	-0.72	-0.91	-1.12	0.27	0.41	0.86	0.99
1985	-0.5	-0.27	-0.44	0.37	0.3	0.34	-0.1	-0.68	-1.21	-1.79	-0.93	-0.94
1986	0.62	1.56	0.84	1.71	1.35	1.28	1.48	0.95	0.02	-0.07	-0.44	-1.25
1987	-0.9	-0.36	0.38	0.17	0.77	1.45	1.63	1.69	1.86	0.08	0.11	-0.28
1988	-1.47	-1.11	1.39	1.27	1.32	1.41	0.58	1.17	1.04	1.06	0.7	0.43
1989	-0.25	-0.52	-0.69	-0.13	-0.23	-0.69	0.13	-0.65	-0.21	0.3	-0.72	-0.76
1990	-1.1	-0.01	0.05	0.27	0.24	0.18	0.1	-0.5	0.05	-0.45	0.85	1.27
1991	1.07	0.3	-1.09	-0.78	-0.21	1.03	0.64	-0.31	-0.77	-1.9	-1.26	-0.19
1992	-0.89	-0.22	-0.63	-0.04	-0.54	-0.39	-0.81	-1.24	-0.71	0.05	1.35	1.59
1993	1.59	0.51	-1.52	-1.41	-0.84	-0.57	1.25	1.29	1.41	1.68	0.07	0.46
1994	0.97	0.64	0.64	0.54	1.05	0.74	-0.08	-0.36	-1.14	-0.8	-0.32	0.24
1995	0.77	1.42	2.13	1.48	1.41	1.35	0.86	1.09	0.45	-0.77	-0.47	-0.24
1996	-1.37	-0.16	-0.28	-1.37	-0.27	-0.5	0.05	0.55	0	0.49	0.62	0.5
1997	0.09	0.05	-1.48	-1.08	-1.06	-0.52	0.51	0.17	0.35	-0.4	-1.49	-0.62
1998	0.23	-0.14	0.42	-0.16	-1.36	-0.94	-1.31	-1.6	-0.01	0.52	1.5	1.48
1999	0.84	1.52	0.41	1.03	1.79	1.54	1.82	1.63	0.81	-0.3	0.49	0.92
2000	0.37	1.62	1.24	0.1	0.42	-0.85	0	0.52	0.79	1.22	0.26	-0.45
2001	-0.43	-0.69	1.64	2.03	1.59	2.02	1.44	0.63	1.91	1	1.19	0.96
2002	-0.81	-0.54	-1.13	-0.58	0.59	-0.01	-0.13	0.48	0	0.97	1.98	1.53
2003	1.44	1.01	-1.29	-1.25	-1.36	-2.04	-1.89	-1.88	-1.9	-0.38	-0.23	-0.03
2004	1.29	0.25	0.3	0.22	-0.25	0.16	0.33	0.21	-0.52	-0.27	-1.07	-0.79
2005	-1.16	-2.39	-1.5	-0.15	0.18	-0.01	0.3	0.46	-0.03	0.25	-0.35	-1.32
2006	-1.41	-1.55	0.98	1.65	1.94	1.33	-0.48	-0.47	-0.81	-0.29	0.47	-1.26
2007	-1.99	-1.68	-0.23	-0.98	-0.59	-0.71	-0.52	1.69	1.66	1.14	0.34	-0.98
2008	-1.16	-0.8	0.09	1.03	0.41	0.28	0.12	-0.49	0.54	1.53	1.16	0.57
2009	-0.09	-1.4	0.34	-0.5	-0.55	-0.22	-0.41	-0.18	-0.1	-0.69	-0.83	0.37
2010	0.33	0.65	-0.19	-1.22	-0.35	-0.16	0.14	0.82	0.4	0.01	-0.15	0.04
2011	-0.17	-0.43	-1.22	-2.2	-2.02	-2	-0.98	-0.42	-0.27	0.14	-1.56	-0.34
2012	0.14	-0.51	-0.26	-1.38	-1.6	-0.47	0.65	1.16	1.56	1.23	1.08	1.35
2013	1.33	1.29	1.01	0.31	1.07	0.71	0.15	-0.54	-1.3	-0.74	0.49	0.58
2014	0.36	-0.06	-1.57	-0.78	-0.5	-0.63	0.47	0.54	0.32	0.29	-0.31	-0.74
2015	-0.24	-0.49	-0.37	0.67	0.71	0.83	-0.18	-1.26	-1.82	-2.05	-1.98	-2.4
2016	-0.77	0.04	-0.05	1.06	0.73	1.24	2.04	1.31	0.21	-0.85	-1.13	-1.49
2017	-0.63	-0.88	-1.48	0.15	-0.7	-1.09	-0.78	-1.24	-0.53	-0.46	-0.56	0.21
2018	0.6	1.24	1.03	-0.51	-1.37	-1.81	-2.47	-1.68	-1.57	-1.32	-1.45	-0.44
2019	-0.25	-0.16	0.7	-0.63	-0.19	-0.38	-0.81	-0.43	-0.87	-0.02	0.23	-0.11
2020	-0.7	-0.85	-0.83	-1.18	-0.9	-1.11	-1.63	-0.75	-1.05	-1.01	-0.97	-1.32

Table 17: SPEI with a timescale of 5 over the 1981-2020 period. In red are showed SPEI values below -1, while in yellow are represented the values below 0 and above -1. 0 values coloured mean that the value is approximated but within the range

$SPEI_5$												
year	Jan	Feb	Mar	Apr	May	Jun	Jul	Aug	Sep	Oct	Nov	Dec
1981	-0.14	0.12	-0.22	-0.6	-0.14	-1.01	-0.48	-0.84	0.79	1.82	2.09	2.26
1982	2.38	2.01	1.21	1	-0.68	-0.81	-0.34	0.43	0.29	1.35	0.8	0.9
1983	0.34	0.98	0.55	0.71	0.81	0.35	-0.74	-1.22	-1.15	-1.75	-1.39	-0.98
1984	0.08	-0.24	-0.11	-0.34	0.01	-0.58	-1.12	-1.06	0.2	0	0.29	0.59
1985	1.01	-0.48	-0.59	0.18	0.38	0.33	-0.29	-0.33	-1.07	-1.61	-1.28	-1.07
1986	0.01	0.55	1.51	1.62	1.64	1.16	1.35	1.84	0.4	-0.14	-0.41	-0.4
1987	-1.49	-0.43	-0.16	0.21	0.58	1.51	1.48	1.51	2.01	1.31	-0.06	-0.24
1988	-0.44	-1.54	1.23	1.06	1.14	1.26	1.71	1	1.06	1.13	0.83	0.89
1989	-0.29	-0.03	-1	0.23	-0.76	-0.48	-0.18	-0.11	-0.8	-0.08	-0.11	-0.9
1990	-1.18	0.23	-0.59	0.04	-0.03	0.85	-0.25	-0.54	-0.2	0.34	0.27	0.65
1991	1.15	0.69	0.07	-0.94	-0.25	0.69	0.44	-0.42	-0.36	-1.09	-1.54	-1.3
1992	-0.82	-0.82	0.09	-0.21	-0.94	-0.32	-0.54	-1.02	-1.43	0.15	1.06	1.28
1993	1.21	1.33	0.15	-1.34	-1.23	-0.84	0.91	1.09	1.15	1.46	1.45	0.37
1994	0.75	0.79	0.47	0.88	1.2	0.56	-0.14	-0.06	-0.12	-1.14	-1.15	0.22
1995	0.86	1.07	1.68	1.82	1.65	1.43	1.11	1.13	1.12	-0.46	-0.81	0.22
1996	-1	-1.41	-0.43	-0.6	-0.78	-0.5	-0.12	0.13	0.32	0.12	0.84	0.54
1997	-0.18	0.29	-0.9	-1.08	-1.51	-0.32	-0.09	0.16	-0.34	0.22	-0.77	-0.86
1998	-0.42	-0.15	-0.24	0.39	-1.1	-1.08	-1.26	-1.47	-0.93	0.52	1.06	1.04
1999	1.33	1.68	1.21	0.63	1.56	1.95	1.45	1.74	1.71	0.4	0.05	0.92
2000	0.55	1.07	1.55	0.69	0.1	-0.18	0.09	0.1	0.75	0.52	1.06	-0.28
2001	-0.02	-0.75	1.51	1.81	1.64	1.81	2.24	1.22	1.53	1.62	1.13	0.82
2002	0.6	-0.62	-0.8	-0.98	0.27	0.09	-0.29	0.3	0.76	0.38	1.73	1.8
2003	1.47	1.25	0.27	-1.39	-1.25	-2.05	-2.12	-1.9	-2.06	-1.28	-0.46	-0.68
2004	0.84	1.09	0.16	-0.24	0.56	-0.05	0.25	-0.27	-0.03	-0.12	-0.77	-1.3
2005	-1.28	-1.31	-2.56	-0.52	-0.14	-0.1	0.05	0.87	-0.02	-0.09	-0.27	-0.38
2006	-1.84	-1.27	0.3	1.66	1.59	1.27	0.58	0.56	-0.4	-1.03	-0.64	0.07
2007	-1.57	-1.86	-0.91	-1.38	-0.73	-0.62	-0.09	0.73	1.5	0.92	0.82	0.51
2008	-1.15	-1.58	-0.31	1.23	0.29	0.01	0.34	0.58	-0.16	1.07	1.04	0.97
2009	0.29	-0.12	-0.33	-0.61	-0.71	-0.21	0.18	-0.88	-0.39	-0.42	-0.29	-0.34
2010	0.02	0.15	0.44	-0.74	-0.57	-0.25	0.02	0.23	0.75	0.02	0.02	0.15
2011	-0.18	-0.77	-1.29	-1.86	-2.06	-2.11	-1.35	-1.05	-0.59	-0.38	-0.59	-0.64
2012	-0.12	-0.53	-1.55	-0.46	-1.31	-0.82	-0.04	0.84	1.2	1.7	1.3	1.53
2013	1.24	1.36	1.22	1.04	0.93	0.68	0.17	-0.34	-0.48	-0.99	-0.24	0.01
2014	0.34	0.38	-0.87	-1.27	-0.62	-0.53	-0.06	0.43	0.3	0.11	0.27	-0.61
2015	-0.48	-0.57	-0.36	0.4	0.82	0.61	-0.11	-0.76	-1.54	-1.89	-2.11	-2.48
2016	-1.2	-0.5	-0.46	0.34	1.26	1.26	1.57	1.46	0.78	0.02	-0.59	-1.81
2017	-1.25	-0.87	-1.19	-0.78	-0.45	-1.12	-0.91	-0.94	-1.02	-0.96	-0.31	-0.2
2018	0.72	0.43	1.17	-0.14	-0.75	-1.75	-2.34	-2.05	-1.78	-1.69	-1.69	-0.45
2019	-0.47	-0.68	-0.19	0.35	-0.16	-0.58	-0.75	-0.64	-0.49	-0.5	-0.23	-0.06
2020	-0.7	-0.08	-1.24	-1.46	-1.24	-0.64	-1.73	-1.25	-1.26	-0.85	-1.37	-0.95

Table 18: SPEI with a timescale of 6 over the 1981-2020 period. In red are showed SPEI values below -1, while in yellow are represented the values below 0 and above -1. 0 values coloured mean that the value is approximated but within the range

$SPEI_6$												
year	Jan	Feb	Mar	Apr	May	Jun	Jul	Aug	Sep	Oct	Nov	Dec
1981	-0.52	-0.46	0.5	-0.88	-0.44	-0.67	-0.68	-0.43	0.17	1.79	1.48	2.4
1982	2.43	2.18	1.95	0.76	0.19	-0.11	-0.66	0.33	0	0.64	1.16	0.89
1983	1	0.46	0.93	0.6	0.96	0.44	-0.58	-1.09	-0.97	-1.45	-1.49	-1.55
1984	-0.68	0.19	-0.73	-0.08	-0.35	-0.25	-0.96	-1.17	0.12	-0.07	-0.11	0.1
1985	0.7	1.02	-0.79	0.04	0.22	0.41	-0.24	-0.41	-0.73	-1.57	-1.12	-1.34
1986	-0.25	-0.01	0.6	1.98	1.55	1.45	1.21	1.55	1.34	0.21	-0.46	-0.36
1987	-0.61	-1.04	-0.31	-0.25	0.6	1.31	1.55	1.32	1.9	1.7	1.06	-0.31
1988	-0.37	-0.51	0.61	0.92	0.95	1.11	1.53	1.81	0.9	1.22	0.86	0.98
1989	0.34	-0.06	-0.5	0	-0.48	-0.92	-0.01	-0.3	-0.29	-0.69	-0.44	-0.28
1990	-1.32	0	-0.28	-0.49	-0.24	0.62	0.56	-0.71	-0.28	0.08	0.93	0.14
1991	0.58	0.86	0.49	-0.05	-0.37	0.61	0.1	-0.43	-0.47	-0.8	-0.7	-1.54
1992	-1.98	-0.74	-0.56	0.29	-1.09	-0.66	-0.46	-0.75	-1.21	-0.7	1.07	1
1993	0.89	0.94	1.11	-0.01	-1.19	-1.17	0.55	0.78	0.97	1.3	1.21	1.53
1994	0.73	0.61	0.65	0.72	1.4	0.78	-0.27	-0.07	0.14	-0.28	-1.36	-0.69
1995	0.88	1.1	1.4	1.5	1.9	1.62	1.24	1.25	1.16	0.25	-0.53	-0.23
1996	-0.4	-1.04	-1.59	-0.76	-0.19	-0.91	-0.15	0.01	-0.08	0.41	0.45	0.76
1997	-0.03	0.05	-0.52	-0.59	-1.53	-0.73	0.08	-0.28	-0.32	-0.44	-0.22	-0.33
1998	-0.72	-0.74	-0.29	-0.17	-0.66	-0.86	-1.37	-1.4	-0.89	-0.43	1.01	0.59
1999	0.93	1.84	1.53	1.19	1.33	1.72	1.93	1.32	1.86	1.46	0.65	0.51
2000	0.62	1.1	1.09	0.99	0.56	-0.41	0.65	0.19	0.34	0.53	0.36	0.58
2001	0.13	-0.24	1.19	1.75	1.41	1.79	1.98	1.97	2.03	1.38	1.67	0.76
2002	0.51	0.72	-0.89	-0.72	-0.03	-0.15	-0.15	0.15	0.58	1.09	1.21	1.48
2003	1.74	1.29	0.73	-0.16	-1.38	-2.02	-2.16	-2.1	-2.04	-1.48	-1.25	-0.75
2004	0.29	0.64	1	-0.41	0.22	0.63	0.03	-0.22	-0.47	0.31	-0.6	-0.95
2005	-1.83	-1.4	-1.55	-1.27	-0.44	-0.34	-0.04	0.59	0.39	-0.11	-0.54	-0.27
2006	-0.82	-1.73	0.21	1.28	1.59	0.97	0.59	1.24	0.57	-0.74	-1.22	-0.85
2007	-0.16	-1.52	-1.23	-1.9	-1.06	-0.73	-0.06	0.91	0.57	0.92	0.58	0.92
2008	0.41	-1.53	-1.16	1	0.48	-0.04	0.07	0.7	0.83	0.4	0.56	0.87
2009	0.78	0.29	0.54	-1.2	-0.81	-0.34	0.17	-0.31	-1.03	-0.71	-0.08	0.07
2010	-0.67	-0.09	-0.04	-0.27	-0.2	-0.43	-0.07	0.15	0.19	0.39	-0.01	0.27
2011	0	-0.64	-1.51	-1.87	-1.82	-2.23	-1.54	-1.3	-1.17	-0.71	-0.95	0.09
2012	-0.44	-0.66	-1.44	-1.46	-0.61	-0.57	-0.43	0.23	0.9	1.44	1.72	1.68
2013	1.44	1.25	1.35	1.18	1.4	0.61	0.2	-0.22	-0.31	-0.25	-0.56	-0.55
2014	-0.19	0.39	-0.31	-0.67	-1.02	-0.62	-0.01	0.01	0.2	0.09	0.07	0
2015	-0.39	-0.73	-0.51	0.37	0.61	0.73	-0.28	-0.6	-1.07	-1.72	-1.87	-2.41
2016	-1.89	-0.93	-0.94	0.01	0.75	1.57	1.55	1.01	0.95	0.59	0.2	-1.13
2017	-1.81	-1.43	-1.18	-0.5	-1.21	-0.88	-0.96	-0.99	-0.75	-1.4	-0.81	-0.03
2018	0.39	0.61	0.43	-0.01	-0.47	-1.24	-2.28	-1.97	-2.11	-1.92	-1.86	-1.04
2019	-0.47	-0.81	-0.73	-0.43	0.55	-0.52	-0.92	-0.55	-0.7	-0.19	-0.66	-0.41
2020	-0.56	-0.13	-0.5	-1.76	-1.48	-0.94	-1.28	-1.32	-1.63	-1.11	-1.16	-1.32

Table 19: SPEI with a timescale of 12 over the 1981-2020 period. In red are showed SPEI values below -1, while in yellow are represented the values below 0 and above -1. 0 values coloured mean that the value is approximated but within the range

$SPEI_{12}$												
year	Jan	Feb	Mar	Apr	May	Jun	Jul	Aug	Sep	Oct	Nov	Dec
1981	0.62	0.41	0.57	0.12	0.25	-0.65	-0.87	-0.64	0.44	0.84	0.75	1.4
1982	1.71	1.68	1.53	1.6	1.09	1.59	1.63	1.82	1.3	0.89	0.93	0.5
1983	0.09	0.48	0.53	0.78	1.35	0.91	0.22	-0.67	-0.19	-0.83	-0.64	-0.95
1984	-0.97	-1.03	-1.24	-1.25	-1.51	-1.46	-1.16	-0.94	-0.22	-0.09	-0.38	-0.2
1985	-0.41	-0.45	-0.39	-0.05	0.11	0.37	0.23	0.37	-0.93	-1.29	-0.81	-0.79
1986	-0.47	-0.52	-0.33	0.27	0.44	0.37	0.78	1.2	1.22	1.53	0.98	1.07
1987	0.57	0.84	0.85	-0.02	0.12	0.89	0.92	0.62	1.22	1.06	1.16	0.94
1988	1.03	0.84	1.73	1.63	1.29	0.73	1	1.24	0.96	1.32	1.31	1.52
1989	1.37	1.53	0.39	0.84	0.33	0.02	0.16	-0.28	-0.43	-0.52	-0.69	-0.95
1990	-0.9	-0.4	-0.46	-0.82	-0.45	0.29	-0.36	-0.61	-0.31	-0.21	0.46	0.55
1991	0.71	-0.14	-0.01	0	0.44	0.56	0.4	0.23	-0.04	-0.64	-0.82	-0.8
1992	-1.17	-0.96	-0.75	-0.48	-1.21	-1.73	-1.48	-1.08	-1.26	-0.35	-0.01	0.18
1993	0.15	-0.11	-0.43	-0.57	0.03	-0.15	0.92	1.12	1.25	0.9	0.03	0.26
1994	0.81	0.97	1.07	1.28	1.65	1.5	0.24	0.33	0.5	0.25	-0.07	0.1
1995	0.29	0.65	1	0.84	0.63	1.04	1.38	1.49	1.51	1.16	1.38	1.34
1996	0.71	0.51	0.03	-0.27	-0.49	-0.88	-0.4	-0.55	-0.81	-0.12	0.14	-0.2
1997	-0.27	-0.09	-0.41	-0.06	-0.64	-0.02	-0.01	-0.2	-0.46	-0.64	-1.12	-0.85
1998	-0.5	-0.82	-0.49	-0.45	-0.56	-0.91	-1.5	-1.72	-0.82	-0.41	0.24	-0.29
1999	-0.57	0.38	0.28	0.46	1.51	1.75	1.9	1.96	1.91	1.6	1.52	1.83
2000	1.87	1.72	1.95	1.52	0.83	0.03	0.81	0.85	0.89	0.96	0.62	0.04
2001	0.48	-0.1	0.98	1.53	1.27	1.8	1.61	1.45	1.84	1.91	2.26	2.02
2002	1.86	2.02	1.17	0.6	1.09	0.4	0.17	0.56	0.04	0.4	0.82	0.93
2003	1.19	1.02	0.83	0.67	0.01	-0.37	-0.39	-1.05	-1.53	-1.3	-1.68	-1.93
2004	-1.68	-1.77	-1.46	-1.44	-0.88	-0.04	0.16	0.23	0.28	0.01	-0.38	-0.25
2005	-1.14	-1.11	-1.22	-0.5	-0.72	-1.01	-1.11	-0.21	-0.43	-0.77	-0.74	-0.53
2006	-0.65	-0.54	0.37	0.77	0.92	0.62	-0.05	0.26	0.56	0.33	0.31	0.18
2007	0.26	0.26	-0.27	-1.55	-1.65	-1.21	-0.19	0.04	-0.13	-0.38	-0.35	0.07
2008	0.1	-0.1	-0.23	1.2	0.73	0.59	0.26	-0.17	0.1	0.89	0.71	0.53
2009	0.47	0.7	0.91	-0.4	-0.09	0.34	0.59	-0.07	-0.5	-1.16	-0.63	-0.28
2010	-0.39	-0.48	-0.97	-0.72	-0.15	-0.3	-0.5	0.08	0.17	0.14	-0.21	-0.2
2011	-0.19	-0.38	-0.71	-0.78	-1.16	-1.48	-1.26	-1.57	-1.65	-1.5	-1.68	-1.57
2012	-1.55	-1.69	-1.69	-1.32	-1.13	-0.4	-0.63	-0.16	0.01	0.28	0.82	0.81
2013	0.69	1.04	1.48	1.62	1.87	1.49	1.1	0.7	0.65	0.6	0.72	0.04
2014	-0.08	-0.07	-0.49	-0.59	-1.06	-0.91	-0.17	0.25	0.04	-0.3	-0.66	-0.54
2015	-0.37	-0.55	-0.19	0.26	0.51	0.57	-0.49	-0.94	-1.1	-1.25	-1.28	-1.57
2016	-1.38	-1.21	-1.4	-1.47	-1.22	-0.62	0.27	0.39	0.29	0.43	0.66	0.68
2017	0.26	0.05	0.07	0.12	-0.61	-1.54	-1.74	-1.66	-1.14	-1.39	-1.32	-0.75
2018	-0.63	-0.63	-0.45	-1.18	-0.92	-0.97	-1.68	-1.54	-1.79	-1.66	-1.77	-1.66
2019	-2.12	-2.36	-2.25	-1.85	-1.36	-1.21	-1.03	-0.93	-0.88	-0.37	-0.18	-0.76
2020	-1.16	-0.72	-0.91	-1.11	-1.42	-1.03	-1.35	-1.3	-1.66	-1.74	-1.66	-1.68

Table 20: SPI with a timescale of 1 over the 1981-2020 period. In red are showed SPI values below -1, while in yellow are represented the values below 0 and above -1. 0 values coloured mean that the value is approximated but within the range

	SPI_1											
year	Jan	Feb	Mar	Apr	May	Jun	Jul	Aug	Sep	Oct	Nov	Dec
1981	0.7	-1.11	1.01	-1.54	0.02	-1.88	0.6	-0.08	2.05	2	-0.42	1.71
1982	1.42	-1.84	-0.26	-0.69	-2.04	1.04	0.57	1.35	-0.85	0.91	0.07	0.64
1983	0.53	0.3	0.14	0.48	0.74	-0.75	-2.01	-1.6	0.77	-1.17	0.53	-1.06
1984	0.76	0.22	-1.45	-0.09	-0.53	-0.93	-0.84	-0.93	2.27	-0.34	0.03	-0.39
1985	0.31	0.05	-0.78	0.81	0.22	-0.06	-1.24	-0.51	-1.07	-3.21	1.1	-0.3
1986	1.47	-0.14	0.11	1.74	0.86	-0.05	0.04	1.19	-1.72	-0.08	-0.73	0.13
1987	-0.36	0.81	-0.1	-0.01	0.62	1.88	-0.03	0.1	1.45	-1.02	-0.1	-0.63
1988	0.09	-0.09	2.38	0.01	0.48	0.31	0.64	1.18	-0.07	0.67	-0.39	0.8
1989	-2.33	0.68	-0.33	1.05	-1.41	-0.84	1.06	-0.38	-0.42	0.45	-1.16	-0.39
1990	-0.73	2.23	-0.57	-0.19	-0.25	1.33	-0.79	-1.5	0.63	0.89	1.4	-0.33
1991	-0.04	-1.54	0	-0.25	0.36	1.57	-1.39	-2.9	0.22	-1.4	0.95	-0.4
1992	-1.62	0.23	0.57	0.45	-2.32	0.28	-0.05	-0.4	-0.66	1.49	1.95	0.15
1993	-1.13	-1.54	-0.61	0.09	-0.01	-0.15	2.27	0.07	-0.25	0.42	-0.46	0.92
1994	0.95	-0.33	0.36	0.64	1.71	-0.96	-1.77	0.4	0.56	-0.18	-0.75	1.2
1995	1.33	1.18	0.86	0.45	1.3	0.44	-0.38	0.94	0.06	-2.79	-0.14	1.22
1996	-2.39	-0.18	-0.68	-0.7	0.54	-0.45	0.72	0.23	-0.96	0.42	0.93	-0.02
1997	-2.43	0.79	-1.41	0.12	-1.68	1.12	0.78	-0.23	-1.26	-0.08	-1.07	1.09
1998	0.55	-0.56	-0.03	0.13	-2.68	0.34	-0.55	-1.12	1.51	1.19	1.14	-1.31
1999	-0.12	2.13	-0.26	0.64	2.03	1.19	-0.42	0.32	0.85	-0.72	0.66	1.16
2000	-0.96	1.73	0.38	-0.57	0.37	-1.22	1.42	0.53	0.75	-0.19	0.06	-1.02
2001	0.89	-0.32	2.64	1.24	-0.04	1.23	0.42	0.14	1.81	0.12	0.51	-0.93
2002	-0.92	0.8	-0.15	-0.09	1.32	-0.62	-0.43	1	0.65	0.94	1.87	0.01
2003	0.13	-0.92	-1.07	-0.59	-0.28	-1.72	-0.06	-0.46	-0.86	1.22	-0.03	-1.12
2004	1.65	-0.59	-0.09	-0.94	0.75	0.42	0.29	-1.16	-0.3	1.04	-1.54	-0.79
2005	-0.92	-0.37	-0.42	1.11	0.14	-0.25	0.31	1.24	-0.97	0.19	-1.42	-0.11
2006	-1.05	0.19	1.75	1.88	0.8	-1.96	-1.66	1.67	0.58	-0.32	-0.63	-0.68
2007	-0.06	0.49	0.9	-2.99	0.35	-0.05	1.16	2.18	-0.39	-2.13	-0.65	0.52
2008	0.02	-0.57	0.58	1.86	-1.21	-0.64	0.29	1.11	0.58	1.28	-1.1	-0.21
2009	-0.55	0	1.1	-1.81	-0.29	0.64	0.92	-1.06	-0.28	-0.7	1.05	0.86
2010	-0.71	-0.32	-0.24	-1.13	0.62	0.25	0.74	0.36	-0.07	-0.81	0.24	0.62
2011	-0.23	-1.22	-1.47	-1.53	-0.41	-0.99	1.15	-0.29	-0.06	-0.17	-1.98	1.59
2012	0.64	-2.27	-1.67	-0.44	-0.26	1.27	0.89	0.95	0.36	0.77	0.63	1.49
2013	-0.05	0.12	-0.09	0.6	1.31	-0.72	-0.79	-0.9	0.28	0.83	1.05	-1.07
2014	-0.14	0.47	-1.12	0.32	-0.01	0.07	1.09	0.06	-0.27	0.08	0.32	-0.5
2015	0.64	-0.75	0.34	1.2	0.82	0.28	-1.86	-1.16	-1.23	-0.97	-0.16	-1.94
2016	1.7	0.8	-0.82	0.71	1.07	1.6	0.92	-1.09	-0.97	-0.32	0.65	-1.98
2017	0.48	-0.09	-0.07	0.72	-1.04	-0.7	0.64	-0.36	0.48	-1.22	0.45	0.72
2018	1.37	-0.43	0.07	-2.3	-0.33	-1.26	-1.24	0.5	-0.1	-0.77	-1.6	1.7
2019	0.08	-0.55	0.25	-0.35	0.44	-0.46	-0.24	0.44	0.04	0.97	-0.28	-0.32
2020	-1.05	1.46	-0.56	-1.22	-0.57	0.35	-1.32	0.71	-1.52	0.44	-1.26	0.02

Table 21: SPI with a timescale of 2 over the 1981-2020 period. In red are showed SPI values below -1, while in yellow are represented the values below 0 and above -1. 0 values coloured mean that the value is approximated but within the range

	SPI_2											
year	Jan	Feb	Mar	Apr	May	Jun	Jul	Aug	Sep	Oct	Nov	Dec
1981	-0.11	-0.12	0.25	-0.07	-0.84	-1.26	-0.63	0.32	1.53	2.7	1.32	1.06
1982	2.11	0.53	-1.23	-0.72	-1.92	-0.31	1.01	1.18	0.54	0.15	0.61	0.42
1983	0.71	0.49	0.16	0.31	0.73	0	-1.87	-2.46	-0.47	-0.19	-0.38	-0.35
1984	-0.14	0.66	-0.83	-0.92	-0.53	-1.17	-1.3	-1.25	1.33	1.48	-0.33	-0.41
1985	-0.15	0.11	-0.61	0.12	0.59	0.01	-0.9	-1.23	-1.23	-2.6	-0.32	0.66
1986	0.93	1.21	-0.12	1.27	1.68	0.52	-0.1	0.74	0.04	-1.16	-0.66	-0.58
1987	-0.27	0.17	0.35	-0.18	0.35	1.78	1.32	-0.04	1.1	0.48	-0.85	-0.69
1988	-0.49	-0.19	1.92	1.68	0.25	0.46	0.56	1.11	0.79	0.35	0.16	0.24
1989	-0.4	-0.87	0.11	0.51	-0.1	-1.73	0.24	0.52	-0.7	-0.03	-0.43	-1.35
1990	-0.92	1.36	1.23	-0.58	-0.4	0.79	0.48	-1.55	-0.55	0.95	1.5	0.95
1991	-0.39	-1.19	-0.88	-0.28	0.01	1.36	0.44	-2.73	-1.58	-0.77	-0.07	0.45
1992	-1.39	-1.12	0.45	0.55	-1.04	-1.16	0.07	-0.36	-0.88	0.78	2.31	1.77
1993	-0.67	-2.36	-1.44	-0.39	-0.06	-0.23	1.62	1.75	-0.25	0.04	-0.1	0.3
1994	1.21	0.53	-0.02	0.56	1.54	0.79	-1.91	-0.81	0.59	0.16	-0.75	0.4
1995	1.69	1.87	1.24	0.75	1.12	1.2	-0.01	0.32	0.67	-1.37	-1.61	0.77
1996	0.01	-1.85	-0.71	-1.01	-0.07	0	0.17	0.58	-0.53	-0.35	0.84	0.66
1997	-1.26	-0.75	-0.32	-0.72	-1.05	-0.09	1.21	0.37	-1.1	-0.94	-0.86	0.13
1998	1.05	-0.03	-0.47	-0.04	-1.48	-1.22	-0.19	-1.15	0.49	1.75	1.52	0.19
1999	-1.11	1.56	1.27	0.21	1.79	2.28	0.54	-0.15	0.75	0.09	-0.04	1.27
2000	0.32	0.75	1.3	-0.19	-0.14	-0.59	0.39	1.28	0.82	0.3	-0.21	-0.8
2001	0.02	0.48	2.09	2.48	0.76	0.83	1.06	0.3	1.44	1.31	0.32	-0.3
2002	-1.48	-0.18	0.31	-0.26	0.86	0.59	-0.81	0.32	1.1	1.01	1.89	1.6
2003	-0.03	-0.69	-1.47	-1.15	-0.66	-1.45	-1.15	-0.4	-1.06	0.44	0.81	-0.96
2004	0.75	1.23	-0.53	-0.74	0.02	0.75	0.39	-0.5	-1.18	0.53	-0.03	-2.01
2005	-1.37	-1.27	-0.66	0.52	0.76	-0.19	-0.03	0.94	0.38	-0.56	-0.8	-1.25
2006	-0.86	-0.86	1.44	2.26	1.74	-0.54	-2.56	0.3	1.59	0.09	-0.79	-1.19
2007	-0.65	0.12	0.85	-0.46	-0.84	0.12	0.74	2.12	1.52	-1.62	-1.92	-0.17
2008	0.28	-0.58	0.05	1.59	0.74	-1.44	-0.28	0.84	1.14	1.22	0.37	-1.14
2009	-0.66	-0.68	0.77	-0.05	-1.21	0.18	0.98	0.09	-1.09	-0.79	0.31	1.36
2010	0.16	-1.07	-0.49	-0.95	-0.17	0.53	0.6	0.67	0.11	-0.71	-0.45	0.53
2011	0.2	-1.23	-1.94	-2.06	-1.21	-1.12	0.24	0.64	-0.38	-0.28	-1.65	0.14
2012	1.5	-0.58	-2.71	-1.3	-0.56	0.74	1.39	1.14	0.87	0.69	0.86	1.52
2013	1.02	-0.17	-0.11	0.27	1.22	0.53	-1.12	-1.19	-0.52	0.69	1.2	0.2
2014	-0.98	0.04	-0.47	-0.43	0.1	-0.07	0.75	0.77	-0.27	-0.24	0.16	-0.22
2015	0.06	-0.03	-0.24	0.96	1.26	0.71	-0.91	-2.07	-1.87	-1.64	-0.88	-1.78
2016	0.42	1.98	-0.06	0.02	1.1	1.85	1.64	0.08	-1.63	-0.98	0.17	-1.04
2017	-1.26	0.18	-0.23	0.37	-0.22	-1.37	-0.04	0.19	-0.02	-0.47	-0.47	0.76
2018	1.41	0.96	-0.31	-1.15	-1.38	-1.23	-1.8	-0.48	0.21	-0.7	-1.79	0.54
2019	1.27	-0.51	-0.22	-0.16	0.03	-0.08	-0.57	0.04	0.25	0.66	0.47	-0.62
2020	-1.05	0.42	0.59	-1.25	-1.21	-0.23	-0.61	-0.36	-0.36	-0.59	-0.49	-1.02

Table 22: SPI with a timescale of 3 over the 1981-2020 period. In red are showed SPI values below -1, while in yellow are represented the values below 0 and above -1. 0 values coloured mean that the value is approximated but within the range

	SPI_3											
year	Jan	Feb	Mar	Apr	May	Jun	Jul	Aug	Sep	Oct	Nov	Dec
1981	-0.58	-0.81	0.52	-0.54	-0.12	-1.84	-0.67	-0.66	1.5	2.44	2	2.14
1982	1.69	1.67	0.15	-1.36	-1.64	-0.67	0.03	1.52	0.7	0.91	0.07	0.83
1983	0.54	0.77	0.33	0.3	0.57	0.17	-1.07	-2.54	-1.55	-1.11	0.08	-1.07
1984	0.1	-0.15	-0.22	-0.72	-1.04	-1.08	-1.63	-1.7	0.57	0.86	1.12	-0.66
1985	-0.28	-0.28	-0.42	0.04	0.13	0.39	-0.76	-1.13	-1.83	-2.4	-0.81	-0.6
1986	1.42	0.78	0.85	1.02	1.35	1.4	0.38	0.53	-0.03	-0.12	-1.35	-0.63
1987	-0.87	0.13	-0.03	0.16	0.16	1.42	1.49	1.16	0.78	0.38	0.25	-1.3
1988	-0.66	-0.71	1.66	1.42	1.5	0.29	0.7	1.05	0.93	0.94	0.01	0.53
1989	-0.78	-0.09	-0.91	0.64	-0.3	-0.65	-0.59	-0.05	0.19	-0.35	-0.62	-0.76
1990	-1.76	0.87	0.66	0.77	-0.64	0.49	0.19	-0.27	-1.02	0.09	1.42	1.23
1991	0.66	-1.31	-0.89	-0.86	-0.07	0.96	0.52	-0.68	-2.2	-2.2	-0.01	-0.42
1992	-0.43	-1.32	-0.4	0.49	-0.53	-0.73	-1.09	-0.22	-0.79	0.39	1.66	2.27
1993	1.02	-1.64	-2.06	-0.97	-0.37	-0.23	1.45	1.42	1.51	-0.03	-0.27	0.4
1994	0.74	1.02	0.5	0.29	1.33	0.89	-0.2	-1.34	-0.48	0.28	-0.3	0.1
1995	1.12	2.31	1.74	1.07	1.21	1.13	0.78	0.44	0.22	-0.46	-1.15	-0.44
1996	-0.25	-0.24	-1.8	-1	-0.41	-0.41	0.38	0.19	0.04	-0.24	0.24	0.69
1997	-0.36	-0.73	-1.38	-0.24	-1.49	-0.1	0.36	0.92	-0.29	-1.03	-1.35	-0.06
1998	0.31	0.74	-0.14	-0.34	-1.21	-0.99	-1.49	-0.78	-0.02	1.07	1.85	0.89
1999	-0.06	0.64	0.95	1.2	1.33	2.12	1.79	0.56	0.27	0.17	0.36	0.62
2000	0.58	1.37	0.66	0.68	0	-0.87	0.48	0.54	1.5	0.48	0.18	-0.88
2001	-0.11	-0.31	2.21	2.13	1.99	1.28	0.87	0.94	1.31	1.17	1.19	-0.28
2002	-0.91	-0.89	-0.32	0.09	0.57	0.36	0.18	-0.13	0.56	1.37	1.75	1.78
2003	1.34	-0.65	-1.18	-1.46	-1.04	-1.59	-1.33	-1.32	-0.92	0.03	0.25	0.17
2004	0.52	0.38	0.76	-0.97	-0.1	0.17	0.73	-0.23	-0.74	-0.2	-0.24	-0.58
2005	-2.44	-1.75	-1.24	0.24	0.39	0.44	-0.06	0.61	0.41	0.32	-1.17	-0.91
2006	-1.85	-0.88	0.77	2.05	2.13	0.79	-1.48	-0.71	0.5	1.09	-0.3	-1.26
2007	-1.17	-0.46	0.58	-0.23	-0.19	-0.81	0.79	1.82	1.84	0.49	-1.64	-1.26
2008	-0.29	-0.14	-0.08	1.2	0.78	0.24	-1.04	0.34	1	1.62	0.51	0.12
2009	-1.46	-0.82	0.29	-0.13	-0.28	-0.58	0.67	0.38	-0.16	-1.42	0.05	0.71
2010	0.75	-0.16	-0.98	-1.03	-0.32	-0.09	0.82	0.63	0.49	-0.44	-0.45	-0.11
2011	0.18	-0.49	-1.8	-2.36	-1.65	-1.71	-0.12	-0.01	0.47	-0.52	-1.26	-0.11
2012	0.38	0.84	-1.34	-2.04	-1.13	0.33	1.1	1.63	1.16	1.07	0.78	1.6
2013	1.18	1.01	-0.27	0.2	0.89	0.66	-0.05	-1.53	-0.99	0.07	1.02	0.62
2014	-0.06	-0.77	-0.63	-0.22	-0.4	0.03	0.6	0.62	0.5	-0.27	-0.08	-0.24
2015	0.11	-0.48	0.1	0.54	1.09	1.17	-0.3	-1.46	-2.71	-2.21	-1.34	-2.18
2016	0.12	0.77	1.09	0.3	0.57	1.79	2.06	1.03	-0.48	-1.6	-0.35	-1.15
2017	-0.62	-1.45	-0.01	0.2	-0.28	-0.68	-0.72	-0.3	0.33	-0.72	-0.16	-0.06
2018	1.42	1.2	0.64	-1.24	-1.08	-2.01	-1.91	-1.19	-0.61	-0.34	-1.37	-0.08
2019	0.36	0.99	-0.28	-0.45	0.06	-0.34	-0.32	-0.31	-0.05	0.73	0.31	0.16
2020	-1.27	0.04	-0.09	-0.14	-1.29	-0.8	-1.02	-0.18	-1.14	-0.1	-1.13	-0.56

Table 23: SPI with a timescale of 4 over the 1981-2020 period. In red are showed SPI values below -1, while in yellow are represented the values below 0 and above -1. 0 values coloured mean that the value is approximated but within the range

SPI_4												
year	Jan	Feb	Mar	Apr	May	Jun	Jul	Aug	Sep	Oct	Nov	Dec
1981	0.09	-1.26	0	-0.2	-0.47	-0.95	-1.37	-0.66	0.6	2.28	1.96	2.63
1982	2.55	1.22	1.21	-0.27	-2.07	-0.74	-0.39	0.68	1.16	0.98	0.75	0.3
1983	0.9	0.6	0.62	0.42	0.54	0.13	-0.82	-1.66	-1.93	-1.96	-0.7	-0.43
1984	-0.55	0.1	-0.86	-0.3	-0.88	-1.48	-1.68	-1.88	-0.01	0.27	0.68	0.88
1985	-0.53	-0.39	-0.72	0.08	0.08	0.01	-0.31	-0.94	-1.72	-2.72	-1.17	-1.01
1986	0.37	1.38	0.61	1.56	1.15	1.17	1.35	0.86	-0.15	-0.15	-0.53	-1.25
1987	-0.88	-0.48	-0.04	-0.11	0.37	1.12	1.34	1.28	1.81	0.22	0.19	-0.1
1988	-1.21	-0.87	1.33	1.28	1.3	1.45	0.57	1.11	0.94	1.04	0.58	0.33
1989	-0.29	-0.5	-0.34	-0.08	-0.07	-0.75	0	-0.74	-0.34	0.31	-0.91	-0.87
1990	-1.17	0.06	0.38	0.36	0.45	0.16	-0.01	-0.46	-0.03	-0.39	0.84	1.21
1991	0.99	0.05	-1.13	-0.91	-0.5	0.75	0.27	-0.47	-0.64	-2.62	-1.17	-0.28
1992	-1.13	-0.44	-0.7	-0.14	-0.45	-0.4	-0.86	-1.18	-0.61	0.22	1.47	1.62
1993	1.68	0.48	-1.77	-1.5	-0.79	-0.49	1.34	1.23	1.26	1.41	-0.34	0.14
1994	0.77	0.54	0.95	0.64	1.08	0.82	0.07	-0.03	-1.05	-0.59	-0.17	0.29
1995	0.8	1.72	2.28	1.53	1.41	1.23	0.87	1.05	0.37	-0.65	-0.56	-0.38
1996	-1.3	-0.48	-0.64	-1.84	-0.48	-0.67	-0.04	0.37	-0.3	0.16	0.26	0.14
1997	-0.14	-0.01	-1.36	-1.04	-0.96	-0.58	0.29	0.15	0.39	-0.37	-1.51	-0.62
1998	0.13	-0.04	0.5	-0.13	-1.32	-0.9	-1.42	-1.84	0.09	0.57	1.45	1.4
1999	0.64	1.3	0.31	0.98	1.89	1.69	1.92	1.64	0.89	-0.15	0.42	0.84
2000	0.07	1.57	1.25	0.21	0.65	-0.61	0.1	0.6	0.82	1.16	0.36	-0.31
2001	-0.3	-0.4	1.81	2.27	1.71	2.31	1.42	0.76	1.82	1.11	1.18	0.79
2002	-0.79	-0.53	-0.89	-0.38	0.72	0.18	0.02	0.6	0.12	0.89	2.15	1.66
2003	1.58	1.01	-1.17	-1.31	-1.29	-1.82	-1.68	-1.4	-1.82	-0.08	-0.07	-0.28
2004	1.1	0.18	0.18	0.18	-0.33	0.04	0.23	0.14	-0.47	-0.07	-0.9	-0.67
2005	-1.08	-2.83	-1.75	-0.23	0.19	0.16	0.51	0.55	0.15	0.35	-0.35	-1.24
2006	-1.45	-1.87	0.62	1.6	1.95	1.42	-0.01	-0.22	-0.46	0.21	0.63	-0.68
2007	-1.28	-1.01	0.16	-0.35	-0.06	-0.28	-0.06	1.76	1.62	1	0.06	-1.24
2008	-1.21	-0.71	0.16	1.04	0.5	0.38	0.3	-0.29	0.53	1.43	0.99	0.32
2009	-0.27	-1.63	0.08	-0.47	-0.31	0.01	-0.04	0.12	0.16	-0.53	-0.54	0.39
2010	0.24	0.55	-0.35	-1.39	-0.45	-0.24	0.27	0.81	0.5	0.02	-0.34	-0.19
2011	-0.34	-0.43	-1.17	-2.24	-1.93	-2.05	-0.8	-0.29	-0.14	0.25	-1.47	-0.19
2012	0.14	-0.42	0.01	-1.35	-1.64	-0.23	0.78	1.32	1.72	1.29	1.16	1.39
2013	1.34	1.21	0.7	0.05	0.78	0.46	0.18	-0.48	-1.4	-0.4	0.58	0.56
2014	0.37	0.07	-1.29	-0.38	-0.24	-0.4	0.62	0.48	0.41	0.39	-0.15	-0.38
2015	0.04	-0.34	-0.25	0.69	0.76	1.05	0.37	-0.8	-2.13	-2.87	-2.03	-2.37
2016	-0.46	0.47	0.19	1.13	0.72	1.27	2.22	1.41	0.59	-0.65	-0.98	-1.43
2017	-0.82	-0.84	-1.28	0.31	-0.34	-0.67	-0.34	-0.84	-0.14	-0.25	-0.44	0.13
2018	0.7	1.26	0.95	-0.23	-1.16	-1.66	-2.85	-1.32	-1.32	-0.96	-1.04	-0.18
2019	-0.16	0.02	0.86	-0.48	-0.16	-0.24	-0.59	-0.11	-0.38	0.42	0.43	0.08
2020	-0.41	-0.31	-0.35	-0.66	-0.44	-0.96	-1.64	-0.52	-0.86	-0.78	-0.71	-1.13

Table 24: SPI with a timescale of 5 over the 1981-2020 period. In red are showed SPI values below -1, while in yellow are represented the values below 0 and above -1. 0 values coloured mean that the value is approximated but within the range

SPI_5												
year	Jan	Feb	Mar	Apr	May	Jun	Jul	Aug	Sep	Oct	Nov	Dec
1981	-0.47	-0.37	-0.46	-0.66	-0.2	-1.19	-0.68	-1.21	0.48	1.57	1.96	2.46
1982	3.04	2.19	0.92	0.67	-0.98	-1.12	-0.51	0.32	0.3	1.37	0.87	0.88
1983	0.4	0.95	0.54	0.67	0.62	0.15	-0.71	-1.33	-1.25	-2.29	-1.54	-1.12
1984	-0.14	-0.54	-0.64	-0.83	-0.52	-1.26	-2.02	-1.84	-0.33	-0.23	0.18	0.42
1985	0.86	-0.6	-0.89	-0.16	0.11	-0.02	-0.61	-0.51	-1.44	-2.52	-1.7	-1.25
1986	-0.15	0.23	1.26	1.46	1.56	0.97	1.13	1.59	0.28	-0.25	-0.51	-0.48
1987	-1.5	-0.53	-0.62	-0.12	0.16	1.18	1.05	1.12	1.86	1.23	0.08	-0.12
1988	-0.19	-1.33	1.22	1.04	1.17	1.25	1.7	0.96	1.01	1.06	0.76	0.82
1989	-0.36	-0.06	-0.77	0.27	-0.64	-0.47	-0.2	-0.2	-1	-0.16	-0.19	-1.05
1990	-1.27	0.23	-0.35	0.14	0.13	0.95	-0.29	-0.59	-0.23	0.35	0.35	0.59
1991	1.04	0.51	-0.07	-1.14	-0.55	0.34	0.16	-0.63	-0.44	-1.17	-1.76	-1.29
1992	-0.91	-1.1	-0.13	-0.4	-0.94	-0.33	-0.53	-0.93	-1.53	0.26	1.22	1.34
1993	1.17	1.27	0.04	-1.44	-1.17	-0.83	0.9	1.1	1.06	1.22	1.1	0.09
1994	0.48	0.58	0.61	1.02	1.27	0.61	0.14	0.19	0.15	-1.09	-0.94	0.39
1995	0.85	1.26	2.02	2.04	1.72	1.41	1.04	1.08	1	-0.43	-0.76	0.08
1996	-1.13	-1.47	-0.93	-0.95	-1.07	-0.7	-0.35	0.02	-0.05	-0.14	0.53	0.16
1997	-0.58	0.15	-0.74	-1.11	-1.56	-0.28	-0.22	0.1	-0.37	0.23	-0.84	-0.75
1998	-0.43	-0.17	-0.17	0.4	-0.99	-1.01	-1.29	-1.69	-0.9	0.63	1.01	0.89
1999	1.21	1.67	1	0.51	1.68	2.15	1.52	1.7	1.91	0.46	0.1	0.86
2000	0.4	0.91	1.59	0.75	0.28	0.12	0.17	0.27	0.85	0.58	1.04	-0.09
2001	0.05	-0.52	1.83	2.05	1.82	2	2.51	1.2	1.57	1.6	1.17	0.73
2002	0.35	-0.45	-0.7	-0.86	0.35	0.37	-0.11	0.44	0.8	0.51	1.72	1.93
2003	1.56	1.28	0.4	-1.35	-1.18	-1.94	-1.91	-1.63	-1.84	-0.86	-0.17	-0.54
2004	0.58	0.85	0	-0.33	0.44	-0.16	0.09	-0.27	-0.06	0.07	-0.68	-1.21
2005	-1.14	-1.34	-2.98	-0.65	-0.17	0	0.22	0.95	0.13	0.14	-0.22	-0.43
2006	-1.75	-1.42	-0.16	1.56	1.56	1.28	0.85	0.78	-0.03	-0.63	-0.13	0.28
2007	-0.81	-1.09	-0.35	-0.73	-0.16	-0.14	0.29	1.05	1.57	0.85	0.64	0.23
2008	-1.29	-1.56	-0.36	1.23	0.4	0.15	0.43	0.72	-0.09	1.05	0.95	0.77
2009	-0.02	-0.36	-0.66	-0.65	-0.55	-0.04	0.42	-0.48	-0.07	-0.21	0	-0.12
2010	0	0.03	0.28	-0.86	-0.73	-0.35	0.07	0.33	0.7	0.07	0.05	-0.07
2011	-0.41	-0.86	-1.19	-1.72	-1.9	-2.22	-1.23	-0.84	-0.4	-0.27	-0.55	-0.38
2012	0.01	-0.53	-1.24	-0.28	-1.2	-0.67	0.17	1.01	1.39	1.78	1.4	1.66
2013	1.23	1.33	1	0.8	0.64	0.4	0.04	-0.23	-0.42	-0.81	0.11	0.11
2014	0.36	0.49	-0.57	-0.92	-0.35	-0.25	0.14	0.5	0.29	0.32	0.42	-0.4
2015	-0.17	-0.32	-0.21	0.45	0.86	0.74	0.38	-0.15	-1.35	-2.39	-2.76	-2.81
2016	-0.96	-0.15	-0.06	0.46	1.31	1.31	1.65	1.53	1.04	0.32	-0.34	-1.9
2017	-1.19	-0.95	-0.93	-0.64	-0.19	-0.67	-0.4	-0.49	-0.67	-0.65	-0.1	-0.11
2018	0.73	0.48	1.13	0.08	-0.38	-1.65	-2.41	-2	-1.42	-1.58	-1.59	0.01
2019	-0.26	-0.46	0.06	0.49	-0.2	-0.41	-0.46	-0.33	-0.17	0.11	0.2	0.21
2020	-0.41	0.3	-0.71	-0.89	-0.82	-0.3	-1.7	-0.99	-1.14	-0.61	-1.31	-0.69

Table 25: SPI with a timescale of 6 over the 1981-2020 period. In red are showed SPE values below -1, while in yellow are represented the values below 0 and above -1. 0 values coloured mean that the value is approximated but within the range

	SPI_6											
year	Jan	Feb	Mar	Apr	May	Jun	Jul	Aug	Sep	Oct	Nov	Dec
1981	-0.83	-0.86	0.17	-1.06	-0.57	-0.84	-0.95	-0.63	-0.07	1.48	1.23	2.38
1982	2.98	2.71	2	0.39	-0.15	-0.4	-0.9	0.14	-0.04	0.64	1.21	0.97
1983	1	0.43	0.9	0.6	0.8	0.26	-0.59	-1.14	-1	-1.75	-1.8	-1.83
1984	-0.82	-0.13	-1.19	-0.65	-0.96	-0.88	-1.76	-2.06	-0.43	-0.55	-0.27	-0.02
1985	0.43	0.8	-1.03	-0.28	-0.09	0.01	-0.59	-0.73	-0.97	-2.31	-1.6	-1.69
1986	-0.44	-0.27	0.19	1.96	1.47	1.37	0.94	1.35	1.11	0.15	-0.55	-0.46
1987	-0.75	-1.13	-0.66	-0.59	0.14	0.95	1.15	0.88	1.68	1.43	1.02	-0.19
1988	-0.2	-0.29	0.55	0.92	0.97	1.12	1.48	1.81	0.87	1.18	0.77	0.94
1989	0.21	-0.15	-0.3	-0.02	-0.35	-0.96	0	-0.34	-0.44	-0.8	-0.59	-0.37
1990	-1.47	-0.05	-0.12	-0.46	-0.06	0.65	0.63	-0.74	-0.37	0.15	0.92	0.16
1991	0.46	0.63	0.41	-0.26	-0.75	0.23	-0.23	-0.6	-0.6	-1	-0.62	-1.79
1992	-1.96	-0.87	-0.8	0.06	-1.17	-0.75	-0.45	-0.63	-1.27	-0.6	1.18	1.11
1993	0.94	0.77	0.93	-0.01	-1.17	-1.16	0.48	0.74	0.95	1.12	0.89	1.29
1994	0.43	0.31	0.66	0.75	1.56	0.83	-0.01	0.23	0.35	-0.02	-1.34	-0.32
1995	0.94	1.22	1.58	1.78	2.13	1.69	1.26	1.17	1.04	0.26	-0.52	-0.16
1996	-0.6	-1.24	-1.86	-1.18	-0.52	-1.2	-0.41	-0.24	-0.38	0.07	0.24	0.42
1997	-0.51	-0.3	-0.45	-0.61	-1.62	-0.78	0.02	-0.31	-0.38	-0.48	-0.2	-0.3
1998	-0.6	-0.68	-0.28	-0.15	-0.53	-0.77	-1.38	-1.51	-0.87	-0.27	1.01	0.52
1999	0.75	2.01	1.46	1.06	1.38	1.93	2.06	1.35	1.97	1.54	0.63	0.53
2000	0.46	1.07	0.98	1	0.69	-0.21	0.76	0.31	0.52	0.66	0.47	0.61
2001	0.23	-0.13	1.41	2.06	1.59	2.07	2.18	2.15	1.95	1.49	1.57	0.76
2002	0.34	0.58	-0.61	-0.69	0.01	0.05	0.12	0.27	0.64	1.13	1.32	1.52
2003	1.9	1.28	0.81	-0.02	-1.24	-1.76	-2.04	-1.79	-2.05	-1.06	-0.85	-0.56
2004	0.31	0.34	0.7	-0.48	0.06	0.5	-0.12	-0.32	-0.47	0.39	-0.46	-0.94
2005	-1.69	-1.32	-1.61	-1.47	-0.5	-0.31	0.05	0.65	0.58	0.12	-0.37	-0.29
2006	-0.92	-1.68	-0.12	1.06	1.52	0.91	0.77	1.33	0.94	-0.24	-0.88	-0.4
2007	0.14	-0.66	-0.56	-1.2	-0.46	-0.22	0.36	1.16	0.85	0.92	0.5	0.72
2008	0.12	-1.54	-1.2	0.91	0.53	0.08	0.2	0.76	0.88	0.51	0.57	0.74
2009	0.48	-0.09	0.24	-1.31	-0.71	-0.26	0.33	-0.01	-0.67	-0.43	0.24	0.3
2010	-0.49	-0.17	-0.18	-0.3	-0.4	-0.6	-0.07	0.15	0.23	0.31	0.09	0.24
2011	-0.28	-0.82	-1.53	-1.7	-1.59	-2.16	-1.48	-1.17	-0.94	-0.54	-0.98	0.22
2012	-0.19	-0.55	-1.23	-1.31	-0.41	-0.43	-0.29	0.48	1.08	1.59	1.79	1.79
2013	1.56	1.2	1.18	1.04	1.19	0.29	0.02	-0.29	-0.19	-0.06	-0.26	-0.29
2014	-0.07	0.46	-0.03	-0.36	-0.78	-0.35	0.22	0.1	0.32	0.23	0.35	0.17
2015	-0.2	-0.46	-0.22	0.5	0.67	0.83	0.11	-0.07	-0.63	-1.78	-2.27	-3.35
2016	-1.51	-0.65	-0.59	0.28	0.81	1.77	1.67	1.08	1.19	0.8	0.5	-1.1
2017	-1.71	-1.27	-1.06	-0.38	-1.01	-0.5	-0.44	-0.5	-0.35	-1.18	-0.45	0.15
2018	0.5	0.53	0.4	0.2	-0.14	-0.85	-2.34	-1.73	-2.09	-1.78	-2.07	-0.53
2019	-0.07	-0.5	-0.41	-0.2	0.52	-0.42	-0.62	-0.25	-0.39	0.24	-0.08	0.01
2020	-0.24	0.2	-0.04	-1.19	-1.02	-0.62	-0.91	-1.09	-1.59	-0.94	-1.04	-1.21

Table 26: SPI with a timescale of 12 over the 1981-2020 period. In red are showed SPI values below -1, while in yellow are represented the values below 0 and above -1. 0 values coloured mean that the value is approximated but within the range

SPI_{12}												
year	Jan	Feb	Mar	Apr	May	Jun	Jul	Aug	Sep	Oct	Nov	Dec
1981	-0.08	-0.44	-0.15	-0.47	-0.26	-1.15	-1.32	-1.1	0	0.5	0.51	1.22
1982	1.57	1.56	1.21	1.32	0.74	1.48	1.55	1.92	1.16	0.66	0.76	0.35
1983	-0.02	0.34	0.47	0.81	1.38	0.83	0.22	-0.64	-0.2	-0.85	-0.61	-1.07
1984	-1.12	-1.2	-1.61	-1.77	-2.06	-2.09	-1.91	-1.7	-1.04	-0.85	-0.92	-0.78
1985	-1.06	-1.16	-1.05	-0.65	-0.33	-0.08	-0.18	-0.08	-1.36	-1.84	-1.23	-1.21
1986	-0.85	-0.94	-0.7	-0.18	0.08	0.08	0.43	0.92	0.9	1.33	0.74	0.82
1987	0.24	0.5	0.46	-0.3	-0.36	0.42	0.42	0.04	0.91	0.7	0.81	0.62
1988	0.75	0.54	1.63	1.6	1.37	0.76	1.02	1.32	0.92	1.37	1.23	1.54
1989	1.31	1.54	0.46	0.84	0.25	-0.08	0.09	-0.42	-0.55	-0.64	-0.74	-1.11
1990	-1.04	-0.44	-0.49	-0.95	-0.54	0.22	-0.43	-0.67	-0.39	-0.22	0.59	0.59
1991	0.76	-0.26	-0.1	-0.11	0.11	0.22	0.1	-0.1	-0.24	-0.93	-1.05	-1.07
1992	-1.54	-1.25	-1.05	-0.75	-1.35	-1.96	-1.64	-1.1	-1.45	-0.45	0.09	0.21
1993	0.26	-0.06	-0.4	-0.51	0.07	-0.07	0.95	1.03	1.21	0.78	-0.14	0.09
1994	0.61	0.81	1.1	1.26	1.73	1.53	0.23	0.33	0.6	0.41	0.34	0.42
1995	0.59	1.01	1.22	1.13	0.82	1.19	1.55	1.66	1.65	1.28	1.34	1.31
1996	0.61	0.25	-0.22	-0.55	-0.82	-1.12	-0.76	-1	-1.35	-0.68	-0.24	-0.66
1997	-0.76	-0.52	-0.66	-0.38	-0.96	-0.37	-0.36	-0.49	-0.59	-0.77	-1.3	-0.92
1998	-0.46	-0.85	-0.54	-0.51	-0.59	-0.91	-1.48	-1.68	-0.85	-0.34	0.36	-0.27
1999	-0.55	0.3	0.26	0.45	1.67	1.94	2.07	2.31	2.27	1.72	1.45	1.97
2000	1.97	1.9	2.13	1.73	0.88	0.15	0.84	0.88	0.92	1.04	0.81	0.22
2001	0.71	0.1	1.24	1.79	1.47	2.12	1.87	1.7	2.22	2.31	2.27	2.24
2002	2	2.33	1.23	0.71	1.11	0.52	0.27	0.54	0.11	0.41	0.95	1.12
2003	1.41	1.09	0.94	0.8	0.14	-0.1	0.01	-0.46	-0.94	-0.81	-1.57	-1.86
2004	-1.35	-1.35	-1.12	-1.15	-0.63	-0.04	0.07	-0.09	0.04	-0.05	-0.34	-0.28
2005	-1.28	-1.29	-1.41	-0.61	-0.77	-1	-1.05	-0.27	-0.44	-0.8	-0.69	-0.53
2006	-0.64	-0.54	0.33	0.72	0.87	0.5	0	0.18	0.6	0.46	0.59	0.44
2007	0.65	0.75	0.38	-0.97	-1.03	-0.54	0.33	0.54	0.31	-0.02	0	0.29
2008	0.31	0.06	-0.05	1.21	0.67	0.51	0.19	-0.28	0	0.88	0.76	0.54
2009	0.42	0.55	0.78	-0.42	-0.13	0.27	0.52	-0.11	-0.39	-1.13	-0.37	-0.05
2010	-0.13	-0.22	-0.71	-0.57	-0.18	-0.32	-0.42	-0.03	0.03	0	-0.27	-0.36
2011	-0.32	-0.51	-0.77	-0.8	-1.07	-1.46	-1.33	-1.51	-1.62	-1.44	-1.91	-1.47
2012	-1.35	-1.53	-1.59	-1.27	-1.07	-0.26	-0.39	0.02	0.15	0.47	1.06	1
2013	0.85	1.21	1.53	1.79	2.08	1.49	1.05	0.52	0.54	0.56	0.7	-0.03
2014	-0.1	-0.02	-0.24	-0.32	-0.82	-0.57	0.08	0.31	0.18	-0.09	-0.33	-0.22
2015	-0.03	-0.33	0.06	0.43	0.67	0.73	-0.09	-0.4	-0.64	-0.94	-1	-1.32
2016	-0.96	-0.61	-0.95	-1.14	-0.89	-0.32	0.47	0.47	0.56	0.7	0.91	0.82
2017	0.36	0.13	0.33	0.33	-0.38	-1.27	-1.48	-1.24	-0.9	-1.13	-1.1	-0.35
2018	-0.06	-0.14	-0.09	-0.78	-0.49	-0.63	-1.3	-0.98	-1.25	-1.15	-1.58	-1.15
2019	-1.86	-1.98	-1.94	-1.48	-1.02	-0.8	-0.56	-0.57	-0.57	0.01	0.29	-0.4
2020	-0.74	-0.18	-0.4	-0.57	-0.84	-0.56	-0.89	-0.77	-1.21	-1.46	-1.55	-1.45

Table 27: Duration of drought for different SPEI and SPI timescale (1, 2, 3, 4, 5, 6, 12). At the bottom average over the periods 1981-2020, 1981-2000, 2001-2020. d = duration

	$SPEI_1$	SPI_1	$SPEI_2$	SPI_2	$SPEI_3$	SPI_3	$SPEI_4$	SPI_4	$SPEI_5$	SPI_5	$SPEI_6$	SPI_6	$SPEI_{12}$	SPI_{12}
year	d	d	d	d	d	d	d	d	d	d	d	d	d	d
1981	1	1	0	4	5	5	0	5	6	8	0	6	0	9
1982	4	4	4	4	4	3	3	4	0	3	0	0	0	0
1983	3	3	6	6	4	4	6	6	6	6	6	6	0	5
1984	0	6	0	6	5	7	4	7	3	10	6	12	12	12
1985	4	5	5	5	6	6	6	6	6	7	6	6	4	12
1986	3	3	3	3	3	4	3	4	0	0	0	0	0	0
1987	3	3	0	0	1	1	0	0	3	4	4	4	0	0
1988	0	0	0	0	0	0	2	2	2	2	0	0	0	0
1989	2	2	3	4	3	0	0	0	0	8	0	0	0	5
1990	2	2	2	2	1	2	2	1	1	1	1	5	0	5
1991	4	4	4	4	3	5	5	5	5	5	5	6	0	5
1992	1	1	5	2	5	5	9	9	6	9	6	6	11	10
1993	6	3	6	6	5	5	4	4	3	3	3	3	0	0
1994	2	2	2	2	3	3	5	4	5	2	3	3	0	0
1995	2	2	2	2	3	3	0	0	0	0	0	0	0	0
1996	1	4	4	4	4	6	6	7	7	7	7	9	0	10
1997	4	4	6	6	5	6	4	6	5	5	4	6	12	12
1998	2	2	4	7	7	7	6	5	5	5	10	10	10	10
1999	0	0	1	1	0	0	0	0	0	0	0	0	0	0
2000	3	1	2	0	2	0	0	0	0	0	0	0	0	0
2001	0	0	0	0	0	0	0	0	0	0	0	0	0	0
2002	0	0	4	2	4	0	4	0	0	0	0	0	0	0
2003	8	8	9	9	9	8	10	10	9	9	9	9	7	5
2004	2	2	2	2	0	0	4	0	5	2	0	0	6	6
2005	4	2	3	3	3	3	4	4	6	6	7	6	12	12
2006	2	2	3	2	2	2	2	2	3	3	3	3	0	0
2007	3	3	3	3	3	2	7	2	7	6	7	5	5	3
2008	2	2	2	2	1	1	2	2	3	3	2	2	0	0
2009	3	3	3	2	3	2	2	2	0	0	4	3	5	5
2010	4	4	0	4	0	5	4	4	0	0	0	0	0	0
2011	6	6	5	5	7	7	9	9	12	12	11	11	12	12
2012	4	4	4	4	3	3	5	3	7	5	7	7	8	7
2013	3	1	3	3	4	3	3	3	0	0	0	0	0	0
2014	4	1	6	0	6	0	5	4	5	0	5	0	7	0
2015	6	6	6	6	6	6	6	5	6	5	6	5	6	6
2016	3	3	3	2	4	4	3	3	3	2	3	3	6	6
2017	2	2	7	3	8	3	7	3	12	12	12	11	8	8
2018	4	4	9	6	9	9	9	9	9	7	9	8	12	12
2019	0	0	3	0	0	0	0	0	0	0	0	0	12	9
2020	3	3	9	9	12	10	12	12	12	10	12	10	12	12
1981-2000	2.4	2.6	3	3.4	3.5	3.6	3.3	3.8	3.2	4.3	3.1	4.1	2.5	4.8
2001-2020	3.2	2.8	4.2	3.4	4.2	3.4	4.9	3.9	5	4.1	4.9	4.2	5.9	5.2
1981-2020	2.8	2.7	3.6	3.4	3.8	3.5	4.1	3.8	4.1	4.2	4	4.1	4.2	5

Table 28: Frequency of drought for different SPEI and SPI timescale (1, 2, 3, 4, 5, 6, 12). At the bottom average over the periods 1981-2020, 1981-2000, 2001-2020. F_e = frequency

	$SPEI_1$	SPI_1	$SPEI_2$	SPI_2	$SPEI_3$	SPI_3	$SPEI_4$	SPI_4	$SPEI_5$	SPI_5	$SPEI_6$	SPI_6	$SPEI_{12}$	SPI_{12}
year	F_e	F_e	F_e	F_e	F_e	F_e	F_e	F_e	F_e	F_e	F_e	F_e	F_e	F_e
1981	8.3	8.3	0	33.3	41.7	41.7	0	41.7	50	66.7	0	50	0	75
1982	33.3	33.3	33.3	33.3	33.3	25	25	33.3	0	25	0	0	0	0
1983	25	25	50	50	33.3	33.3	50	50	50	50	50	50	0	41.7
1984	0	50	0	50	41.7	58.3	33.3	58.3	25	83.3	50	100	100	100
1985	33.3	41.7	41.7	41.7	50	50	50	50	50	58.3	50	50	33.3	100
1986	25	25	25	25	25	33.3	25	33.3	0	0	0	0	0	0
1987	25	25	0	0	8.3	8.3	0	0	25	33.3	33.3	33.3	0	0
1988	0	0	0	0	0	0	16.7	16.7	16.7	16.7	0	0	0	0
1989	16.7	16.7	25	33.3	25	0	0	0	0	66.7	0	0	0	41.7
1990	16.7	16.7	16.7	16.7	8.3	16.7	16.7	8.3	8.3	8.3	8.3	41.7	0	41.7
1991	33.3	33.3	33.3	33.3	25	41.7	41.7	41.7	41.7	41.7	41.7	50	0	41.7
1992	8.3	8.3	41.7	16.7	41.7	41.7	75	75	50	75	50	50	91.7	83.3
1993	50	25	50	50	41.7	41.7	33.3	33.3	25	25	25	25	0	0
1994	16.7	16.7	16.7	16.7	25	25	41.7	33.3	41.7	16.7	25	25	0	0
1995	16.7	16.7	16.7	16.7	25	25	0	0	0	0	0	0	0	0
1996	8.3	33.3	33.3	33.3	33.3	50	50	58.3	58.3	58.3	58.3	75	0	83.3
1997	33.3	33.3	50	50	41.7	50	33.3	50	41.7	41.7	33.3	50	100	100
1998	16.7	16.7	33.3	58.3	58.3	58.3	50	41.7	41.7	41.7	83.3	83.3	83.3	83.3
1999	0	0	8.3	8.3	0	0	0	0	0	0	0	0	0	0
2000	25	8.3	16.7	0	16.7	0	0	0	0	0	0	0	0	0
2001	0	0	0	0	0	0	0	0	0	0	0	0	0	0
2002	0	0	33.3	16.7	33.3	0	33.3	0	0	0	0	0	0	0
2003	66.7	66.7	75	75	75	66.7	83.3	83.3	75	75	75	75	58.3	41.7
2004	16.7	16.7	16.7	16.7	0	0	33.3	0	41.7	16.7	0	0	50	50
2005	33.3	16.7	25	25	25	25	33.3	33.3	50	50	58.3	50	100	100
2006	16.7	16.7	25	16.7	16.7	16.7	16.7	16.7	25	25	25	25	0	0
2007	25	25	25	25	25	16.7	58.3	16.7	58.3	50	58.3	41.7	41.7	25
2008	16.7	16.7	16.7	16.7	8.3	8.3	16.7	16.7	25	25	16.7	16.7	0	0
2009	25	25	25	16.7	25	16.7	16.7	16.7	0	0	33.3	25	41.7	41.7
2010	33.3	33.3	0	33.3	0	41.7	33.3	33.3	0	0	0	0	0	0
2011	50	50	41.7	41.7	58.3	58.3	75	75	100	100	91.7	91.7	100	100
2012	33.3	33.3	33.3	33.3	25	25	41.7	25	58.3	41.7	58.3	58.3	66.7	58.3
2013	25	8.3	25	25	33.3	25	25	25	0	0	0	0	0	0
2014	33.3	8.3	50	0	50	0	41.7	33.3	41.7	0	41.7	0	58.3	0
2015	50	50	50	50	50	50	50	41.7	50	41.7	50	41.7	50	50
2016	25	25	25	16.7	33.3	33.3	25	25	25	16.7	25	25	50	50
2017	16.7	16.7	58.3	25	66.7	25	58.3	25	100	100	100	91.7	66.7	66.7
2018	33.3	33.3	75	50	75	75	75	75	75	58.3	75	66.7	100	100
2019	0	0	25	0	0	0	0	0	0	0	0	0	100	75
2020	25	25	75	75	100	83.3	100	100	100	83.3	100	83.3	100	100
1981-2000	19.6	21.7	24.6	28.3	28.8	30	27.1	31.2	26.3	35.4	25.4	34.2	20.4	39.6
2001-2020	26.3	23.3	35	27.9	35	28.3	40.8	32.1	41.3	34.2	40.4	34.6	49.2	42.9
1981-2020	22.9	22.5	29.8	28.1	31.9	29.2	34	31.7	33.8	34.8	32.9	34.4	34.8	41.3

Table 29: Severity of drought for different SPEI and SPI timescale (1, 2, 3, 4, 5, 6, 12). At the bottom average over the periods 1981-2020, 1981-2000, 2001-2020. S_e = Severity

	$SPEI_1$	SPI_1	$SPEI_2$	SPI_2	$SPEI_3$	SPI_3	$SPEI_4$	SPI_4	$SPEI_5$	SPI_5	$SPEI_6$	SPI_6	$SPEI_{12}$	SPI_{12}
year	S_e	S_e	S_e	S_e	S_e	S_e	S_e	S_e	S_e	S_e	S_e	S_e	S_e	S_e
1981	1.3	1.9	0	2.8	2.8	3.8	0	3.6	3.3	5.2	0	4.1	0	5
1982	3.6	4.8	3	4.2	2.7	3.7	2.3	3.5	0	2.6	0	0	0	0
1983	3.8	4.4	4.6	5.7	5.4	6.3	6.4	7.5	7.2	8.2	7.1	8.1	0	3.4
1984	0	4.8	0	6	3.3	6.5	3.1	7.1	2.8	8.4	3.5	9.7	10.5	17
1985	4.4	6.1	5.2	6.3	5.7	6.9	5.7	7.9	5.7	8.1	5.4	7.9	3.8	10.2
1986	2.6	2.5	2.6	2.4	2.1	1.5	1.8	2.1	0	0	0	0	0	0
1987	2	1.7	0	0	1.4	0.9	0	0	2.1	2.8	2.2	3.1	0	0
1988	0	0	0	0	0	0	2.6	2.1	2	1.5	0	0	0	0
1989	1.9	2.3	1.8	2.5	2.2	0	0	0	0	3.9	0	0	0	3.5
1990	2.1	2.3	1.8	2.1	1.5	1.8	1.1	1.2	1.2	1.3	1.3	2.2	0	3.5
1991	1.9	4.3	4.3	5.1	4.4	5.1	4.4	5.2	4.7	5.3	3.9	4.8	0	3.4
1992	1.7	2.3	3.8	2.5	3.7	3.4	5.5	5.9	4.5	6.8	4.9	4.9	10.5	12.5
1993	3.9	3.3	5.3	5.2	5.2	5.3	4.3	4.6	3.4	3.4	2.4	2.3	0	0
1994	2.4	2.7	2.6	2.7	2.6	2	2.7	1.8	2.6	2	2.3	1.7	0	0
1995	2.2	2.9	3.1	3	2.1	1.6	0	0	0	0	0	0	0	0
1996	1.6	4	2.8	3.6	2.6	4.1	4	5.5	4.8	6.6	5	7.6	0	7.4
1997	3	2.6	4.5	4.2	4.4	4.3	4.1	4.1	3.9	3.9	3.4	4.3	4.8	8.1
1998	1.8	2.7	4	4.6	5.2	5	5.4	5.6	5.8	5.9	7.5	7	8.2	8.2
1999	0	0	1.2	1.1	0	0	0	0	0	0	0	0	0	0
2000	1.7	1.2	1.6	0	1.3	0	0	0	0	0	0	0	0	0
2001	0	0	0	0	0	0	0	0	0	0	0	0	0	0
2002	0	0	2.2	1.7	2.7	0	3.1	0	0	0	0	0	0	0
2003	8.1	6	10	8.1	11.1	9.5	12.3	10.9	13.2	11.4	13.3	11.4	8.2	5.6
2004	2.2	2.3	1.8	2	0	0	2.7	0	2.5	1.9	0	0	7.3	5.6
2005	2.6	1.7	3.1	3.3	4.7	5.4	5.2	5.9	5.9	6.3	6.9	6.9	9.5	10.1
2006	3.3	3.6	3.1	3.1	2.7	2.7	3	3.3	3.1	3.3	2.8	2.7	0	0
2007	2.2	3.2	3	3.7	2.7	1.6	6.7	2.3	7.2	3.3	6.7	3.1	4.9	2.5
2008	2.1	1.9	1.9	1.7	1.1	1	2	1.9	3	3.2	2.7	2.7	0	0
2009	2.4	2.1	2.3	1.9	1.9	2.3	3.5	1.9	0	0	2.4	2.3	2.6	2.1
2010	2.2	2.4	0	2.7	0	2.6	1.9	2.4	0	0	0	0	0	0
2011	6.9	5.9	8.7	7.6	8.3	8.1	9.7	9.4	12.9	12	13.7	13.2	13.9	14.2
2012	5.3	4.6	5.3	5.2	4.6	4.5	4.2	3.2	4.8	3.9	5.6	4.4	8.6	7.5
2013	2.6	1.1	3	2.8	2.7	2.6	2.6	2.3	0	0	0	0	0	0
2014	1.8	1.1	3.4	0	3.7	0	3.5	2.3	3.4	0	2.6	0	3.4	0
2015	7.6	7.3	9	9.1	10.1	8	9.7	10.2	8.9	9.5	7.9	8.1	6.6	4.4
2016	2.9	2.4	2.9	2.6	3.8	2.4	3.5	3.1	2.4	2.2	3.8	2.8	7.3	4.9
2017	2.3	1.7	3.9	1.6	6	2.1	5.4	3	10	7	11.9	8.8	10.1	7.8
2018	5.2	5.1	10.5	6.4	12	9.7	12.6	10.7	12.6	11	12.9	11.5	14.9	9.6
2019	0	0	1.5	0	0	0	0	0	0	0	0	0	15.3	10.8
2020	2.8	2.3	8	6.1	10.8	5.9	12.3	8.8	12.8	9.1	13.2	9.7	15.7	10.6
1981-2000	2.1	2.8	2.6	3.2	2.9	3.1	2.7	3.4	2.7	3.8	2.4	3.4	1.9	4.1
2001-2020	3.1	2.8	4.2	3.5	4.4	3.4	5.2	4.1	5.1	4.2	5.3	4.4	6.4	4.8
1981-2020	2.6	2.8	3.4	3.3	3.7	3.3	3.9	3.7	3.9	4	3.9	3.9	4.2	4.4

Table 30: Intensity of drought for different SPEI and SPI timescale (1, 2, 3, 4, 5, 6, 12). At the bottom average over the periods 1981-2020, 1981-2000, 2001-2020. I_e = Intensity

	$SPEI_1$	SPI_1	$SPEI_2$	SPI_2	$SPEI_3$	SPI_3	$SPEI_4$	SPI_4	$SPEI_5$	SPI_5	$SPEI_6$	SPI_6	$SPEI_{12}$	SPI_{12}
year	I_e	I_e	I_e	I_e	I_e	I_e	I_e	I_e	I_e	I_e	I_e	I_e	I_e	I_e
1981	1.31	1.88	0	0.7	0.57	0.77	0	0.73	0.55	0.65	0	0.69	0	0.55
1982	0.91	1.21	0.75	1.04	0.68	1.23	0.76	0.87	0	0.87	0	0	0	0
1983	1.25	1.45	0.76	0.95	1.35	1.57	1.06	1.25	1.21	1.37	1.19	1.35	0	0.67
1984	0	0.79	0	1	0.65	0.93	0.77	1.01	0.92	0.84	0.59	0.81	0.87	1.42
1985	1.11	1.22	1.04	1.26	0.94	1.16	0.94	1.31	0.94	1.15	0.9	1.32	0.95	0.85
1986	0.86	0.84	0.87	0.8	0.7	0.38	0.59	0.52	0	0	0	0	0	0
1987	0.67	0.58	0	0	1.44	0.87	0	0	0.69	0.69	0.55	0.78	0	0
1988	0	0	0	0	0	0	1.29	1.04	0.99	0.76	0	0	0	0
1989	0.95	1.17	0.58	0.63	0.74	0	0	0	0	0.49	0	0	0	0.69
1990	1.03	1.15	0.89	1.05	1.53	0.88	0.56	1.17	1.18	1.27	1.32	0.43	0	0.69
1991	0.48	1.07	1.08	1.29	1.46	1.02	0.89	1.04	0.94	1.06	0.79	0.81	0	0.68
1992	1.74	2.32	0.77	1.26	0.73	0.67	0.61	0.66	0.74	0.76	0.81	0.81	0.95	1.25
1993	0.65	1.09	0.88	0.86	1.04	1.05	1.09	1.14	1.14	1.15	0.79	0.78	0	0
1994	1.22	1.37	1.32	1.36	0.87	0.67	0.54	0.46	0.52	1.02	0.77	0.56	0	0
1995	1.08	1.47	1.56	1.49	0.69	0.54	0	0	0	0	0	0	0	0
1996	1.59	0.99	0.69	0.91	0.66	0.68	0.66	0.78	0.69	0.94	0.72	0.85	0	0.74
1997	0.75	0.66	0.76	0.7	0.89	0.72	1.03	0.68	0.78	0.78	0.84	0.71	0.4	0.67
1998	0.92	1.34	1	0.65	0.74	0.71	0.9	1.12	1.17	1.18	0.75	0.7	0.82	0.82
1999	0	0	1.21	1.11	0	0	0	0	0	0	0	0	0	0
2000	0.56	1.22	0.78	0	0.65	0	0	0	0	0	0	0	0	0
2001	0	0	0	0	0	0	0	0	0	0	0	0	0	0
2002	0	0	0.56	0.83	0.68	0	0.77	0	0	0	0	0	0	0
2003	1.01	0.74	1.12	0.9	1.24	1.19	1.23	1.09	1.47	1.27	1.48	1.26	1.18	1.13
2004	1.09	1.17	0.9	1.02	0	0	0.66	0	0.5	0.94	0	0	1.21	0.94
2005	0.64	0.86	1.04	1.1	1.55	1.81	1.3	1.47	0.98	1.05	0.98	1.15	0.79	0.84
2006	1.64	1.81	1.02	1.55	1.33	1.36	1.48	1.66	1.03	1.11	0.93	0.91	0	0
2007	0.75	1.06	1.01	1.24	0.88	0.82	0.96	1.14	1.02	0.55	0.95	0.62	0.97	0.85
2008	1.03	0.93	0.96	0.86	1.14	1.04	0.98	0.96	1.01	1.07	1.35	1.37	0	0
2009	0.79	0.7	0.76	0.94	0.65	1.14	0.74	0.95	0	0	0.59	0.76	0.53	0.41
2010	0.54	0.6	0	0.67	0	0.51	0.48	0.61	0	0	0	0	0	0
2011	1.15	0.98	1.73	1.51	1.19	1.16	1.08	1.04	1.07	1	1.25	1.2	1.16	1.18
2012	1.32	1.16	1.33	1.29	1.53	1.5	0.85	1.07	0.69	0.79	0.8	0.63	1.07	1.07
2013	0.86	1.1	1	0.94	0.69	0.86	0.86	0.76	0	0	0	0	0	0
2014	0.45	1.12	0.56	0	0.62	0	0.71	0.58	0.67	0	0.53	0	0.48	0
2015	1.26	1.22	1.51	1.52	1.68	1.34	1.62	2.04	1.48	1.89	1.32	1.62	1.1	0.73
2016	0.96	0.79	0.98	1.3	0.96	0.61	1.16	1.02	0.8	1.12	1.25	0.92	1.22	0.81
2017	1.16	0.87	0.56	0.54	0.75	0.69	0.77	1.01	0.83	0.58	1	0.8	1.27	0.98
2018	1.31	1.28	1.16	1.06	1.33	1.08	1.4	1.19	1.4	1.57	1.43	1.44	1.24	0.8
2019	0	0	0.5	0	0	0	0	0	0	0	0	0	1.27	1.2
2020	0.92	0.78	0.89	0.68	0.9	0.59	1.03	0.73	1.06	0.91	1.1	0.97	1.31	0.88
1981-2000	0.85	1.09	0.75	0.85	0.82	0.69	0.58	0.69	0.62	0.75	0.5	0.53	0.2	0.45
2001-2020	0.84	0.92	0.88	0.9	0.86	0.79	0.95	0.87	0.7	0.69	0.75	0.68	0.74	0.59
1981-2020	0.85	1.01	0.81	0.88	0.84	0.74	0.77	0.78	0.66	0.72	0.62	0.61	0.47	0.52

Table 31: Trees samples. Some data are not provided because they are not available.

Species	Category	Birth	Plantation year	Area	Street	Number
Dead in 2018						
Pyrus communis	Park tree	1939	1950	Langstrasse	Zeughausstr.	AU-4678
Robinia pseudoacacia Unifoliola'	City tree	1994		Werd	Kaesernenstr. 10	AU-27
Robinia pseudoacacia 'Unifoliola'	City tree	1996		Werd	Kaesernenstr.	AU-26
Dead in 2019						
Acer platanoides	City tree	1984		Altstetten	Badenerstr.	AL-1728
Acer platanoides	City tree	2003	2011	Altstetten	Badenerstr. 537	AL-5004
Aesculus hippocastanum 'Baumannii'	City tree	2012		Altstetten	Badenerstr. 520	AL-3425
Betula pendula	Park tree	1952	1970	Albisrieden	Freibad Letzigraben 5/Edelweissstr.	AR-1612
Catalpa bignonioides	Park tree	1969	1980	Langstrasse	Lutherwiese /Stauffacherstr.	AU-6141
Crataegus laevigata	City tree	1968	1980	Langstrasse	Schulhaus Feld 89/Feldstr.	AU-3816
Platanus x hispanica	City tree	2013	2016	Langstrasse	Herman-Greulich-Str. 48	AU-5811
Platanus x hispanica	City tree	2013	2018	Langstrasse	Herman-Greulich-Str. 48	AU-6861
Platanus x hispanica	City tree	2013	2016	Langstrasse	Herman-Greulich-Str. 48	AU-5810
Platanus x hispanica	City tree	2013	2018	Langstrasse	Herman-Greulich-Str. 48	AU-6860
Platanus x hispanica	City tree	2013	2018	Langstrasse	Herman-Greulich-Str. 48	AU-5813
Robinia pseudoacacia 'Unifoliola'	City tree	1976		Langstrasse	Kanzleistr. 137	AU-553
Robinia pseudoacacia 'Unifoliola'	City tree	1984		Langstrasse	Kanzleistr. 126	AU-550
Sophora japonica	City tree	1998	2004	Langstrasse	Lutherstr. 6	AU-3578
Tilia x europaea 'Euchlora'	City tree	1971		Langstrasse	Kasernenstr.	AU-1072
Dead in 2020						
Acer rufinerve	Park tree		1960	Langstrasse	Baeckeranlage 67+91/Hohlstr.	AU-5969
Betula pendula	Park tree	1957	1960	Sihlfeld	FH Sihlfeld 151/Aemtlerstr.	WD-5514
Betula pendula	Park tree	1928	1960	Sihlfeld	FH Sihlfeld 31/Albisriederstr.	WD-7635
Cercidiphyllum japonicum	Park tree	1926		Sihlfeld	FH Sihlfeld 31/Albisriederstr.	WD-7750
Crataegus x lavalleei	City tree	1983		Langstrasse	Baeckerstr. 1	AU-815
Magnolia kobus	City tree	2000		Sihlfeld	Seebahnstr. 155	WD-3167
Magnolia kobus	City tree	2000		Sihlfeld	Seebahnstr. 155	WD-3166
Paulownia tomentosa	Park tree	1994		Sihlfeld	FH Sihlfeld 151/Aemtlerstr.	WD-6449
Picea omorika 'Pendula'	Park tree	1935	2011	Sihlfeld	FH Sihlfeld 151/Aemtlerstr.	WD-5494
Picea omorika 'Pendula'	Park tree	1937	2012	Sihlfeld	FH Sihlfeld 151/Aemtlerstr.	WD-5497
Prunus 'Umineko'	City tree	2000	2011	Sihlfeld	Seebahnstr. 105	WD-5853
Prunus 'Umineko'	City tree	2006		Sihlfeld	Seebahnstr.	WD-6234
Prunus 'Umineko'	City tree	2003		Sihlfeld	Seebahnstr. 105	WD-5852
Robinia spec.	Park tree	1996		Sihlfeld	FH Sihlfeld 151/Aemtlerstr.	WD-7030
Robinia pseudoacacia	Park tree	1996		Sihlfeld	FH Sihlfeld 31/Albisriederstr.	WD-7203
Robinia pseudoacacia 'Unifoliola'	City tree	1982		Langstrasse	Engelstr.	AU-591
Tilia x europaea 'Euchlora'	City tree	1980		Gewerbeschule	Josefstr.	IQ-1839
Dead in 2021						
Acer platanoides	Park tree	1986	1995	Albisrieden	Sportplatz Utogrund 43/Dennlerstr.	AR-2602
Acer pseudoplatanus	City tree	1940		Sihlfeld	Albisriederstr. 22	WD-1818
Acer platanoides	City tree	1947	1990	Sihlfeld	Albisriederstr. 132	WD-7436
Ailanthus altissima	City tree	1967	1970	Sihlfeld	Birmensdorferstr. 377	WD-1303
Ailanthus altissima	City tree	1918		Sihlfeld	Albisriederstr. 80	WD-1736
Ailanthus altissima	City tree	1907		Sihlfeld	Albisriederstr. 84	WD-1742
Ailanthus altissima	City tree	2000	2004	Sihlfeld	Albisriederstr.	WD-2642
Amelanchier lamarckii	Park tree	1994	2015	Sihlfeld	Brahmsstr. 65-71	WD-9839
Betula pendula	Park tree	1974	1985	Friesenberg	Schulhaus Ältschi 182	WD-6351
Betula pendula	Park tree	1949	1980	Sihlfeld	FH Sihlfeld 151/Aemtlerstr.	WD-6467
Fraxinus excelsior	City tree	1932	1970	Alt-Wiedikon	Wasserschäpfi	WD-707
Pinus mugo	Park tree	1950	1960	Sihlfeld	FH Sihlfeld 31/Albisriederstr.	WD-7795
Prunus cerasifera	City tree	1983		Sihlfeld	Bertastr. 57	WD-1653
Prunus cerasifera	City tree	1982	1998	Sihlfeld	Bertastr. 36	WD-1832
Prunus cerasifera	City tree	1981		Sihlfeld	Aemtlerstr. 86	WD-1851
Prunus 'Umineko'	City tree	1991	2004	Sihlfeld	Zentralstr. 162	WD-2742
Prunus cerasifera	City tree	1996	2006	Sihlfeld	Bertastr. 31	WD-3210
Prunus cerasifera	City tree	1985	2004	Alt-Wiedikon	Wasserschäpfi 6	WD-680
Prunus cerasifera	Park tree	1988	1995	Sihlfeld	Brahmsstr. 54-92	WD-8465
Prunus x	Park tree	2006	2010	Sihlfeld	Brahmsstr. 73-77	WD-9834
Robinia pseudoacacia	City tree	1973		Sihlfeld	Bertastr. 88	WD-1625
Robinia pseudoacacia	City tree	1977		Sihlfeld	Bertastr. 50	WD-1649
Robinia pseudoacacia	City tree	1953		Sihlfeld	Zentralstr. 129	WD-1863
Robinia pseudoacacia	City tree	1975		Sihlfeld	Zurlindenstr.	WD-2167
Robinia pseudoacacia	City tree	1975		Sihlfeld	Rotachstr. 73	WD-2221
Robinia pseudoacacia	City tree	2000	2006	Sihlfeld	Zurlindenstr. 31	WD-2774
Robinia pseudoacacia	Park tree	1954	1970	Sihlfeld	Kindergarten Gutstr. 1+2 126-128/Gutstr.	WD-4025
Robinia spec.	Park tree	1967	1970	Sihlfeld	Zurlindenstr. 230-236	WD-4610
Robinia pseudoacacia	Park tree	1988	1970	Sihlfeld	Schulhaus Aemtler A 101/Aemtlerstr.	WD-6038
Tilia cordata	City tree	1952	1965	Sihlfeld	Gutstr. 127	WD-1458
Tilia x europea	City tree	1912		Sihlfeld	Aemtlerstr.	WD-1712
Tilia cordata	City tree	1975		Sihlfeld	Fritschistr.	WD-2003
Tilia cordata	Park tree	1972	1950	Sihlfeld	Fritschiwiese	WD-2016

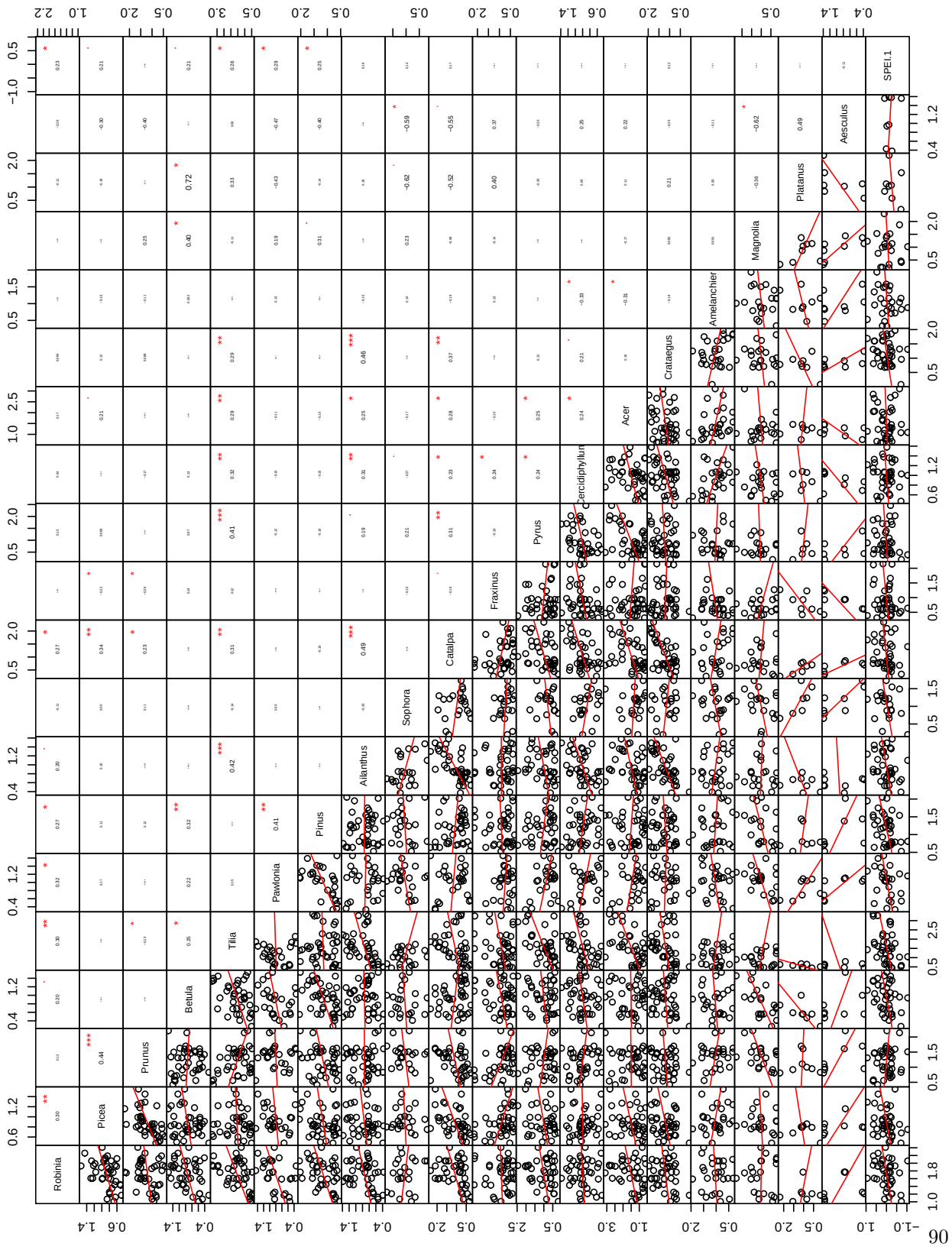

Figure 11: Correlation matrix showing the Mann - Kendall statistics for all the tree species and the vegetative SPEI with a timescale of 1.

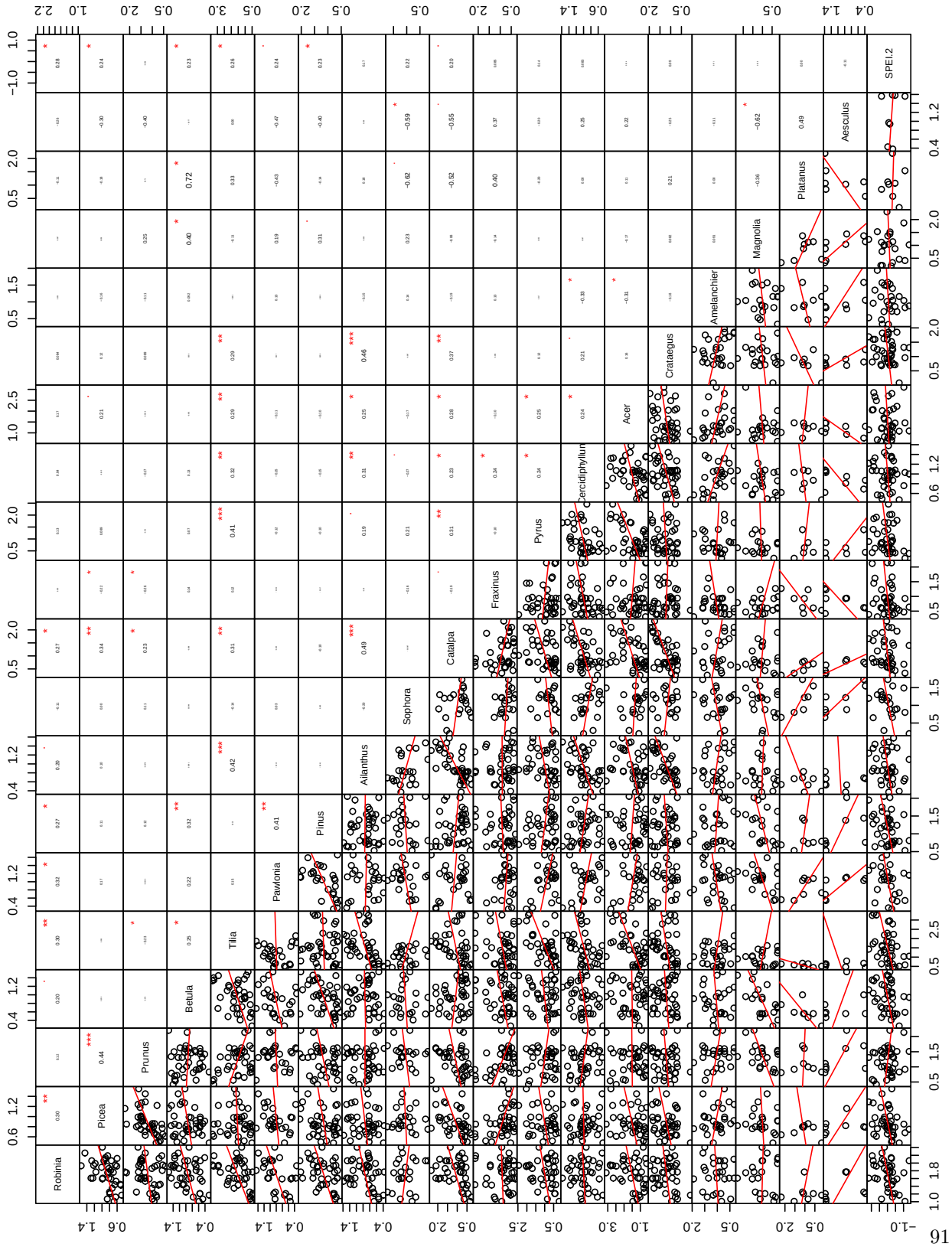

Figure 12: Correlation matrix showing the Mann - Kendall statistics for all the tree species and the vegetative SPEI with a timescale of 2.

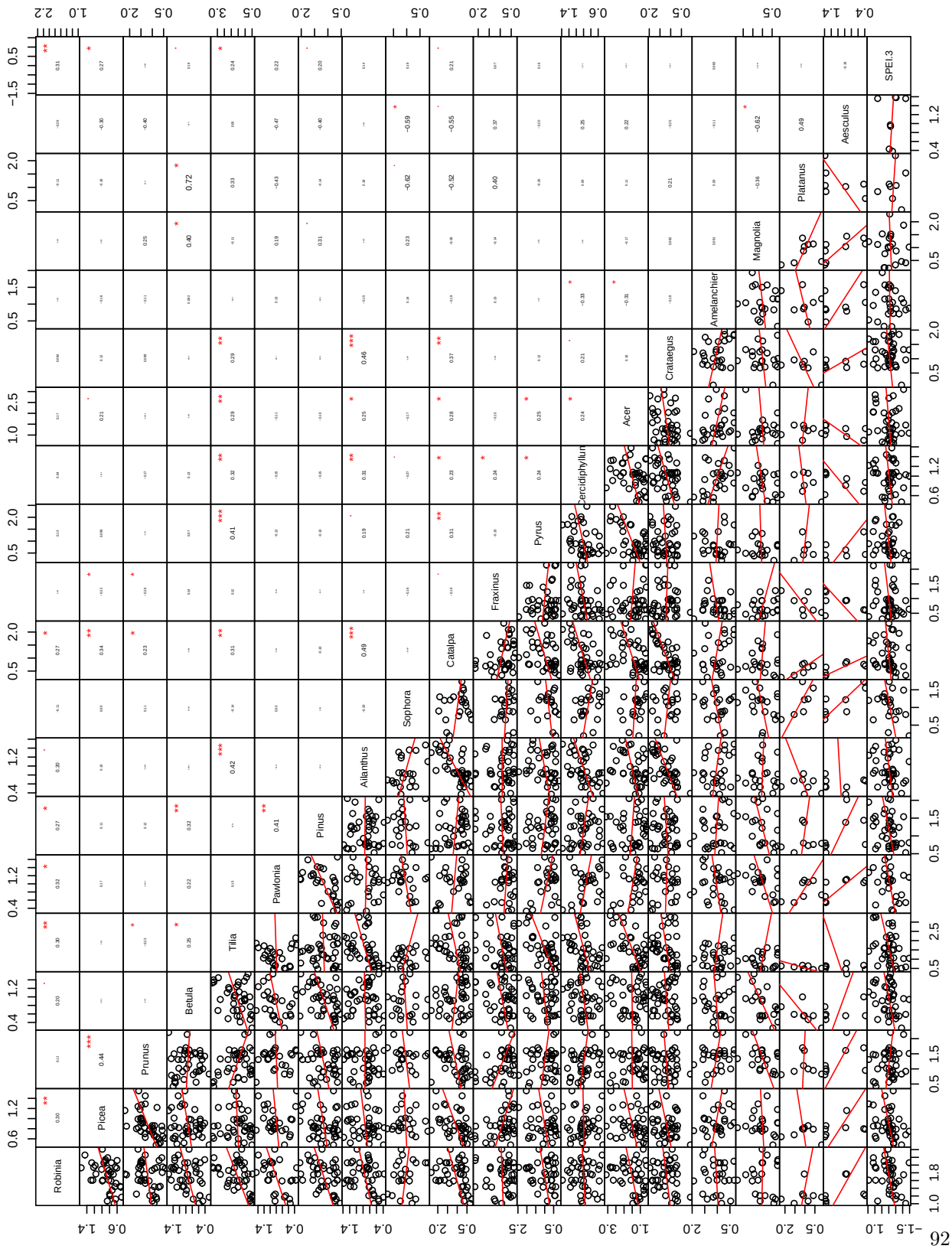

Figure 13: Correlation matrix showing the Mann - Kendall statistics for all the tree species and the vegetative SPEI with a timescale of 3.

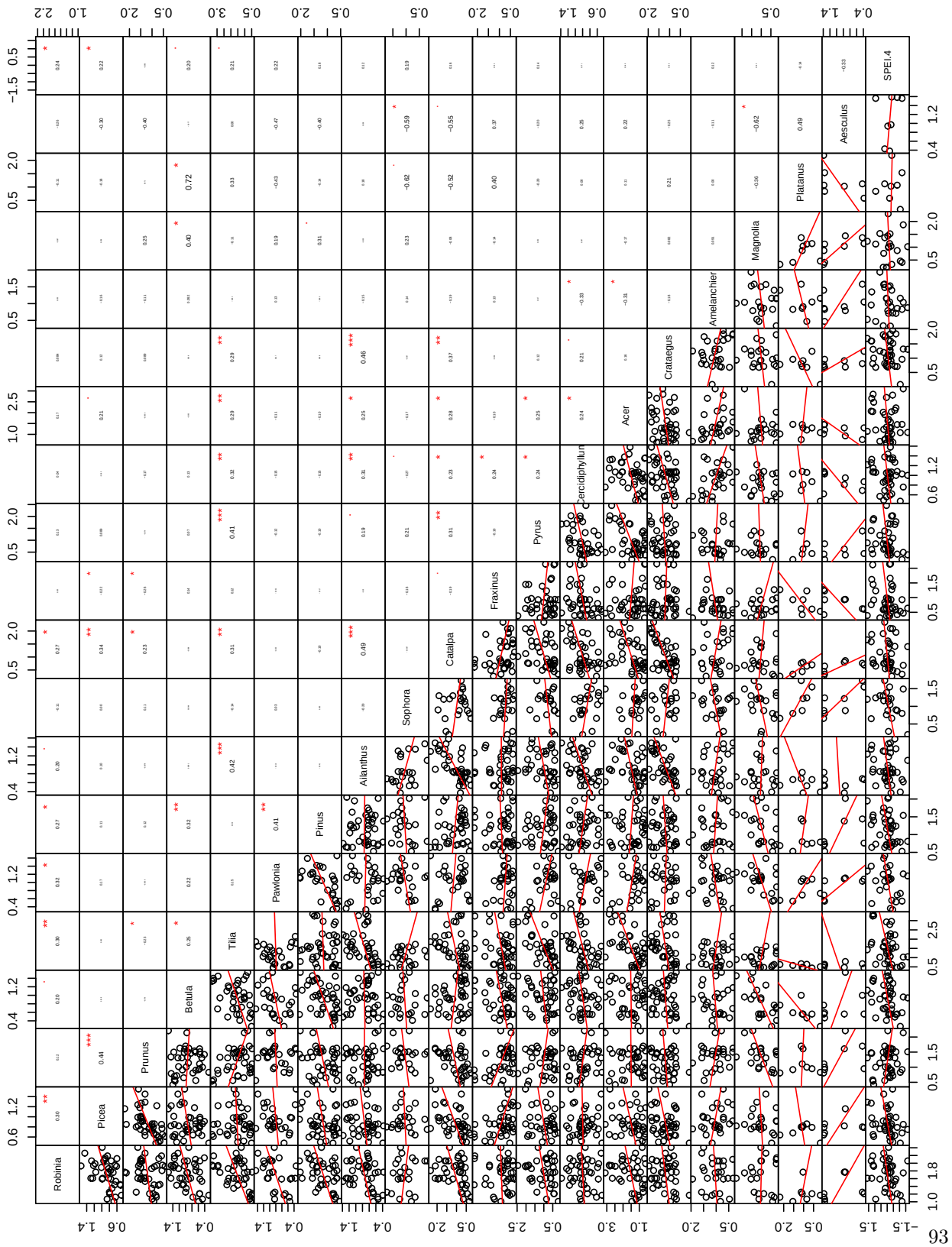

Figure 14: Correlation matrix showing the Mann - Kendall statistics for all the tree species and the vegetative SPEI with a timescale of 4.

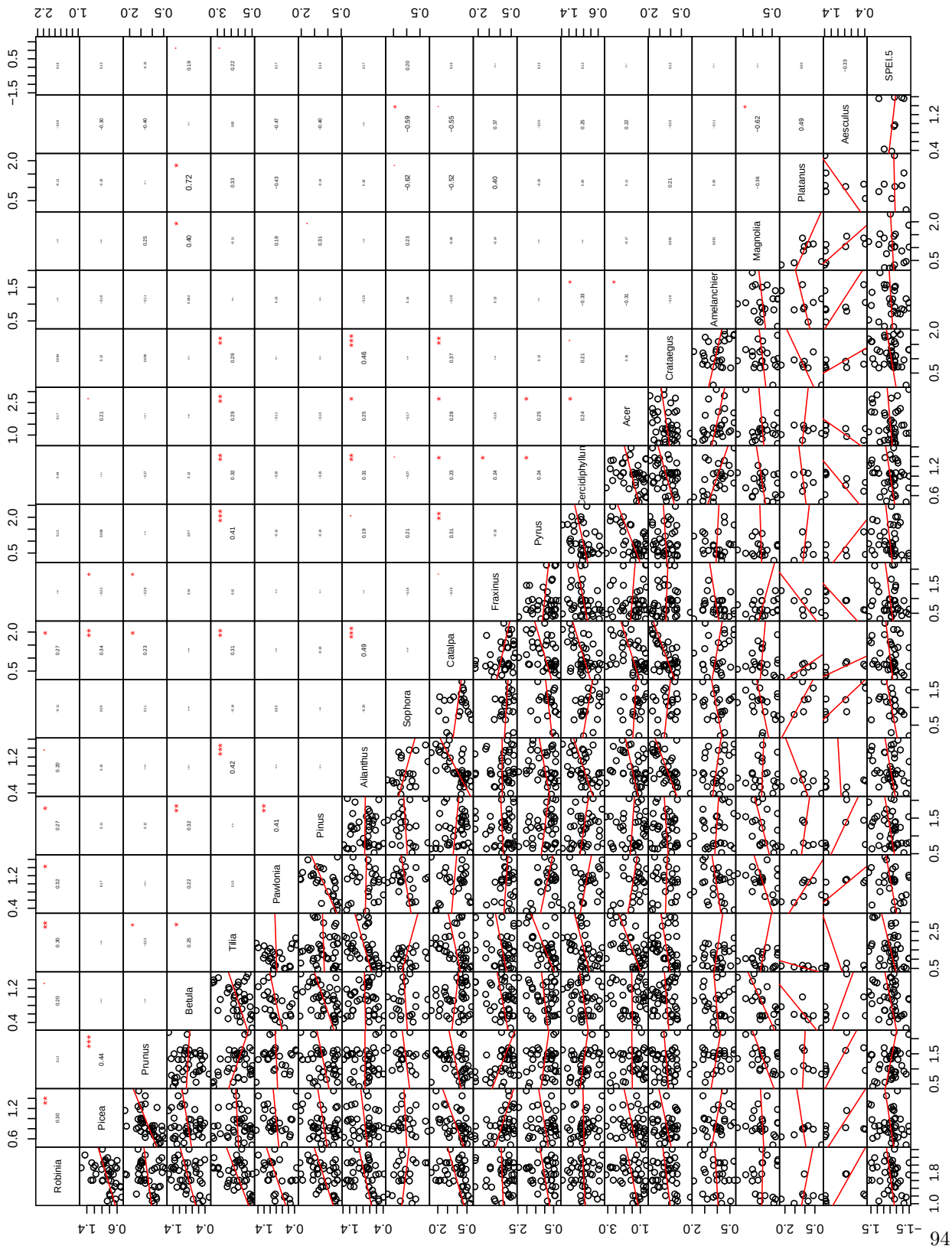

Figure 15: Correlation matrix showing the Mann - Kendall statistics for all the tree species and the vegetative SPEI with a timescale of 5.

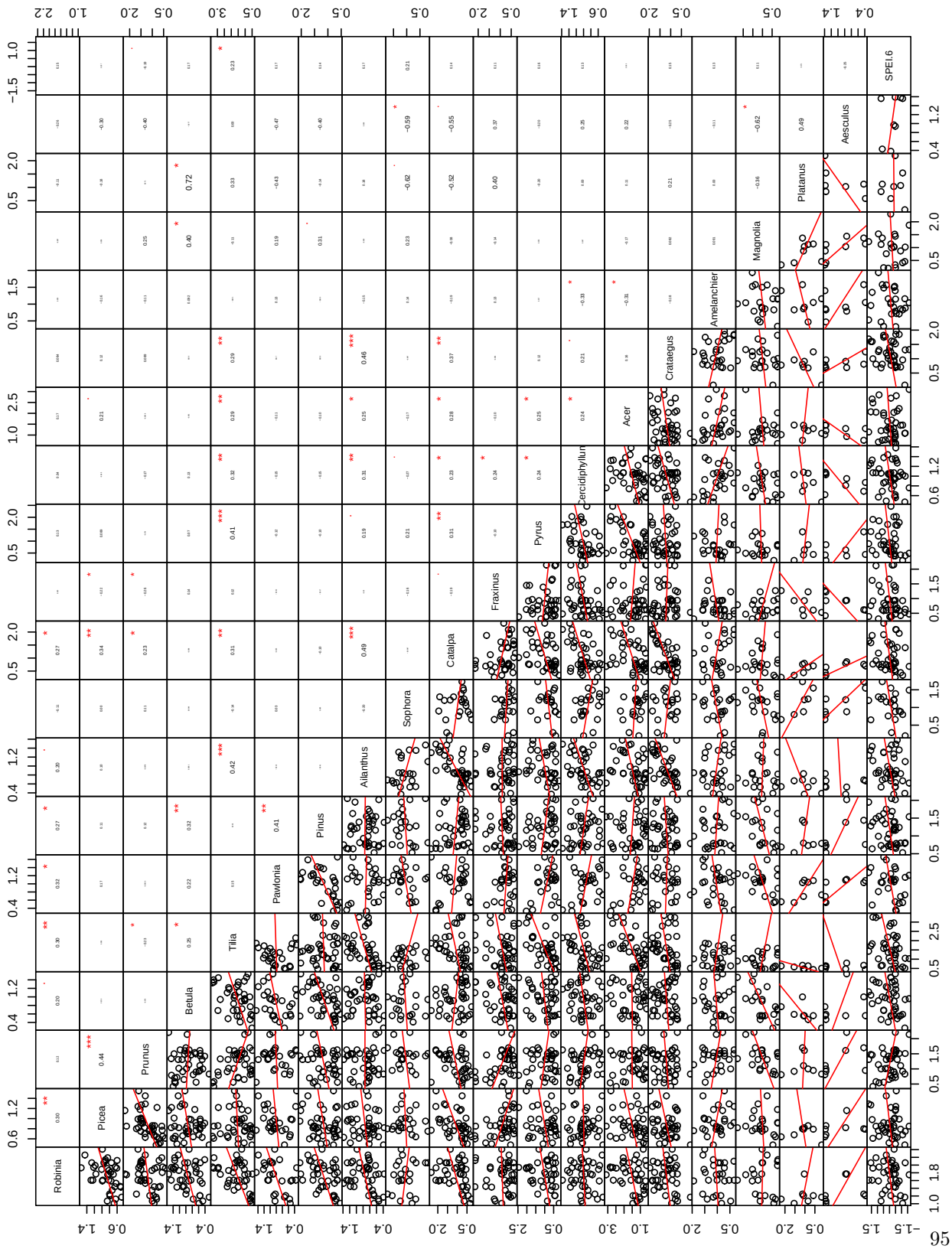

Figure 16: Correlation matrix showing the Mann - Kendall statistics for all the tree species and the vegetative SPEI with a timescale of 6.

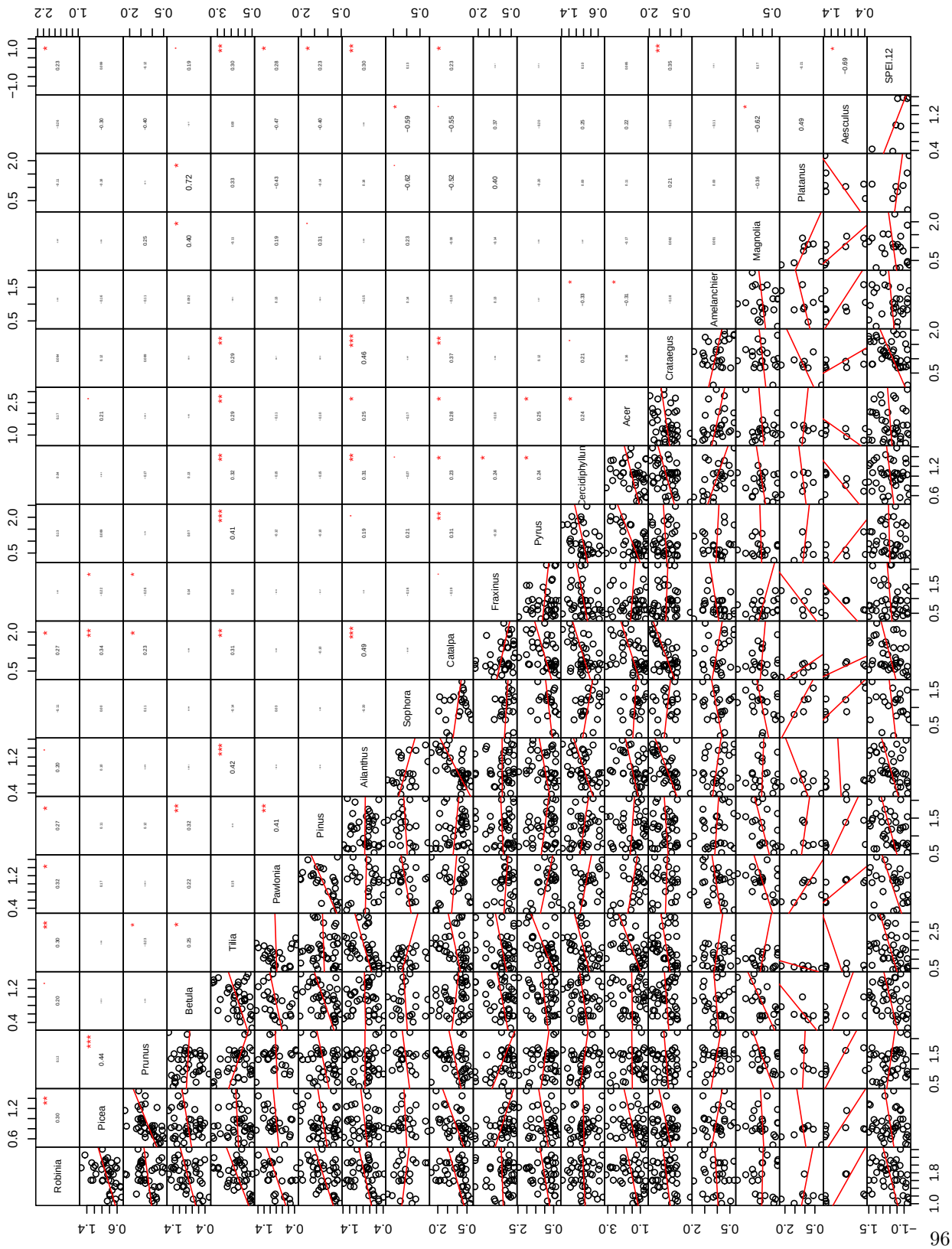

Figure 17: Correlation matrix showing the Mann - Kendall statistics for all the tree species and the vegetative SPEI with a timescale of 12.

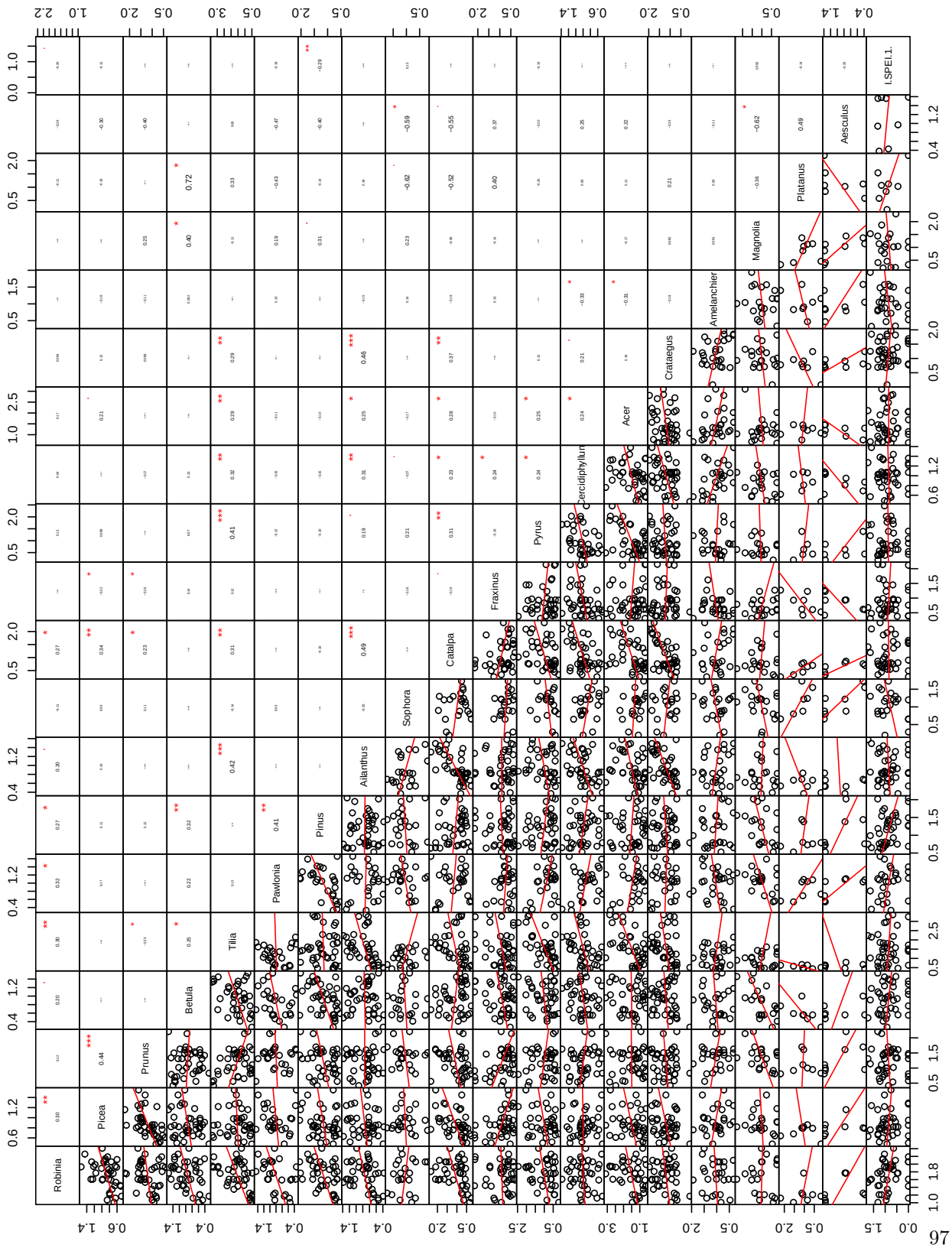

Figure 18: Correlation matrix showing the Mann - Kendall statistics for all the tree species and the intensity of drought with a timescale of 1.

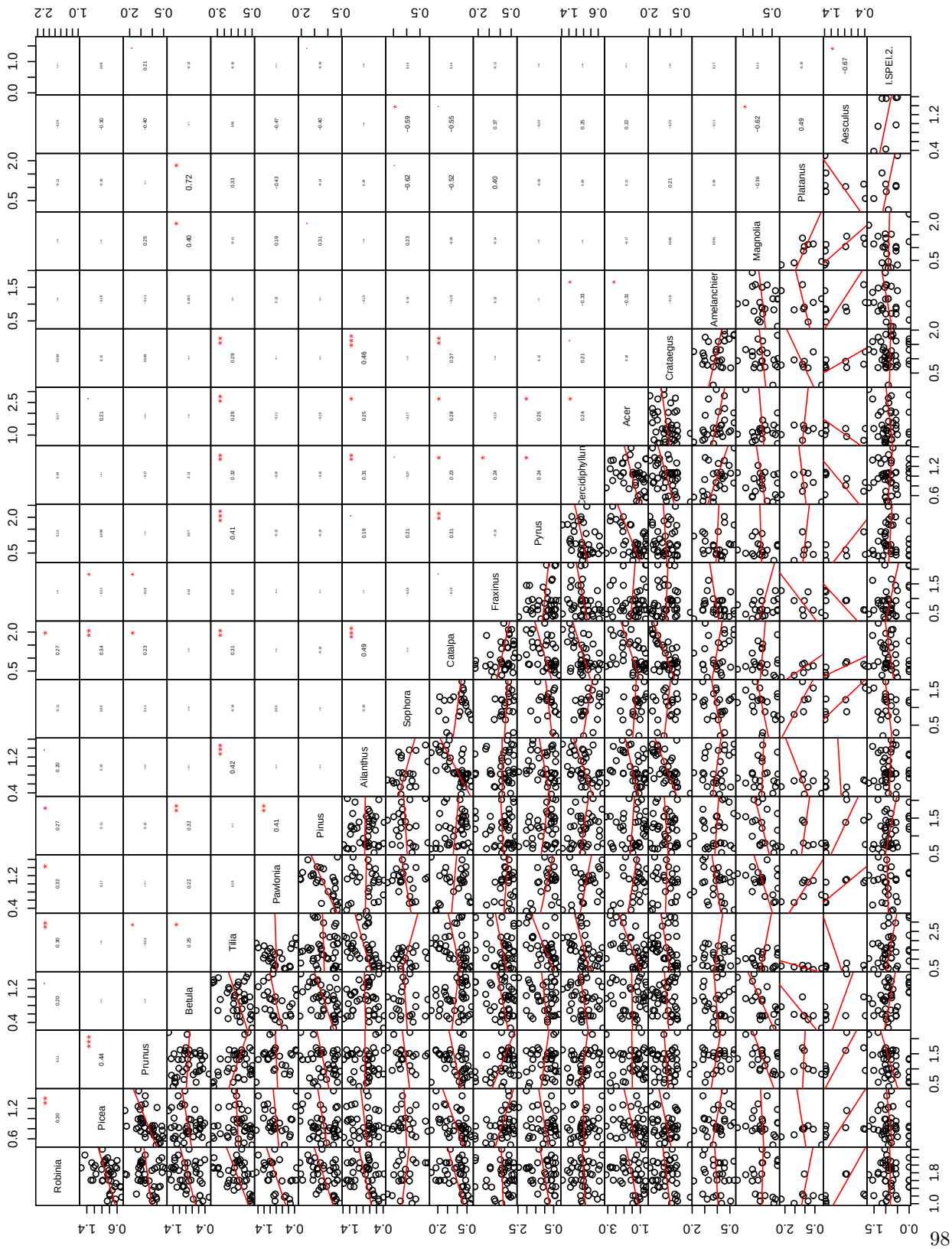

Figure 19: Correlation matrix showing the Mann - Kendall statistics for all the tree species and the intensity of drought with a timescale of 2.

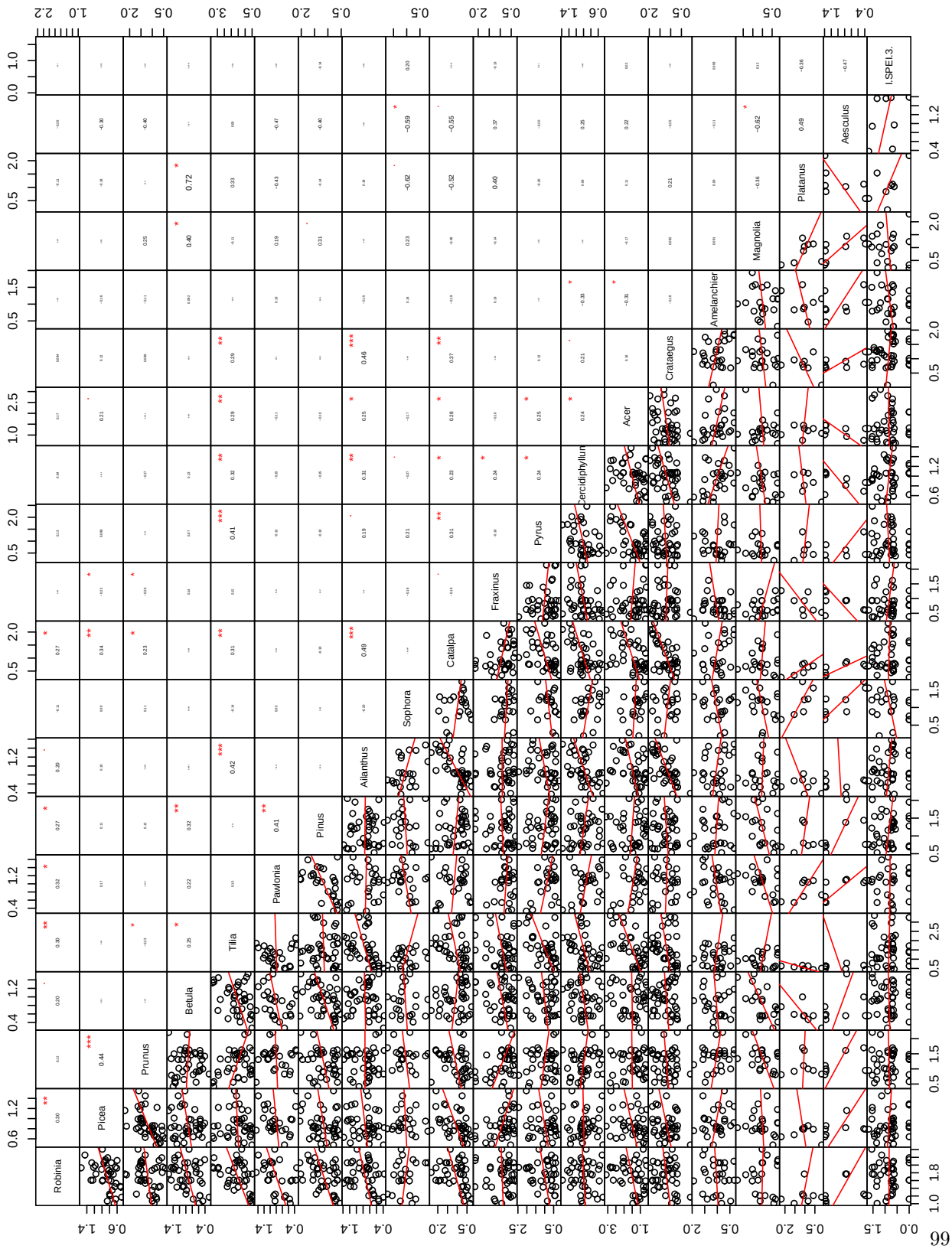

Figure 20: Correlation matrix showing the Mann - Kendall statistics for all the tree species and the intensity of drought with a timescale of 3.

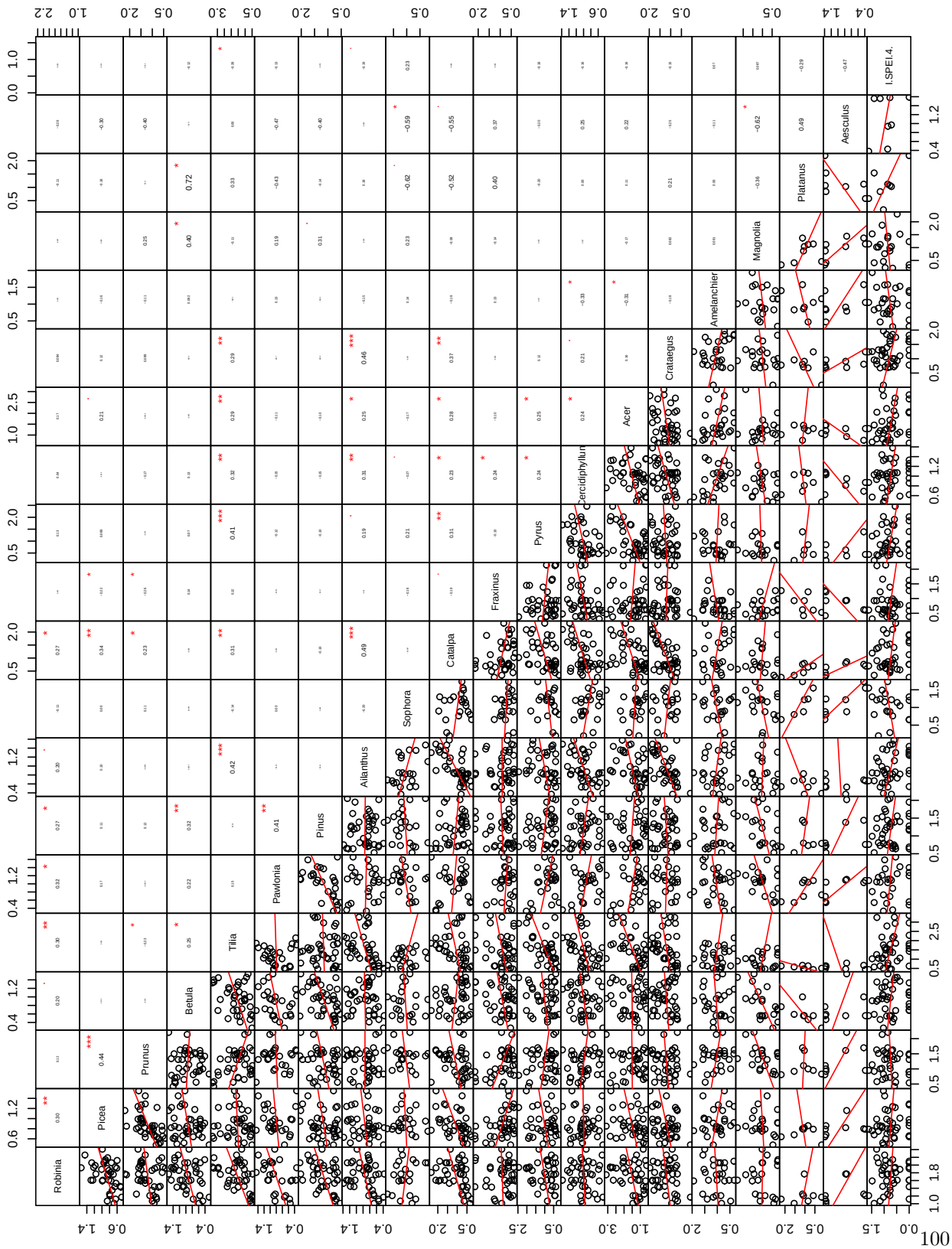

Figure 21: Correlation matrix showing the Mann - Kendall statistics for all the tree species and the intensity of drought with a timescale of 4.

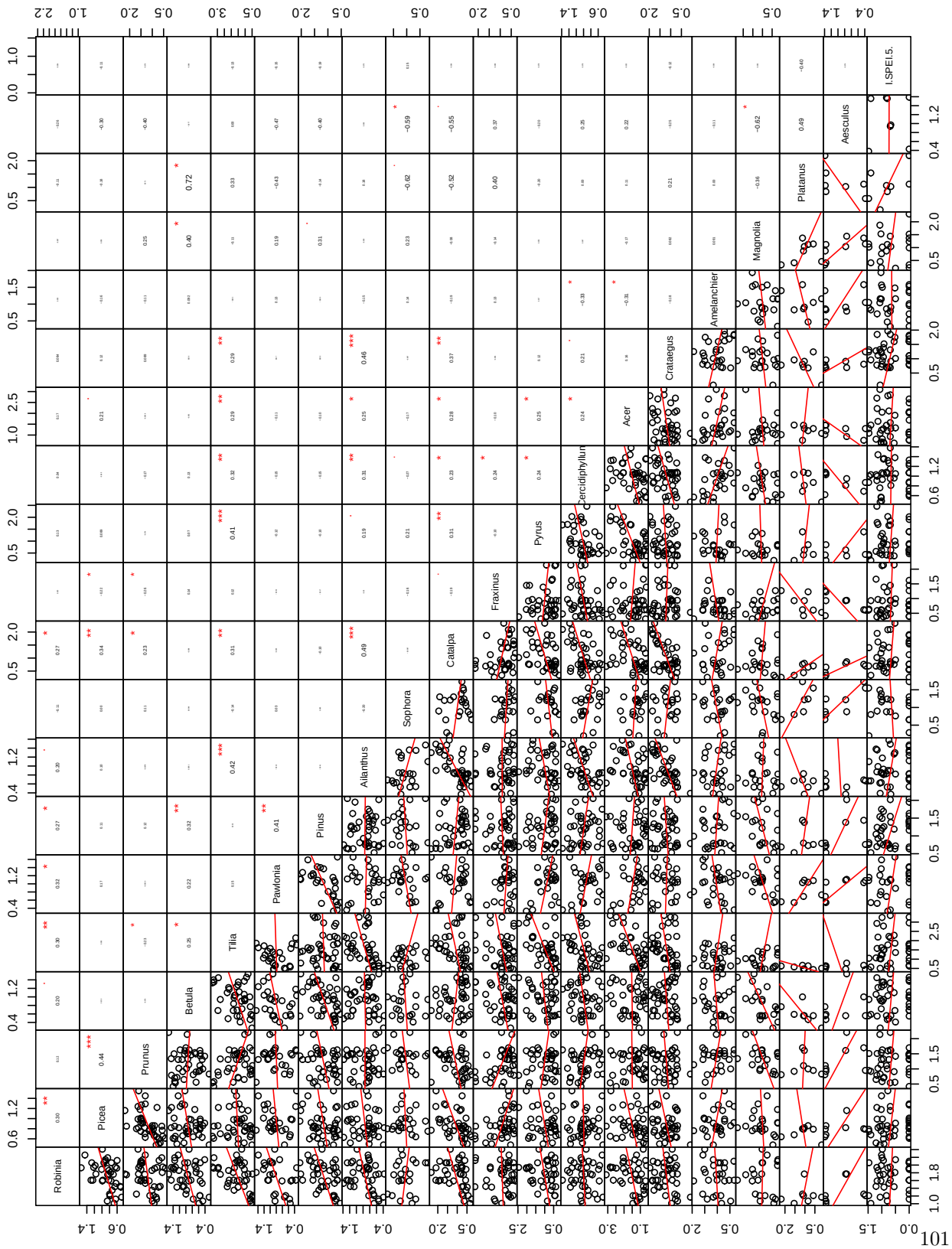

Figure 22: Correlation matrix showing the Mann - Kendall statistics for all the tree species and the intensity of drought with a timescale of 5.

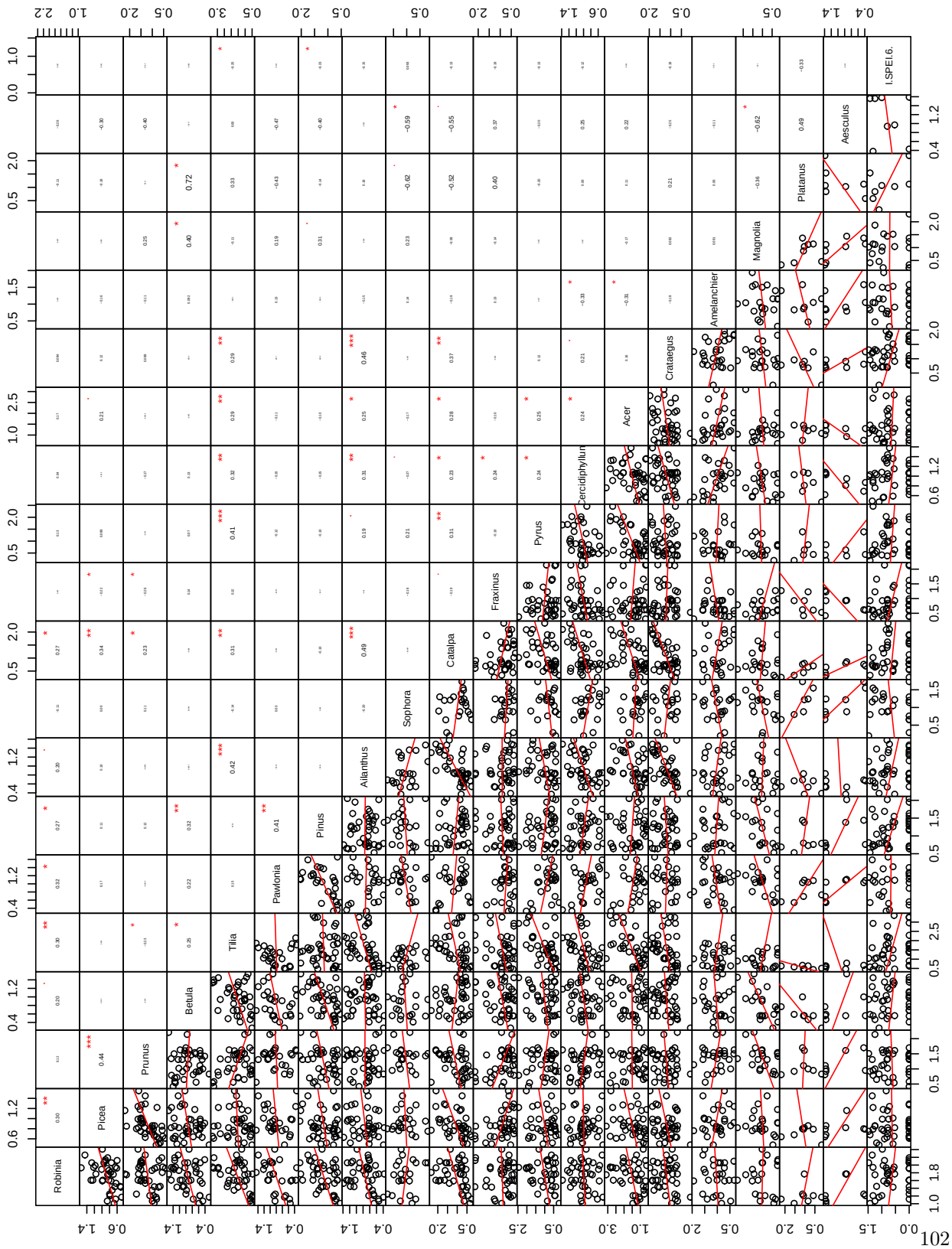

Figure 23: Correlation matrix showing the Mann - Kendall statistics for all the tree species and the intensity of drought with a timescale of 6.

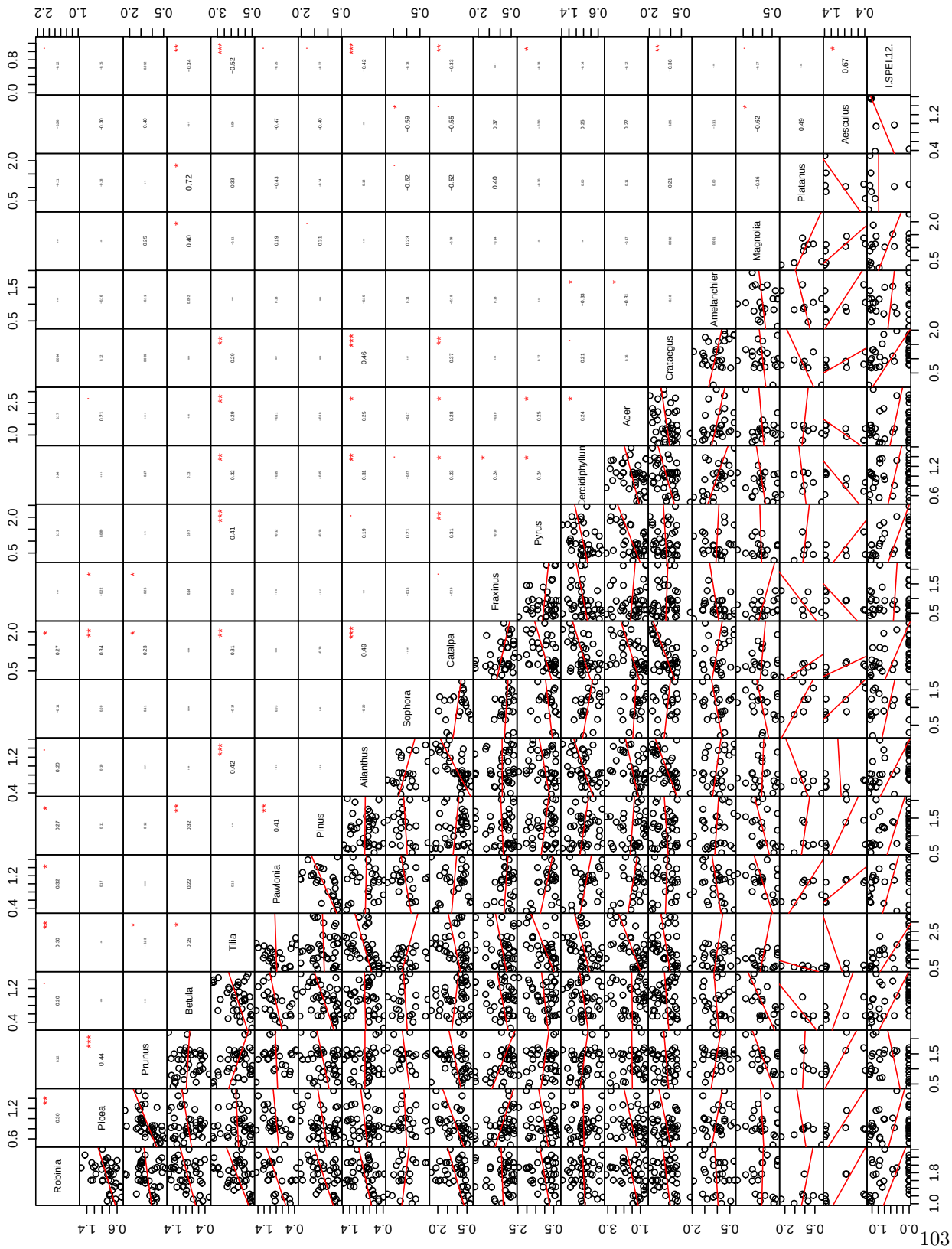

Figure 24: Correlation matrix showing the Mann - Kendall statistics for all the tree species and the intensity of drought with a timescale of 12.

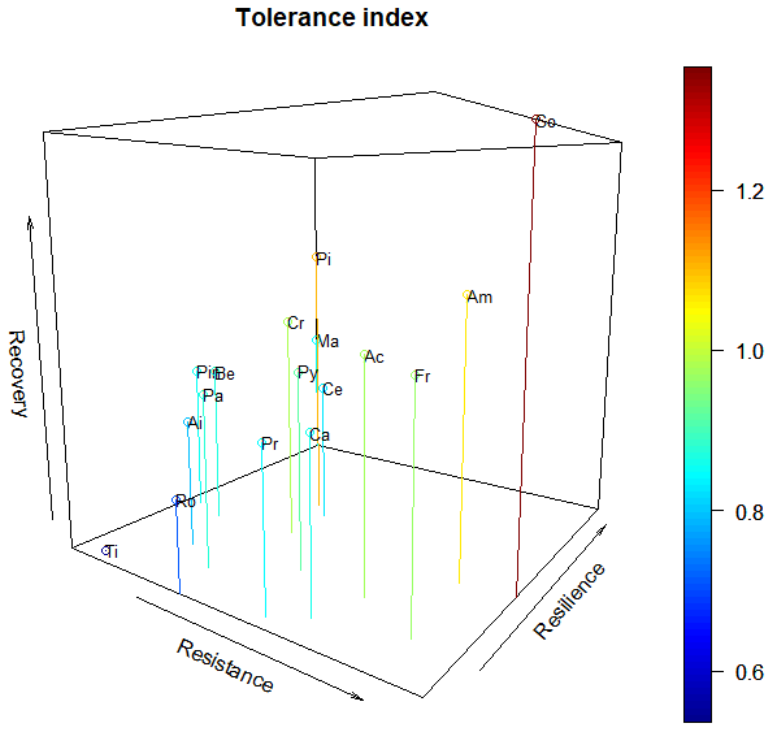

Figure 25: Resistance, resilience and recovery plot for each tree species. Ac = Acer, Ai = Ailanthus, Am = Amelanchier, Be = Betula, Ca = Catalpa, Ce = Cercidiphyllum, Cr = Crataegus, Fr = Fraxinus, Ma = Magnolia, Pa = Paulownia, Pi = Picea, Pin = Pinus, Pr = Prunus, Py = Pyrus, Ro = Robinia, So = Sophora, Ti = Tilia

Personal declaration: I hereby declare that the submitted Thesis is the result of my own, independent work. All external sources are explicitly acknowledged in the Thesis.